This project has received funding from the European Union's Horizon 2020 research and innovation programme under grant agreement No 101016608.

BEYOND 5G – OPTICAL NETWORK CONTINUUM
(H2020 – Grant Agreement № 101016663)

Deliverable D5.2

Final experimental B5G-OPEN validation

Editor Behnam Shariati

Contributors HHI, CNIT, TIM, BT, NOKIA, CTTC, TID, INF-G, Adtran, PLF

Version 1.0

Date October 30, 2024

Distribution PUBLIC (PUP)

Disclaimer

REVISION HISTORY

Revision	*Date*	*Responsible*	*Comment*
0.1	*10 Sept 2024*	*Hussein Zaid*	*Initial version*
0.2	*20 Oct 2024*	*All Partners*	*Partner Contributions*
1.0	*22 Oct 2024*	*Behnam Shariati*	*Final Version*
2.0	*29 Oct 2024*	*Lutz Rapp*	*Quality check*

LIST OF AUTHORS

Partner ACRONYM	Partner FULL NAME	Name & Surname
HHI	Fraunhofer Institute for Telecommunications, Heinrich-Hertz-Institut, HHI	Behnam Shariati, Hussein Zaid, Abdelrahmane Moawad
TID	Telefonica I+D	Oscar Gonzalez De Dios
TIM	Telecom Italia	Marco Quagliotti
CTTC	Centre Tecnològic de Telecommunicacions de Catalunya	Laia Nadal, Ramon Casellas, Ricardo Martínez, Francisco Javier Vílchez, Michela Svaluto Moreolo, Carlos Manso, Luca Vettori
CNIT	CNIT	Filippo Cugini, Alessio Giorgetti, Andrea Sgambelluri
NOKIA	NOKIA	Patricia Layec, Fabien Boitier
BT	British Telecommunications plc	Albert Rafel, Paul Wright, Kris Farrow
INF-G	Infinera Germany	Antonio Napoli, Carlos Castro
ELIG	E-Lighthouse Network Solutions	Francisco Javier Moreno, Pablo Pavón, Enrique Fernandez
TuE	Eindhoven University of Technology	Shiyi XIa, Nicola Calabretta
UPC	Universitat Politecnica de Catalunya	Luis Velasco, Marc Ruiz, Jaume Comellas
ADTRAN	Adtran Networks SE	Lutz Rapp, Dominic Schneider, Achim Autenrieth, Vignesh Karunakaran, Nikhil D Silva
OLC-E	OpenLightComm Europe s.r.o.	Evangelos Kosmatos, Chris Matrakidis, Alexandros Stavdas

GLOSSARY

Acronyms	Description
AI	*Artificial Intelligence*
AP	*Access Point*
B2B	*Back to Back*
BVT	*Bandwidth Variable Transceiver*
BVT	*Bandwidth Variable Transceiver*
CAPEX	*Capital Expenditure*
CD	*Chromatic Dispersion*
CD	*Chromatic Dispersion*
CO	*Central Office*
DL	*Deep Learning*
DoA	*Description of Action*
DRL	*Deep Reinforcement Learning*
DSCM	*Digital Subcarrier Multiplexing*
DSP	*Digital Signal Processing*
DWDM	*Dense Wavelength Division Multiplexed*
EDFA	*Erbium Doped Fibre Amplifier*
ENP	*E-lighthouse Network Planner*
FaaS	*Function as a Service*
HP	*High Power*
IPoWDM	*IP over WDM*
KPI	*Key Performance Indicator*
LP	*Low Power*
MB	*Multiband*
MBoSDM	*Multiband over Space Division Multiplexing*
ML	*Machine Learning*
NOS	*Node Operating System*
OADM	*Optical Add Drop Multiplexer*
OFDM	*Orthogonal Frequency Division Multiplexing*
oFEC	*Open Forward Error Correction*
OLS	*Optical Line System*
OLT	*Optical Line Terminal*
OPEX	*Operational Expenditure*
OSA	*Optical Spectrum Analyzer*
OSNR	*Optical Signal to Noise Ratio*
OT	*Open Terminal*
PCE	*Path Computation Element*
PDL	*Polarization Dependent Loss*
PIC	*Photonic Integrated Circuit*
PLI	*Physical Layer Impairment*
PON	*Passive Optical Network*
Pre-FEC	*Pre Forward Error Correction*

PtMP	*Point to Multi Point*
PtP	*Point to Point*
PVOA	*Programmable Variable Optical Attenuator*
QoT	*Quality of Transmission*
ROADM	*Reconfigurable Optical Add Drop Multiplexer*
RSA	*Routing and Spectrum Allocation*
RSA	*Routing and Spectrum Allocation*
SC	*Subcarrier*
SDN	*Software Defined Network*
SNMP	*Simple Network Management Protocol*
SoA	*Semiconductor optical Amplifier*
SSMF	*Standard Single Mode Fiber*
TAPI	*Transport API*
TAPI	*Transport Application Programming Interface*
TDD	*Time Division Multiplexing*
TDM	*Time Division Multiplexed*
TL	*TeraLight*
VNF	*Virtual Network Function*
VOA	*Variable Optical Attenuator*
WSS	*Wavelength Selective Switch*

TABLE OF FIGURES

TABLE OF CONTENTS

1 EXECUTIVE SUMMARY

This deliverable reports several final demonstrations that validate the B5G-OPEN solutions. In order to map the contributions of the demonstrations to the overall project objectives and KPIs, chapter 3 provides an overview of the overall B5G-OPEN solutions with the goal of mapping the key achievements of each work package to the demonstrations that are reported in the deliverable. The main demonstrations reported in the deliverable are:

- Autonomous Service Provisioning and Self-Healing in Multi-band Multi-Domain IPoWDM Networks for Live Video Traffic
- Disaggregated and Transparent Multi-band Optical Continuum across Access, Horseshoe Aggregation, and Metro IPoWDM Networks
- Filter-less Metro-Access Network
- Chromatic Dispersion Monitoring in Multi-band Optical Transmission Systems
- Packet-Optical Network using Coherent Pluggable Transceivers

The deliverable presents the data plane and control plane architecture of each demonstration followed by demonstration workflows and the carried-out experiments. There is a significant emphasize on the KPIs that are validated in each demonstration using the experimental setup built for each one of them. The document aims to highlight the significant achievements of the project across the three years run time mapped into highly integrated demonstrations and showcase the high level of the interoperability and integrations that could not be achieved without close cooperation among the partners and across different work packages.

2 INTRODUCTION

This deliverable reports on the experimental demonstration and validation of the B5G-OPEN solutions. In this regard, the deliverable covers five demonstrations in which the data plane components developed in WP3 and the control plane components developed in WP4 are integrated to go beyond functional validation of individual components. The integrated demonstrations are evaluated based on the project objectives and the defined KPIs.

In the next chapter, we review the project objectives and KPIs that are validated through the different demonstrations or alternative studies in the project. For each KPI, the experimentally validated measurements are reported based on the corresponding demonstration that are later described in detail. Moreover, for those KPIs that are not evaluated in the demonstration, the corresponding studies are mentioned and referred to accordingly.

The third chapter discusses one of the largest integrated demos of the project focused on Autonomous Service Provisioning and Self-Healing in Multi-Band Multi-Domain IPoWDM Networks for Live Video Traffic. The demonstration is carried out at the Fraunhofer HHI's premises using their large-scale photonic testbed into which several additional data plane (e.g., multi-band node and transceiver prototype) and control plane components (e.g., LiFi controller, optical multi-band controller, orchestrator) developed in the project are integrated. We experimentally validated the control plane architecture of B5G-OPEN using a data plane consisting of IPoWDM smart pluggable, multi-band domain built using prototypes developed in the project, C-band domain using commercial ROADMs and transponders, and access technologies (i.e., PON and LiFi) to create an end-to-end service that carries live traffic.

In the fourth chapter, we report on another large-scale demo focused on Disaggregated and Transparent Multi-band Optical Continuum across Access, Horseshoe Aggregation, and Metro IPoWDM Networks. This demonstration is carried out at the premises of TIM. The demonstration validates an innovative multi-band disaggregated optical network that transparently connects cell-site access in the O band, an aggregation horseshoe utilizing both C- and O-bands, and a C-band metro-core network.

In the fifth chapter, we report a filter-less metro-access network demonstration, that was carried out at BT labs. The demonstration and experiment showed a metro-access network using Infinera's XR Optics connecting a mobile site with a Metro network node through a chain of OADMs that were used to aggregate and drop local traffic. The partners involved included BT, Infinera, OLC-E, CTTC, TuE, and E-Light.

In the sixth chapter, we report a demonstration of chromatic dispersion monitoring in multi-band optical transmission systems. The demonstration took place in CTTC labs in Castelldefels focusing on the monitoring of chromatic dispersion (CD) in multiband (MB) access and metro converged optical networks, using a multiband bandwidth/bitrate variable transceiver (MB BVT). The partners involved in the demo were NOKIA and CTTC.

In the seventh chapter, a demonstration of a Packet-Optical Network using Coherent Pluggables is presented. The experiment was carried out at TID premises in Madrid laboratory. The aim was to evaluate the performance of the proposed B5G-OPEN architecture in which coherent pluggable are hosted in packet optical routers.

3 OVERALL B5G-OPEN SOLUTION AND KPIS

3.1 OVERALL SOLUTION

The overall B5G-OPEN solution used in the final demonstrations involved the data-plane systems and prototypes developed within WP3 and the control plane software solutions developed within WP4. The delivered data and control plane prototypes enabled the design and the development of the innovative concept of "optical continuum" applied to MultiBand (MB) data-plane infrastructures. The delivered solution incorporates heterogeneous nodes and transmission solutions demonstrated within WP5, with different degrees of capacity, complexity, and flexibility, involving innovative prototypes or emerging optical technologies such as pluggables. It encompasses all network domains ranging from metro-core to aggregation and access, also including effective transport for 5G X-haul and LiFi small cells.

Table 1: List of optical data plane prototypes involved in the final demonstration experiments.

Prototypes	Description
MB S-BVT (PtMP transceiver)	B5G-OPEN has developed a multi band (MB) sliceable bandwidth/bit rate variable transceiver (S-BVT) prototype capable to operate within the C- and S-bands. The proposed transceiver enables network scalability and flexibility as the different building blocks can be enabled and disabled according to the traffic demand and network needs, providing an efficient use of the available resources. Additionally, this approach facilitates and supports the coexistence of both point-to-point (PtP) and point-to-multi point (PtMP) high-capacity optical connections within the metro-aggregation and regional networks. The MB S-BVT prototype has been used in different experiments described in deliverables D3.1-D3.3 and in the joint Nokia/CTTC demo "Demonstration of Chromatic Dispersion Monitoring in Multi-Band Optical Transmission Systems", reported in section 7 of this deliverable. In the demo, an additional slice/transceiver working within the L-band, developed in SEASON project (G.A. 101096120), has been also used as joint collaboration between the two projects.
(Semi-) Filterless Node Prototype	The filter-less Optical Add/Drop Multiplexer (OADM) and low-cost Semiconductor Optical Amplifiers (SOAs) have been integrated into a compact, energy-efficient circuit with potential for high-volume production. This design leverages the flexibility and performance of DSCM-based coherent pluggable transceivers. The filter-less OADM, introduced in M3.3 and D3.2, is applied in Metro-Aggregation networks using 400G Open XR pluggable optics and has also been demonstrated in filter-less Metro-Access Network setups.
MB Filter-less Node Prototype	The MB filter-less node prototype with add-drop stage covering S-, C-, L-bands is designed by Fraunhofer HHI by extending a commercial matrix switch with passive band splitters instead of active components. The prototype is a 2x2 node (unidirectional) that offers band switching. The full details of the design are reported in D3.2. The MB node prototype is used in the final integrated demonstration reported in section 4 of the current

	deliverable. The prototype is used to add, drop, or carry out pass-through of an entire band (S, C, or L) in the demonstration.
2-degree C ROADM 2-degree O,C,L ROADM	To address the challenges posed by high-throughput traffic, MBT has demonstrated a cost-efficient and flexible solution. The core components of Multiband ROADM (2-degree-C ROADM, 2-degree-C+O ROADM, and N-degree-C+O+L ROADM) have been explored for use as metro-hubs and metro-access nodes within the MB Optical Metro-Access Network [Xia23]. These ROADMs are also involved in the demo of disaggregated and transparent multi-band optical continuum across access, horseshoe aggregation, and Metro IPoWDM networks. [Xia23] S. Xia, M. Rombouts, H. Santana and N. Calabretta, "Performance Assessment of Multiband OADM in Metro-Access Network for Converged Xhaul Traffic", in 49th European Conference on Optical Communications, 2023
MCS switch PIC	Within the filterless architecture of the Metro-Access Network, high-speed coherent transceivers are used to allocate subcarriers for point-to-multipoint operations and traffic distribution. Upstream and downstream data are transmitted through separate optical fibers. In the downstream link, SOAs are used for power compensation to counteract signal attenuation over long distances. In the upstream link, power balancing is essential for proper subcarrier demodulation. Before transmitting upstream signals, power compensation is applied at the previous node, followed by further compensation for transmission losses through a BOOST-type SOA. A multicast selective (MCS) switch is introduced in both the transmitter and receiver sections to accommodate more users by controlling different optical paths. This MCS switch, based on low polarization-dependent bulk SOA co-integrated with passive waveguides, serves as an optical bypass and amplifier for both uploaded and downloaded signals from the access network. [Zal24] A. R. Zali, N. M. Tessema, S. Kleijn, L. Augustin, R. Stabile and N. Calabretta, "Assessment of Low Polarization Dependent Multicast and Select Switch Based on Bulk SOA for Data Center Application," in Journal of Lightwave Technology, vol. 42, no. 2, pp. 780-792, 15 Jan.15, 2024,
C- and L-band WSS PIC	As a core component of the WSS with splitters in the ROADM for the Metro-Aggregation Network, a C+L band wavelength selective switch has been designed and fabricated. The chip architecture features a single input port branching into eight WDM modules, each with eight output ports. Each WDM module processes eight channels spaced 400 GHz apart, and includes an AWG as a demultiplexer to separate the WDM channels, along with an array of SOAs for amplification. Mukit, M., Prifti, K., Kleijn, S., Augustin, L., Stabile, R., & Calabretta, N. (2023, October). Experimental assessment of C-and L-band photonic integrated SOA-based-1× 8 wavelength selective switch. In ECOC 2023, Vol. 2023, pp. 1138-1141). IET.

Power Profile Monitoring DSP Software	The core concept of the prototype is to offer a monitor that delivers a per-channel longitudinal power profile along the fiber link. This is possible thanks to the non-commutative relationship between the chromatic dispersion and the nonlinear interference induced by the channel on itself, i.e., self-phase modulation (SPM). This non-commutativity permits characteristics of the channel be uniquely determined by applying a reverse-order operation. Therefore, at the Receiver DSP, one can estimate channel properties from the digitized samples by using a DSP chain. By analysing the power profile, interesting results are obtainable such as gain and tilt of amplifiers of the system. It also enables studies concerning anomaly detection, in which optical amplifier anomalies, such as, gain, tilt and narrowband gain compression are observed. The software is reported in D3.1 (section 6.1.2.1).
MB Offline Transceiver Prototype	This prototype enables S-band transmission by employing standard C-band components-off the shelf (COTS). As a reference, similar investigations were conducted for the C- and L-band. To achieve an OSNR penalty reduction, Volterra based system identification (SI) and nonlinear digital predistortion (NLPD) are employed. Using single channel 64 GBd polarization division multiplexed (PDM) 64- and 32-ary quadrature amplitude modulation (QAM) data signals, bandwidths of ~150 nm (32-QAM) and ~140 nm (64-QAM) are achieved at a bit error ratio (BER) below the soft-decision forward-error correction (SD FEC) in a back-to-back (b2b) configuration. The prototype is reported in MS3.2 (section 4.4) and is used in the final integrated demonstration reported in section 4 of the current deliverable. The prototype is used to generate S-band and L-band signals in the MB domain of the end-to-end demonstration.
C-Band ROADM Ring with TAPI	The C-Band Micro ROADM Ring network is deployed and implementations are made for flexible Channel provisioning. The ROADMs are controlled with OLS controller as shown in section 4.1. The ONF-TAPI driver is adapted to support the following task, To provision a service with a flexible channel bandwidth. This helps to support end-to-end service provisioning in a cross-domain use case.
Physical Layer Impairment validation tool	In D3.3 (section 3.1.8), a prototype software suite that optimizes and assesses the performance of a multi-band transmission system is reported. To achieve a flat OSNIR performance over the E- to L-band, the launch power per band is specifically utilized as an optimization variable. This method manifests a very good balance between complexity and accuracy, it applies to an arbitrary number of bands, while not requiring frequent adjustments and tweaks of the corresponding optical amplifiers. Moreover, the method allows to tailor the launch power down to each individual wavelength channel in each band to allow a tight control of the performance of each channel in any optical band. The implicit assumption that is made is that SRS tilt due to the previous fiber link is compensated at every node and that the node is based on WSS elements able to regulate the power level of all channels between the given I/O fibers.

7-node mesh network	This prototype was upgraded with additional nodes and enhanced telemetry systems. During B5G-OPEN project, we run two joint demonstrations. The first one focused on a distributed telemetry system relying on data collected from our optical mesh network testbed. It showed that the telemetry agent could be integrated within the Nokia node agent paving the way to multi-vendor data source integration. Part of this work was reported in D4.3 and D4.4, published in [Go23]. The second demonstration aimed at implementing a telemetry system for power profile monitoring as well as running live for the first time the novel monitoring algorithm in a meshed network testbed with commercial products (see obj. 5). This has been showcased in ECOC 2024 and is reported in D6.3, Section3.6.
Packet-optical white box with SONiC Operating System, OpenZR(+) transceivers, P4 switch	During B5G-OPEN, we envisioned the availability of a programmable IPoWDM white box, i.e. a switch equipped with coherent pluggable transceiver and P4-programmable ASIC. Such a box became commercially available around the end of the project, confirming the potential of the envisioned technology. During project execution, the combined functionalities of the considered box where successfully emulated relying on two separate boxes. In B5G-OPEN, the programmable IPoWDM solution has been investigated, together with its specifically designed software components (OpenConfig Agent and SONIC-based Packet Optical Node), to successfully demonstrate innovative IP over WDM telemetry and networking functionalities. This includes for example the in-network processing and exchange of telemetry data of computing, packet, and optical parameters (see Obj. 6). Results reported in two B5G-OPEN publication in the JOCN Journal and several Conference proceedings.
Multiband Amplifier	Different technologies for signal amplification in various bands have been investigated and compared with each other. Rare-earth base amplifiers offer the advantage of high energy efficiency and can be easily installed in parallel configurations without interaction among the bands. Transient control is a major issue in wavelength-division multiplexing networks and becomes even more critical with the transition to multi-band transmission. In contrast to single-band solution, transient control requires to control tilt and gain of each involved amplifier in a coordinated way. A novel feedforward control solution developed by Adtran has been verified with an experimental setup. The results have been document in a dedicated document and more details are reported with regards to KPI 3.3.
LiFi Access	The LiFi access protocol developed for this project introduces an innovative approach to light-based data transmission by leveraging existing lighting infrastructure. This protocol ensures reliable, high-speed, and low-latency communication, meeting the needs of dynamic indoor environments. In the HHI demonstration, the protocol is implemented within the LiFi Access Point (AP), which transmits data to a user device equipped with a LiFi USB dongle. The demo uses a webcam application to illustrate the seamless, end-to-end data flow provided by the LiFi AP, showcasing the protocol's capability to

	support real-time, high-bandwidth applications in multi-band network environments.

Table 2: List of control plane prototypes involved in the final demonstration experiments.

Prototypes	Description
B5G-ONP	The B5G-ONP is a control plane component aimed at providing an optimal solution for jointly managing multi-layer IT and network resources by integrating advanced algorithms across multiple domains. Additionally, this component plays a role in coordinating service provisioning with full support of standard communication with other orchestrators or controllers in the project, such as the TAPI-enabled orchestrator, the path compute element or the PON controller. Its novelty lies in its ability to handle multi-band resource information and plan across multiple network domains, and as a result a B5G-ONP-based asset has been recognized on the EU innovation radar for the lifetime of this project. In WP5 dedicated demonstrations, B5G-ONP participates in demonstrations presented in Sections 4, 5, and 6. In Sections 4 and 5, it is utilized as a multi-domain IP-over-WDM (IPoWDM) planner, where it coordinates the design and optimization of network resources across multiple domains. In the demonstration in section 4, the component monitors the IP and optical segments of the network and coordinates with domain-specific controllers via standardized interfaces, ensuring continuity of operations at the access, metro and core layers of the network. Also, for section 5 work the multi-domain IPoWDM network orchestrator (B5G-ONP) interacts with the NBIs of a prototype IP SDN controller and the TAPI-based Network Orchestrators for optical domains, and an external inventory database. It has been enhanced to unify and control multi-domain optical and IP layers, offering a comprehensive IPoWDM multilayer network view. Finally, in the Filter-less Metro-Access Network demonstration (section 6), B5G-ONP acts as central controller to coordinate the domain-oriented controllers in the E2E network orchestration.
TAPI-enabled Optical Network Orchestrator with externalized Path Computation	The TAPI-enabled Optical Network Orchestrator is a functional element of the architecture that is responsible for the following functions: i) providing a uniform, open and standard view and interface to the higher levels and components of the B5G-OPEN control, orchestration, and telemetry system; ii) Compose a complete Context to be consumed by B5G-OPEN network planner and additional consumers combining information retrieved from subsystems and sub-controllers (Optical Controller, external databases, monitoring systems, etc), iii) Enable single entry point for provisioning DSR and Photonic Media services, including externalized path computation and iv) provide an event telemetry data source that reports events that happen asynchronously in the network. The novelty of B5G-OPEN is many-fold: integrate with MB-PCE, implement the native interface to the ONOS SDN controller to delegate path provisioning. Support flexi-grid multi-band networking and path computation/resource allocation, interwork with the B5G-ONP and improve

	support for OpenROADM device driver with additional link profiles for multiband as well as initial support for TAPI extensions. This software has been used in all key B5G-OPEN demos: "Disaggregated and Transparent Multi-band Optical Continuum across Access, Horseshoe Aggregation, and Metro IPoWDM Networks" (TIM), "Autonomous Service Provisioning and self-healing in multi-band multi-domain IPoWDM networks for live vide traffic" (HHI); "Filter-less Metro-Access Network Demonstration" (BT premises) and joint Nokia/CTTC demo "Demonstration of Chromatic Dispersion Monitoring in Multi-Band Optical Transmission Systems" (CTTC)
Path Computation Elements – MB-PCE	The Multi-Band Path Computation Engine (MB-PCE) is based on a multi-band routing engine which ensures that: i) routing is implemented by means of an efficient spectrum and modulation-format assignment; and ii) the impact of physical layer effects over the selected optical paths is estimated and the results are benchmarked against QoT target values (BER, OSNIR, OSNR, etc). In this way, the planning tool ascertains the conditions that maximize the total capacity of the network while it minimizes the global blocking probability and prevents network misconfiguration. The main novelty introduced for B5G-OPEN is the Multi-Band physical layer impairment model utilised, and in addition the interfacing with TAPI and B5G-ONP. The MB-PCE was used in the "Disaggregated and Transparent Multi-band Optical Continuum across Access, Horseshoe Aggregation, and Metro IPoWDM Networks" (TIM) demo.
Optical Controller	The optical controller is based on ONOS SDN controller that provides a wide environment that is used to control and configure optical devices and transceiver equipped within packet/optical white boxes. In particular, the main roles of the optical controller are: (i) retrieve devices description from data plane and abstract them toward the upper control layers; (ii) receive the service configuration requests by the upper control layers and translate such requests in a set of configuration messages to be forwarded to each involved device. During the project, several innovative developments within the ONOS controller have been implemented at different levels of the ONOS architecture (i.e., in the NBI, in the SBI and in the Core) for introducing B5G-OPEN specific features: 1. Enable integration with T-API orchestrator (NBI) 2. Develop drivers toward new devices and update existing drivers against most recent versions of standard models (SBI) 3. Introduce the support of flexible grid (NBI, core, SBI) 4. Introduce the support of multi-band (NBI, core, SBI) 5. Import/Export physical impairment device manifest (SBI, NBI) 6. Activate intents using as end-points the ROADM's ports (Core)
Access / PON Controller	The B5G-OPEN TDM-PON infrastructure is realised using an XGS-PON OLT pluggable transceiver (e.g., TiBit pluggable) and a couple of pluggable ONUs (e.g., Tibit ONUs). The OLT is interfaced directly to a whitebox switch while the OLT is interconnected to the ONUs by means of splitters, forming up an ODN branch. The PON vendor (Tibit) will provide the pluggable software and the PON controller software. The integration of Tibit PON Controller with the

	B5G OPEN platform is realised with the development of an Access Controller. The Access Controller is responsible to: a) monitor the PON network and receive any requests for PON reconfiguration; b) translate these requests into high level traffic requests that is reported to the B5G-ONP App; c) execute the appropriate actions in the PON Controller in order to support the new requests. In addition, the Access Controller communicates with the LiFi Controller for retrieving any connection/traffic requests. This is a new component developed exclusively for B5G-OPEN. The main features are the TiBit controller, LiFi and B5G-ONP integrations. The Access/PON Controller was used in the "Autonomous Service Provisioning and self-healing in multi-band multi-domain IPoWDM networks for live vide traffic" (HHI) and the "Filter-less Metro-Access Network Demonstration" (BT) demos.
LiFi Controller and LiFi Agent	The LiFi controller and LiFi agent developed in this project enable streamlined management of LiFi Access Points (APs) within a broader network system. Positioned between the PON controller and LiFi agents, the LiFi controller facilitates device discovery and essential configurations, such as setting SSIDs, IP addresses, and toggling APs on or off, with minimal processing overhead. Each LiFi agent operates directly on the APs, using the NETCONF protocol to communicate with the controller to manage configurations and update AP status. In the demonstration, this setup is tested for effective communication with the access controller, validating the system's responsiveness and reliability in dynamically managing the LiFi APs within the multi-band network.
OpenROADM Agent	The TIM OpenROADM agent is an implementation of a NETCONF server controlling optical network elements using OpenROADM device models. It's basically an evolution of the agent developed for the H2020 Metro-Haul project enhanced to cover MultiBand technology exploiting the latest OpenROADM models. It has been used for the field trial of multi-band disaggregated optical network integrating access, aggregation horseshoe and metro-core networks operating with both C and O bands, described in sect. 5.
OpenConfig Agent	B5G-OPEN has produced two different implementations of the OpenConfig agent. One implemented at CTTC with the main aim of integrating it with the CTTC developed multi-band transceiver and one implemented at CNIT with the main aim of integrating it into the packet-optical SONiC based node. Since the software architecture, interfaces, and proposed KPIs are the same, both implementations are described in this section. OpenConfig agent is an implementation of an SDN agent using NETCONF/YANG with the OpenConfig data models. It implements a subset of the data models, namely the OpenConfig platform and optical transport as well as some extensions devised in the context of B5G-OPEN to report details about the transceiver operational modes. The software relies on ConfD free, a Tail-f/Cisco management agent software framework for network elements. It enables the industry adoption of NETCONF and YANG, and provides a simple mechanism to develop SDN agents focusing on the business logic and on the actual data models and semantics. CTTC OpenConfig agent has been used with the demos involving the S-BVT at the CTTC premises, including joint Nokia/CTTC demo "Demonstration of

	Chromatic Dispersion Monitoring in Multi-Band Optical Transmission Systems" (CTTC) and has been integrated with the Optical Network Orchestrator and with the ONOS Optical Controller.
SONIC-based Packet Optical Node	SONiC has been used as network operating system (NOS) of packet-optical white-box nodes and extended with some components to enable the integration with other B5G-OPEN components: (1) docker container running the OpenConfig agent to control external transponders, local coherent transceivers, and IP interfaces; (2) REST-based APIs enabling the control of coherent transceivers, Ethernet/IP interfaces and routing processes; (3) exporter/adapter of monitoring information from SONiC system and transceivers to the telemetry server. The proposed technology has been used to provide the first validation of the MANTRA Options. Furthermore, they have been used to validate an innovative monitoring solution (in-network processing and exchange of telemetry data of computing, packet, and optical parameters - see Obj. 6). Results have been reported in two B5G-OPEN publication in the JOCN Journal and several Conference proceedings. In addition, the innovations related to IPoWDM have been demonstrated in the final demos described in Sections 4, 5, and 8.
AI/ML models for PSD and Power Management	The best performance is obtained as a compromise between linear and nonlinear contributions. It is the so-called nonlinear threshold which is operating in the weakly nonlinear regime. Monitoring ASE and NL signal to noise ratios is quite complex in a live network and has some limitations which make this problem attractive for artificial neural networks (ANN). We proposed to monitor the optical spectrum contains knowledge regarding linear and nonlinear impairments specifically the shape is different if operating in linear or nonlinear regime. In addition, we also proposed to monitor the SNR-induced fluctuations from the polarisation dependent loss (PDL) also show a pdf with a different shape in linear and nonlinear regimes. To this end, we need to monitor the SNR per polarization. Therefore, we can use either of these 2 shapes at the input of the ANN to get an optimal power correction to be applied. These works are novel proposals in the community and have been reported in D4.2, D4.3 and D4.4, also published in [And24.1] and [And24.2].
Telemetry System	Several telemetry architectures are available. In general, telemetry data is collected from observation points in the devices and send to a central system running besides the SDN controller. Although protocols specifically devised for telemetry, like gRPC, compress data, the amount of data that can be collected and the frequency of collection make those architecture not practical. The main novelty of the proposed telemetry system is that it is distributed and supports intelligent data aggregation nearby data collection. The system integrates measurements and event data collection and telemetry agents receive and analyse measurements before sending to a centralized manager. This work was reported in D4.3 and D4.4, published in [Ve23.1] and demonstrated in [Go23] The telemetry system has been demonstrated as part of the control plane of the demonstration of automation and real-time management of a multi-band, multi-domain IPoWDM network.
Mesarthim – Failure management	The performance of optical devices can degrade because of aging and external causes like, for example, temperature variations. Such degradation might start with a low impact on the Quality of Transmission (QoT) of the

Using a SNR Digital Twin	supported lightpaths (soft-failure). However, it can degenerate into a hard-failure if the device itself is not repaired or replaced, or if an external cause responsible for the degradation is not properly addressed. MESARTHIM compares the QoT measured in the transponders with the one estimated using a QoT tool. Those deviations can be explained by changes in the value of input parameters of the QoT model representing the optical devices, like noise figure in optical amplifiers and reduced Optical Signal to Noise Ratio (OSNR) in the Wavelength Selective Switches. By applying reverse engineering, MESARTHIM estimates the value of those modelling parameters as a function of the observed QoT of the lightpaths. This work was reported in D4.3 and D4.4 and published in [Ve23.2]. The MESARTIM methodology was initially based on a SNR digital twin that was later replaced by OCATA.
OCATA- Digital Twin for the Optical Time Domain	The development of Digital Twins to represent the optical transport network enables multiple applications for network operation, including automation and fault management. OCATA is a deep learning-based digital twin for the optical time domain that is based on the concatenation of deep neural networks (DNN) modelling optical links and nodes, which facilitates representing lightpaths. The DNNs model linear and nonlinear noise, as well as optical filtering. Additional DNN-based models extract useful lightpath metrics, such as lightpath length, number of optical links and nonlinear fibre parameters. OCATA exhibits low complexity, thus making it ideal for real-time applications. This work was reported in D4.3 and D4.4 and published in [Ru22] OCATA has been demonstrated as part of the control plane of the demonstration of disaggregated and transparent MB Optical Continuum.

Using the above protypes in the demonstration experiments, as documented in this deliverable, the following features were demonstrated:

- Flexibility to adapt to the specific network domain with the proposal of different optical switching technologies in order to cope with the specific needs in term of node size, scalability, cost, power consumption and numerosity.
- Transparent interoperation (Optical Continuum) allowing transparent crossing of network domains with an expected relevant cost saving.
- Native support for optical disaggregation with horizontal and vertical standard interfaces and in particular the integration with the packet layer (IP over dense wavelength division multiplexing, DWDM)
- Use of Point to Multi Point (PtMP) connectivity at the optical layer, that efficiently provide traffic in the metro aggregation segment and particularly in short and medium term.
- Efficient use of available optical bands (Multi band).

With respect to the control plane involved in the experiments, this involved the following software prototypes:

- Network planning and orchestration mechanism focusing on the use of P2MP pluggable and using deep reinforcement learning for solving Routing and Spectrum Assignment (RSA) problem.

- Failure management mechanism for soft-failure detection, identification, localization and severity estimation. The developed mechanism, named MESARTHIM makes use of a network Digital Twin (DT) for assisting in the process of failure detection and localization by analyzing the estimation of the value of the modelling parameters of the devices. In essence, MESARTHIM methodology targets at:
    - detecting and localizing the optical device responsible for the soft failure
    - identifying the modeling parameters that explain the observed effects in the QoT
    - estimating the evolution of the value of such parameters to find whether the soft-failure will degenerate into a hard-failure
- Failure recovery and restoration employing a DRL-based agent that was developed for the autonomous restoration of disrupted lightpaths.

In addition to the above-mentioned solutions for the control plane, part of the effort was devoted to developing a digital twining (DT) solution for failure management (named OCATA and which was based on Deep Neural Networks) as well as on solutions for autonomous network operations. The latter included actions both on the physical layer and the network layer. For example, optical power optimization was used to gain knowledge on the network physical parameters or detection of large flows at the network level to be handled differently by the data plane.

3.2 PROJECT OBJECTIVES AND KPIS

Obj. 1 (O1): Design a cost-effective, energy-efficient, programmable, and disaggregated end-to-end optical network, which removes terminations between network domains, thus drastically reducing electronic hops, to provide an optical network continuum between access, metro, and core segments.
Description (DoA): The main objective is to redesign the overall end-to-end network infrastructure to meet the B5G requirements in terms of bandwidth, latency, mobility, dynamicity, power-efficiency, while cost-efficiently supporting massive small-cell deployments. This involves new data and control plane technologies that are expected to radically transform the way optical networks are deployed, notably MB technology, pluggable-enabled packet-optical white box with open network operating system, coherent point-to-multipoint technology, telemetry-driven and AI-empowered domain-less control plane, Li-Fi small-cells seamlessly integrated with (B)5G access. B5G-OPEN will bring about a remarkable impact and new business models related to (*i*) LiFi- access points fully integrated in the transport and control architecture; (*ii*) new MB node and transmission technologies; (*iii*) open white box and SDN solutions supporting AI-empowered predictive control; and (iv) enabling high-capacity cost-efficient passive optical networks (PON)
KPIs (DoA): This overall objective is addressed through all subsequent specific project objectives and KPIs, and is validated in two comprehensive demonstrations focusing on both infrastructure and user needs.

Obj.1 (O1) Project results

All subsequent specific project objectives and KPIs have been successfully achieved.

In this document, objectives and KPIs related to experimental validation are reported. For objectives and KPIs related to techno-economic validations, please refer to D5.3.

Obj. 2 (O2): Design and validation of an innovative optical transport infrastructure supporting MB connectivity and transparent network continuum from User Equipment to DC.
Description (DoA): B5G-OPEN will explore a wide range of transport solutions that will co-exist to provide a novel high-bandwidth and cost-effective infrastructure ranging from front/mid-haul to data-centre interconnection and metro/core. This objective drives R&D on: (*i*) MB technology beyond C+L, enabling spectrum usage of up to 53 THz, including MB transmission modelling with impairment assessment for differentiated transparency within and across network segments (X-haul, metro, core, inter-DC); (*ii*) Optical MB subsystems (*iii*) per-band filter-less solutions; (*iv*) Packet-opto white box supporting flexible pluggable coherent modules; (*v*) PtMP systems applied beyond access scope (e.g. metro), across network segments, and in MB; (*vi*) Techno-economic analysis of different disaggregated transport solutions.
KPIs (DoA): KPI 2.1: Reduction of total power consumption from 30% to 50% with respect to SoA architectures (e.g. H2020 METRO-HAUL results) and legacy solutions; KPI 2.2: CAPEX reduction above 50% in the end-to-end "domain-less" architecture relative to fixed-domain metro-access/regional/core segments; KPI 2.3: KPI Increase of 10x in-service bandwidth w.r.t. currently deployed C-band transport solutions.

Obj.2 (O2) Project results

All KPIs of this Objective have been successfully achieved. Reported in D5.3.

Obj. 3 (O3): Design of novel optical network devices for switching, amplification and transmission to enable B5G-OPEN solutions and demonstration.
Description (DoA): (*i*) Switching: Design and development of MB Optical Switching nodes and a MB filter-less add-drop stage. The innovative prototypes will operate at multiple bands, beyond the conventional C or C+L bands; (*ii*) Amplification: design and implementation of an optical amplification system to a wide bandwidth range beyond the currently used C-band. Control of the amplification system will minimize gain variations between channels and ensure a fast response to changes in the transmission system. This will enable an expansion of the optical bandwidth available for data transmission; (*iii*) Transmission: Upgrade a scalable and modular S-BVT capable of establishing high-capacity connections beyond the C and L bands. MB/multi-carrier technology will be adopted within the S-BVT to promote the system's flexibility/adaptability. S-BVT programmable interfaces/agents will be enhanced to ensure smooth integration with the control plane. Moreover, innovative pluggable modules for flexible PtP transmission (e.g. ZR+), pluggable PtMP DSCM transmission (e.g. XR), and pluggable PONs

(e.g. TiBIT) will be adopted within the packet-optical white box for flexible operations, studying their application within the B5G Architecture and their evolution for MB.
KPIs (DoA): KPI 3.1: MB Optical Switching Matrix with bandwidth covering S-, C-, L- and O-band, supporting multiband operation on 50-100 GHz-grid, reducing the overall switching time to < 1 ms, and enabling multiband reconfiguration with added flexibility (dynamicity) in order to improve effective and agile usage of the traffic pipes. The modularity of the architecture will help to scale the node capacity to 3 Pb/s in a pay as it grows approach. Moreover, photonic integrated technology improves the power consumption by 4×... KPI 3.2: MB filter-less add-drop stage with bandwidth covering at least S-, C-, L- and O-band, supporting flexible MB operation based on passive components and thus negligible power consumption. KPI 3.3: MB amplification with cumulative gain bandwidth of at least three times the bandwidth of SoA EDFAs, sufficient gain flatness to allow four transmission spans without gain equalization, and gain control response time in the millisecond range. KPI 3.4: MB transceivers: Increase the capacity of SoA transceivers up to 2× - 4× by exploiting multiple transmission bands while enabling appropriate slice/band selection according to the network path. Pluggable solutions fully integrated within the white box enabling the removal of stand-alone network elements (e.g. xPonders, OLTs, etc.) to reduce footprint.

Obj.3 (O3) Project results

All KPIs of this Objective have been successfully achieved.

KPI 3.1

In section 3.7 of D3.3, some node architectures are presented as possible solutions to obtain a multiband node capable of switching signals belonging to many bands combining also many parallel fibers (or many cores of a multi core fiber) on the same topological degree. Even though these architectures are not yet commercially available, they are made of mature components (band filters, space cross connect S-OXC, WSS operating in a single o double/multi band) and can be easily obtained in near future. Each degree of such switches is capable of carry up to a few hundred of Tb/s and a node with some node degrees (greater than four) reach easily Pb/s overall switching capacity. SOA have been demonstrated the switching time ~10 ns which have been included in D3.3. Concerning the achievement of power saving in the optical switching matrix (a factor x4 is required), the solution focuses on lowering power consumption of the WSSs, the most demanding power component of the switch (excluding the amplifiers). The 90-channels SOA based WSS power consumption will reduce from 405W to 49W by applying photonics integration technology.

[Sou24] Andrè Souza et al., “Node Architectures for High-Capacity Multi-band Over Space Division Multiplexed (MBoSDM) Optical Networks”, invited paper at ICTON 2024, Bari (Italy), July 12-14 2024

KPI 3.2

HHI has designed, assembled, and experimentally evaluated a MB filter-less node prototype with add-drop stage covering S-, C-, L-bands. The design is based on extending a commercial matrix switch with passive band splitters instead of active components. The passive nature of the MB switching aspect results in negligible power consumption. The baseline of comparison of this prototype during the proposal preparation was switching capability covering C-band only. As a means to measure the KPI, we decided on device characterization including measurements of insertion loss, PDL and band of operation as well as practical analysis of full-band switching capabilities within multiband WDM systems. The full details of the design are reported in D3.2.

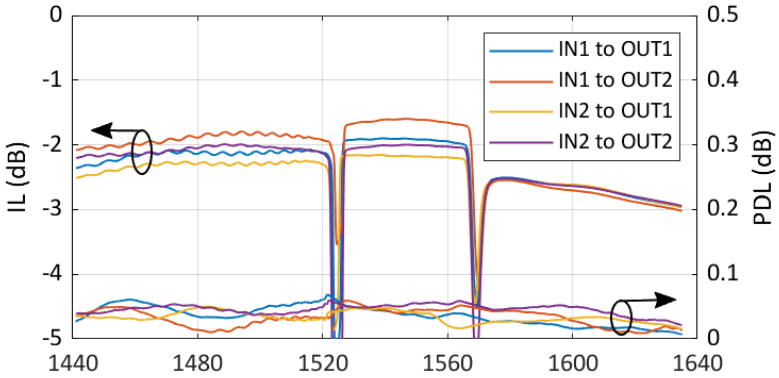

Figure 3-1: Insertion Loss (IL) with respect to wavelength

Table 03: Prototype specifications

Parameter	Specification
Operation Bands	S-band: 1460-1522 nm C-band: 1527-1565 nm L-band: 1574-1640 nm
Insertion Loss	< 3.0 dB
PDL	< 0.1 dB

The prototype was also integrated in the final demo of the project in which different functionalities (e.g., band switching, adding and dropping a band) have been experimentally validated. The validation was achieved in an SDN controlled fashion due to its provided programmability and north bound interface.

KPI 3.3

Tilt control is an important control mechanism for maintaining transmission performance in meshed networks with varying number of transmitted channels. The main task is to compensate for the power exchange among channels occurring during propagation in the transmission fiber. For multiband transmission, existing solutions need to be extended.

In single-band systems, the impact of stimulated Raman scattering (SRS) on system performance is reduced by setting a pre-tilt in the gain profile of the amplifier in front of the respective span while keeping the average amplifier gain at a constant level. However, multiband systems require to adjust both, gain and tilt of the band-specific amplifiers. Dropping or adding of

channels typically requires to increase the gain of some amplifiers, whereas the gain of other amplifiers needs to be reduced. In contrast, all amplifiers are set to the same tilt. For this adjustment, each amplifier needs to be aware of the power levels at the input of all optical amplifiers operated in parallel. Therefore, concepts for fast transmission of control data between different amplifier cards have been conceived. In view of this KPI, an experimental setup demonstrating combined gain and tilt control has been realized.

The amplifiers used in parallel cover in total a bandwidth of 150 nm. However, the used band combiners require band gaps of 5 nm and 7 nm, respectively, between the bands. Thus, the effective bandwidth amounts to 138 nm, which corresponds to almost four times the bandwidth offered by state-of-the-art C-band EDFAs supporting a bandwidth of around 35 nm. Performance data obtained with the amplifiers embedded into the setup indicate suitability for data transmission over 4 spans. A response time in the millisecond range has been measured.

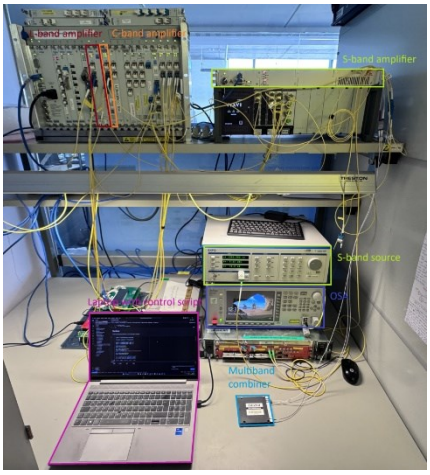

Figure 3-2: Experimental setup for demonstrating tilt and gain control in a multiband scenario

[Rapp23-01] L. Rapp, “Amplification in Multiband Systems: Challenges and Solutions”, Europ. Conf. on Opt. Commun., Glasgow, paper Tu.A.6.4, 2023

[Rapp24-01] L. Rapp, “Amplifiers in Multi–Band Scenarios — Output Power Requirements, Control and Performance Characteristics”, Journ. Lightw. Technol., pp. 1991 – 1999, 2024

[Rapp24-02] L. Rapp, “Challenges for Multiband Optical Amplification and Solutions Therefore”, Journ. Lightw. Technol., pp. 4202 – 4212, 2024

KPI 3.4

A programmable MB S-BVT prototype has been successfully implemented and experimentally validated in B5G-OPEN enabling full-reconfigurability, sliceability and scalability following a pay-as-you grow approach. C+L transmission has been demonstrated considering different paths of the network/testbed while extending achieved overall capacity and available spectral resources/bandwidth. The work has performed in the framework of WP3 and reported in several scientific publications [Nad23, Nad24]. Pluggable solutions have been successfully integrated within the IPoWDM white box enabling the removal of stand-alone network elements (e.g.

xPonders, OLTs, etc.). In B5G-OPEN, we designed and implemented both *single* and *dual* solutions, enabling the effective control of pluggable transceivers equipped within IP nodes. An experimental testbed, comprising an IPoWDM node running an extended version of the open-source SONiC network operating system has been deployed to validate these solutions, with a comprehensive analysis of the time required to provision and recover a real traffic flow that spans both the packet and optical domains. The work, reported in WP4 deliverables, has been also published in several scientific publications, including:

[Gio23] A Giorgetti, D Scano, A Sgambelluri, F Paolucci, E Riccardi, R Morro, P Castoldi, and F. Cugini, "Enabling hierarchical control of coherent pluggable transceivers in SONiC packet–optical nodes", Journal of Optical Communications and Networking 15 (3), 163-173, 2023

[Sga24] A. Sgambelluri, D. Scano, R. Morro, F. Cugini, J. Ortiz, J. M. Martinez, E. Riccardi, P. Castoldi, P. Pavon, A. Giorgetti, "Failure recovery in the MANTRA architecture with an IPoWDM SONiC node and 400ZR/ZR+ pluggables", Journal of Optical Communications and Networking, Vol. 16, Is. 5, Pages B26-B34, 2024

[Nad23] L. Nadal, R. Casellas, J. M. Fàbrega, F. J. Vílchez, and M. Svaluto Moreolo, "Capacity scaling in metro-regional aggregation networks: the multiband S-BVT," J. Opt. Commun. Netw. 15, F13-F21 (2023).

[Nad24] L. Nadal, M. Svaluto Moreolo, J. M. Fàbrega, F. J. Vílchez and R. Casellas, "Enabling Capacity Scaling in Metro Networks with Multi Band Sliceable Transceiver Architectures", Photonics West, SPIE, Jan. 2024, San Francisco.

Obj. 4 (O4): Design and validation of next-generation optical access & X-haul for B5G applications enabling massive cost-efficient 5G and Li-Fi small cell deployment.
Description (DoA): Design and validate a novel MB optical access and X-haul infrastructure (both cost-effective data plane and scalable control) enabling massive small cell deployments based on: (*i*) MB (> 4 optical bands); (*ii*) heterogeneous PtP and PtMP services; (*iii*) power-efficient pluggable-based multi-technology (TDM PON, DSCM-based coherent transceivers) over low-cost bare metal switches; and (*iv*) The X-haul infrastructure will enable the deployment of a massive WDM channel fixed-line connectivity, with technology-agnostic hybrid connectivity schemes in the last-drop, and supporting QoS-guaranteed services over both 5G and innovative Li-Fi access.
KPIs (DoA): KPI 4.1: 50% CAPEX reduction in the X-haul infrastructure compared to NG-PON2, by leveraging on open disaggregated solutions over MB, pluggable technology, and avoiding stand-alone OLT/SBT; KPI 4.2: 100x offered capacity increase of fixed-line systems compared to NG-PON2 by leveraging on standardized cost-effective 100GHz channel spacing technology and pay-as-you-grow strategy for MB; KPI 4.3: 50% energy reduction in small cell deployments as of today, by leveraging on power efficient Li-Fi small-cells and AI-based throughput optimization algorithms; KPI 4.4: LiFi handover: QoS-guaranteed handover with minimum throughput higher than 50% of the capacity by predicting the mobility and anticipating flow rerouting and parallel

delivery to adjacent APs. In case of blockage of the line-of-sight link, the auto-reconnection time < 2× blockage period.

Obj.4 (O4) Project results

All KPIs of this Objective have been successfully achieved.

KPI 4.1

Reported in D5.3

KPI 4.2

100x offered capacity increase of fixed-line systems compared to NG-PON2 has been demonstrated relying on multiple Point-to-MultiPoint OpenXR interfaces, each operating at 400Gb/s, which can be deployed with 100GHz channel spacing technology following a pay-as-you-grow strategy. In the Demo performed at BT Lab, one XR at 400G was used in the aggregation network. In particular, a "Filter-less Metro-Access Network" demonstrator was built at BT labs using two XR-Systems (each at a different wavelength) and two XGS-PON systems straddling a metro and access network through OADMs allowing the optical bypassing of an access node. The OADMs were filter-less and used SOAs and passive optical splitters. One of the XR systems was configured as a 400G P2MP connection and the second XR as a 100G PtP system that was used to connect to a Mobile network through both the metro and access network segments. The XR PtP 100G system coexisted in the same access fibre infrastructure as the residential XGS-PON system. This is further described in Section 5. The demonstration showed a metro network segment with a capacity of 500Gbit/s and an access network with a capacity of 110Gbit/s with 100Gbit connected between a mobile site in the access network and a metro network node optically bypassing the access node and sharing the access infrastructure.

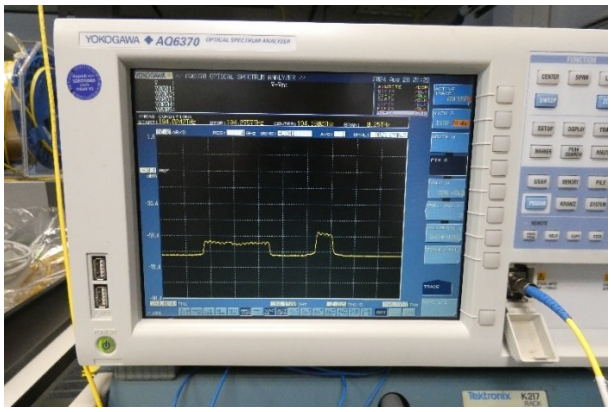

Figure 3-2: Captured spectrum traces showing the two XR systems in the downstream (P2MP left trace and PtP right trace) in the metro section of the network.

KPI 4.3

The KPI has been realised and the power consumption measurements indicate a significant reduction compared to traditional small cell technologies.

The energy-intensive nature of 5G small cells is primarily due to their need to support high data rates and dense user populations. Femtocells, typically used for indoor coverage, consume 10-30 W per cell for scenarios like residential or small business environments.

By adopting LiFi technology, we achieved KPI 4.3, targeting a 50% reduction in energy consumption in small cell deployments. This achievement is supported by the following power measurements:

> The LiFi Access Point (AP) demonstrated a power consumption of only 3.64 W. user device USB dongle used **1.405 W**.

Figure 3-3: Measured power consumption: (a) LiFi AP; (b) User dongle.

These power consumption values are substantially lower compared to traditional femtocells, which typically consume 10-30 W per cell. The inherent efficiency of LiFi, combined with the reuse of existing lighting infrastructure, contributes to significant energy savings, making LiFi a sustainable and energy-efficient alternative for indoor coverage scenarios.

KPI 4.4:

The LiFi system has successfully demonstrated QoS guaranteed handover capabilities, maintaining throughput above 50% of the maximum capacity during mobility and achieving rapid recovery in case of signal blockage.

Specifically, for a setup with throughput of 37 Mbps (both downlink and uplink, where 43 Mbps is the device capability), we observed minimum throughput values of 28.4 Mbps (downlink) and 26.6 Mbps (uplink) at a user movement speed of 1 m/s. Furthermore, auto-reconnection times for interrupted links were achieved as follows: less than 1 second for link interruptions of up to 5 seconds, and less than 2 seconds for link interruptions lasting up to 1 minute.

Table4: Auto-reconnection time

Link interruption duration (s)	Auto-reconnection time (s)
2	< 1
5	< 1
10	< 2
30	< 2
60	< 2

The reduced coverage overlaps in LiFi compared to traditional 5G deployments necessitates frequent handovers but also results in more precise and localized communication. This characteristic, coupled with LiFi's lower power consumption and enhanced indoor security, positions it as an effective alternative to RF-based solutions, particularly in controlled indoor environments requiring stringent energy efficiency and security.

Obj. 5 (O5): Development of an end-to-end monitoring platform covering the optical MB transmission, switching and the packet layer.
Description (DoA): Design and implementation of massive monitoring of the key physical layer performance parameters of transmission and the network elements. To this end, this objective will: (*i*) Establish new monitoring methods to monitor physical layer transmission parameters (e.g. chromatic dispersion, OSNR) and device behaviour (e.g., temperature, current) agnostic to waveforms, form factors, frequency bands, and vendors. (*ii*) Minimize the cost and economic impact of the physical layer monitoring methods using HW-accelerated performance/impairment models, low-cost devices, and AI-algorithm; (*iii*) Develop drivers/agents monitoring features to interface with MB switching elements and white boxes; (*iv*) Develop an e2e platform gathering and processing monitoring information to extract additional information such as hidden physical parameters and statistics (e.g. mean, standard deviation); and (*v*) Adapt the data acquisition rate to specific monitoring objectives.
KPIs (DoA): KPI 5.1: 10x more physical monitored data than what is today available in the field; KPI 5.2: 20% OPEX reduction (in combination with O8 and ZTN) by minimizing the power consumption impact of this massive new monitoring platform; KPI 5.3: Accurate measurements over different bands, e.g. < 1.5 dB uncertainty of OSNR measurements.

Obj.5 (O5) Project results

All KPIs of this Objective have been successfully achieved.

KPI 5.1

A distributed telemetry platform has been proposed, implemented, and tested, with agents receiving and analysing data before sending to a centralized manager. Intelligent data aggregation on optical constellations telemetry largely reduces data rate without introducing significant error. In particular, intelligent data aggregation covers several techniques including: i) data compression using autoencoders; ii) supervised feature extraction by means of using

Gaussian mixture models; and iii) data summarization by means of statistics. Thanks to that reference telemetry architecture fuelled with such sophisticated data processing engines, processing 1 order of magnitude more monitoring data that current centralized monitoring platforms without extending the capacity of data communication infrastructure is achieved.

Next figure presents the telemetry data rate when the telemetry period ranges from 1s to 1min for gRPC messages with: i) samples X using scalar values; ii) Z vectors with the latent space encoded as json objects; and iii) features F encoded as json objects. The inset summarizes the size of every object. Assuming a maximum data rate for telemetry collection of 9600 b/s (e.g., for a typical serial interface), the minimum telemetry period for optical constellations would be 14.5s. With such period, the telemetry data rate reduces one order of magnitude to only hundreds of b/s.

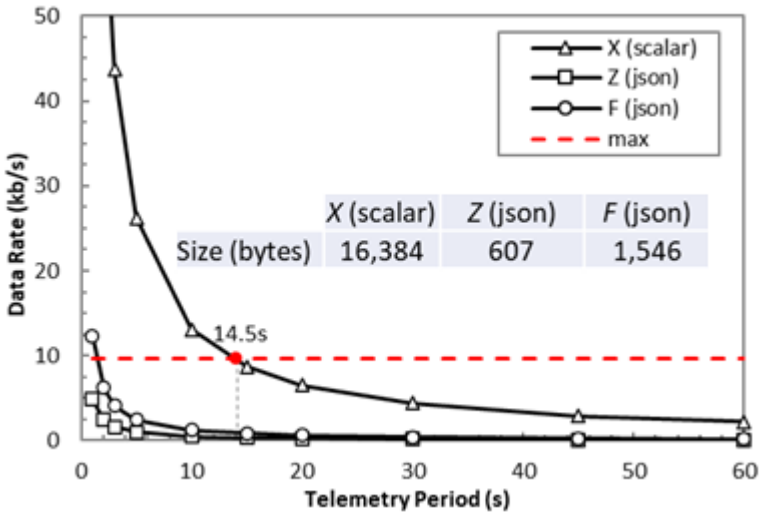

Figure 3-4: Telemetry data for different time perios

Details about the methods and performance evaluation results can be found in [Ve23], as well as in deliverable D5.3.

[Ve23] L. Velasco, P. González, and M. Ruiz, "An Intelligent Optical Telemetry Architecture," in Proc. OFC, 2023.

KPI 5.2

The distributed telemetry platform proposed in this project enables scalable dynamic optical capacity management in point-to-multipoint connections, which leads to remarkable energy consumption reduction. In particular, dynamic optical capacity management based on local monitoring allows accurate and efficient allocation of optical subcarriers according to actual traffic needs, which in multipoint-to-point connections open the opportunity to effectively explore oversubscription. Such dynamic operation leaded to remarkable benefits in terms of capacity utilization, as well as in OPEX savings, since an average energy consumption reduction around 20% was achieved for several traffic scenarios.

As an example of energy consumption in a configuration with 4Txs, the number of subcarriers (SC) in use and the power savings compared to the static method are presented in the next

figure. We observe that power savings are around 20% on average under two extreme traffic scenarios.

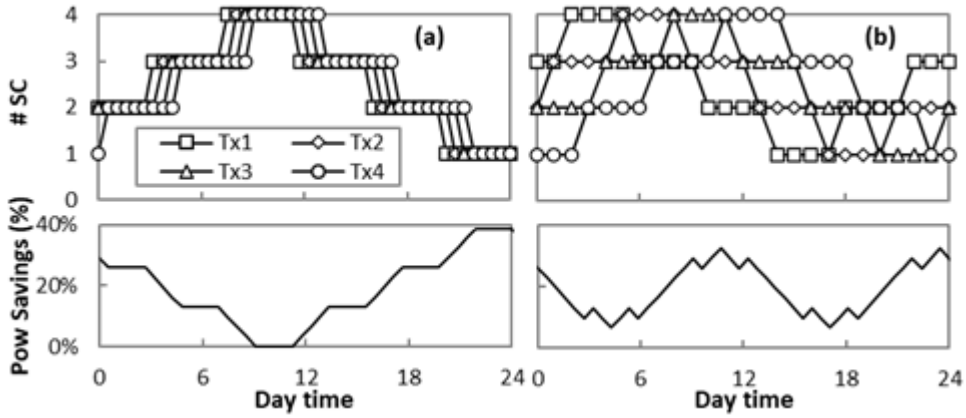

Figure 3-5: Power consumption saving.

Details about the methods, traffic scenarios, and performance evaluation results can be found in [Sh22], as well as in deliverable D5.3.

[Sh22] H. Shakespear-Miles, M. Ruiz, A. Napoli, and L. Velasco, "Dynamic Subcarrier Allocation for Multipoint-to-Point Optical Connectivity," in Proc. PSC, 2022.

KPI 5.3

A key monitoring technique that attracted numerous research works in the past couple of years is longitudinal power profile monitoring. It has been firstly introduced to estimate and localize a power loss in a lightpath by simply relying on the coherent transponder with no need to deploy extra hardware. It is a very accurate estimation technique. For instance, we designed and implemented a C+L experiment for which we estimated the launch power at each span input. We superposed our estimations with OSA traces in the figure below. The average estimation error of 0.04 dB for span #1 up to 0.76 dB for span #4.

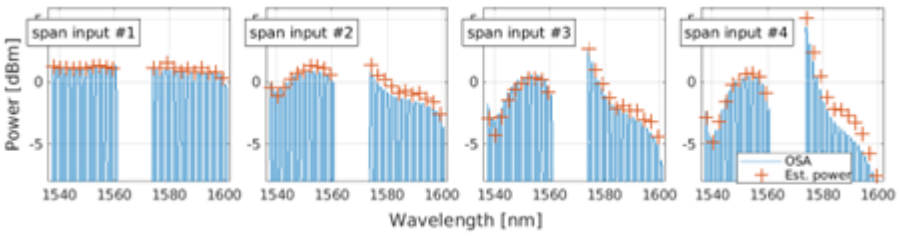

Span input	average (dB)
#1	0.04
#2	0.51
#3	0.40
#4	0.76

The performance and new capabilities of this revolutionary monitoring technique from B5G-OPEN project have been reported in many scientific publications and in the different deliverables (D3.1, D3.2 and D3.3). We also investigated the accuracy in terms of root mean square error (RMSE) for different transmission setups ranging from 400km to 2500km distance with different modulation formats. We showed in [May24] that the estimation error is lower than 0.5dB for a distance up to 2500km with QPSK modulation format. As the modulation format increases this error can even be reduced to 0.2dB.

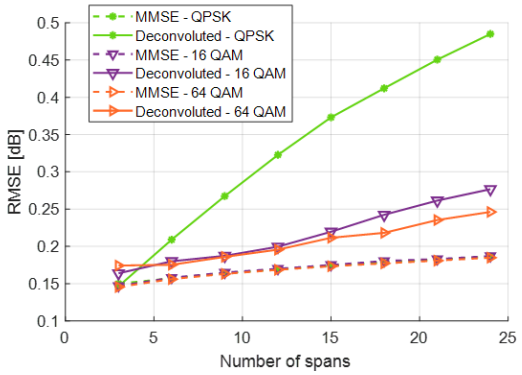

This monitoring technique has also been demonstrated at ECOC 2024 conference.

[May24] A. May, F. Boitier, A. Ore Remigio, P. Layec, "On the Accuracy of Power Profile Estimation using MMSE or Deconvoluted Correlation-Based Profiles," in Proc. OFC, 2024

Obj. 6 (O6): Design, implementation and validation of an operating system for the novel network elements.
Description (DoA): Design and development of a NOS (Node Operating System) which combines P4 packet switching and forwarding with flexible optical transmission. The NOS will adapt and extend existing initiatives like Telecom Infra Project (TIP) or SONIC and implement the required interfaces towards the service orchestration and infrastructure control system and node local control loops.
KPIs (DoA): KPI 6.1: Flow adaptation/control/monitoring capabilities in the millisecond time scale, enabled by AI prediction and wire-speed P4 operations with no SDN Controller intervention; KPI 6.2: Service Provisioning. Multi-vendor operations through fully specified models and APIs, enabling seamless support of optical adaptation functionalities within the packet-optical white box; KPI 6.3: 50% CAPEX reduction by avoiding node solutions designed specifically for the telecom market while leveraging and enhancing white boxes designed for the much wider computing market.

Obj.6 (O6) Project results

All KPIs of this Objective have been successfully achieved.

KPI 6.1

Flow adaptation/control/monitoring capabilities in the ms time scale have been successfully validated. In B5G-OPEN, the adoption of IPoWDM white box supporting both coherent pluggable modules and P4-based network programmability has been explored considering a remote vehicle control application (RVCA) with low-latency requirements. An innovative Function as a Service (FaaS) deployment has been designed and implemented to dynamically perform traffic steering between different edge nodes based on their actual CPU load. When one of its edge

nodes reaches overload, a telemetry packet is generated and processed by the intermediate IPoWDM node, which successfully reacts in the ms time scale rerouting the flow towards an alternative edge node, with no SDN Controller intervention. The FaaS application, specifically adapted to handle stateless behaviour, successfully operated without observable latency increase. The work has been published in [Pel23]. This work also determined an invited talk at ECOC 2024 Conf.

[Pel23] I. Pelle, F. Paolucci, B. Sonkoly, F. Cugini, "P4-based Hitless FaaS Load Balancer for Packet-Optical Network Edge Continuum", OFC 2023

KPI 6.2

The KPI on service provisioning, considering multi-vendor operations within the packet-optical white box, has been successfully achieved (see WP4 deliverables). Multi-vendor operations have been performed at two distinct levels. The first level applies between the SDN Controller and the IPoWDM box. In B5G-OPEN, by leveraging specifically designed OpenConfig-based SDN Drivers/Agents it was possible to control IPoWDM boxes from different vendors including EdgeCore, Juniper, and Cisco. The second level applies within the IPoWDM box, being able to control coherent pluggable modules manufactured by different Vendors, including Neophotonics/Lumentum, Acacia/Cisco, and Ciena. The collaborative work in [Mor24] successfully validates both levels in a complex field trial of IPoWDM optical continuum between access, horseshoe aggregation, and metro mesh networks also operating over multiple bands.

In Section 3 (Autonomous Service Provisioning and Self-Healing in Multi-Band Multi-Domain IPoWDM Networks for Live Video Traffic), from the perspective of B5G-ONP as the IPoWDM orchestrator, we validated successful operate with the following key components:

- The IP SDN controller based on OpenConfig that manages two EdgeCores.
- Two TAPI optical controllers from different vendors.
- PON Controller information to control the coherent pluggables modules.
- The Telemetry Platform, which provided reconfiguration alerts to trigger autonomous service adjustments.

[Mor24] R. Morro, E. Riccardi, A. Chiado' Piat, A. Pagano, A. Giorgetti, E. Kosmatos, S. Xia, H. Freire Santana, N. Calabretta, P. Gonzalez, L. Velasco, A. Sgambelluri, P. Pavon-Marino, E. Fernandez, J. Ortiz, A. Stavdas, C. Matrakidis, F. Cugini, L. Nadal, R. Casellas, O. Gonzales De Dios, "Field Trial of Transparent Multi-band Multi-domain Disaggregated IPoWDM Networks", ECOC 2024

KPI 6.3

Reported in D5.3.

Obj. 7 (O7): Design, implementation and validation of the service orchestration and infrastructure control system.
Description (DoA): Design, development and validation of a generalized orchestration and control plane system for the B5G-OPEN MB infrastructure, able to deploy and manage the lifecycle of services. The system shall enable the provisioning of operational and user-driven services. It will rely on microservice-based lightweight virtualization approaches, such as containers, uni-kernels and serverless approaches. The system shall have support for a generalized form of slicing and multi-tenancy.
KPI 7.1: High level service provisioning (e.g. interconnected cloud native functions and containers) relying on low level service setup performed in the sub-second time scale (data connectivity services, leveraging on the MB fully integrated packet-optical infrastructure and supported predictive capabilities); KPI 7.2: Reduction on the average setup time of connectivity service by 30% compared to serialized provisioning, exploiting approaches relying on parallelism and concurrency; KPI 7.3: 10x number of controlled devices, based on advanced SDN deployments with microservice-based lightweight virtualization and hierarchical arrangements and device / node abstraction; KPI 7.4: 10x rate of e2e provisioning supported services (e.g. number of requests per hour) leveraging on telemetry-empowered SDN Controller communication across multiple domains of visibility and cluster-based deployments for load sharing between controllers.

Obj.7 (O7) Project results

All KPIs of this Objective have been successfully achieved.

KPI 7.1

The KPI on high level service provisioning has been addressed under the common framework of WP4 and WP5, and validated and reported in the post-deadline paper submitted to OFC24 [Mor24]. The baseline numbers measured in average are: i) for optical OLS path provision in domain 1, 0.289 s; ii) in domain 2, 0.338 s; iii) while the total IP config time was of 4.1 s on each node; this makes a total end-to-end multi-domain and multi-layer service provisioning time of 8.579 s in the sequential approach, and 4.1s in the parallel approach. This numbers also validate the KPI 7.2, giving a mean reduction of 30% in the parallel experiment.

In the figure below (extracted from the HHI demo, reported in section 3), we demonstrated the provisioning of IPoWDM in a multidomain scenario. The metrics of this provisioning process are also validated by KPI 7.4.

Regarding the VNF provisioning associated to the service deployment, it was not covered in any joint demo, but we validated it in a standalone experiment using B5G-ONP, which applied deployments to Kubernetes clusters. As presented in section 4.1 the deployment took approximately 1 second, plus additional time to provision all the required computational resources. This standalone experiment could be applied on top of the IPoWDM provisioning demonstrated in the HHI and TIM demos, resulting in a high-level service that also includes the VNF provisioning subprocess.

KPI 7.2

This KPI on setup time of connectivity service comparing the serialized provision and the parallel approach has been addressed and validated in HHI demo. After 10 executions, we measured a general reduction of a 30% in the average setup time was reported comparing the parallel approach respect to the sequential one. Even in the case of topology context discovery, the parallel approach has a reduction of 30% compared with the sequential approach.

In the demo paper presented in [Mor24], the baseline metric for topology context with a sequential approach was 8.8 s. The parallel approach performs with a mean metric of 5.74 s, giving a reduction of 37% (see image below).

The gain of parallel approach is expected to be even higher with more domains.

Level	Timestamp	Message
Info	2024-03-20 16:51:01.303	Received a request to perform a multidomain topology discovery...
Info	2024-03-20 16:51:01.318	Start parallel discovery
Info	2024-03-20 16:51:01.321	Start optical domain 1 network discovery...
Info	2024-03-20 16:51:01.323	Start IP network discovery...
Info	2024-03-20 16:51:01.325	Start optical domain 2 network discovery...
Info	2024-03-20 16:51:02.411	End optical domain 2 network discovery (successful)
Info	2024-03-20 16:51:02.612	End optical domain 1 network discovery (sucessful)
Info	2024-03-20 16:51:07.058	End IP network discovery (successful)
Info	2024-03-20 16:51:07.060	Start inventory read and IP & optical layers correlation
Info	2024-03-20 16:51:07.077	End of inventory read and IP & optical layers correlation
Info	2024-03-20 16:51:07.080	End multidomain topology discovery

Figure. Parallel topology discovery extracted by PDP demo paper experiment.

KPI 7.3

KPI on 10-fold increase of number of controlled devices has been successfully achieved and described in D4.2 Sect. 6.5. The KPI baseline was set on the value demonstrated in the Metro-Haul project (tenths of controlled devices). The tests were performed on three simplified networks, representing real TIM DWDM network of different size. The first is a small size poorly meshed core network of only 16 nodes of which 15 are hubbed to a single Metro hub node. The second network includes both the core, made of only two hub nodes, and the aggregation in a single medium size meshed network (48 nodes, of which 2 are Core nodes and 46 are Aggregation nodes). The third network is the biggest core network among the TIM metro regional DWDM infrastructures with 107 nodes and 5 hub nodes and it constitutes the most challenging scenario among the Italian core networks for a network SDN controller. For example, here the ROADM with the highest nodal degree (9) employed in Italy can be found.

Table 5: Summary of the three networks

Network	Total Nodes	Metro Core Hub nodes	Aggregation nodes	Total Links	Core links	Extension links	Total devices	Total links	Total intents
Small	16	1	15	19	19	0	46	49	30
Medium	48	2	46	63	2	61	144	159	96
Large	107	5	102	163	163	0	331	383	224

The table summarizes the features of the three networks.

The first aspect that was analysed to assess the KPI was the loading of the networks (devices and links) into the controller.

Table 6: KPI values obtained on the three networks

Network	Total devices	Network setup time	Setup time per device
Small	46	16 s	0.35 s
Medium	144	44 s	0.31 s
Large	331	120 s	0.36 s

The table shows the values obtained on the three networks as the average value of three separate executions. The device loading times (about 350 ms) are pretty much independent from the number of devices in the network.

The second aspect that has been analysed is the ability to setup a set of connections that represent a realist pattern of the TIM network traffic demand.

Table 7: Results of the connection setups

Network	Intents setup time	Average #nodes per intent	Maximum #nodes per intent	Total time / # of intents
Small	45 s	5.53	7	1.5 s
Medium	180 s	6.12	11	1.875 s
Large	407 s	5.84	10	1.825 s

The above table reports the results for the three networks. Since the length of the intents (in terms of number of devices) is, on average, quite the same for the three networks, one might expect a difference in setup times between the networks to be due to network dimensions having an impact on path calculation times. However, this is not the case because the average intent setup time (last column of the table) shows a small difference only for the first network, while between the second and the third the difference is negligible, although the third is more than double the second (both in terms of devices and links),

The performed tests allow stating that the B5G-Open controller scales very well and is able to manage networks as wide as 331 devices and 383 links, supporting up to 224 connections.

KPI 7.4

This KPI was handled and partially achieved in [Mor24]. Total provisioning time of IP adjacency (including IPoWDM coherent pluggable set-up time): Non-parallel version: <10 seconds (360 per hour), parallel version <6 seconds (600 per hour). If domain was emulated, then number of provisioning per hour: 1000s.

From the HHI demo reported in section 3 using an example of end-to-end (E2E) service provision, we observe how the parallel configuration achieves a significant reduction in processing time, with a decrease from 10663 ms in sequential mode to 7099 ms in parallel mode. This represents a major improvement of 34%.

Obj. 8 (O8): Build a framework for an AI-assisted autonomous and dynamic network supporting real-time operations and ZTN.
Description (DoA): Development of autonomous cognitive networking that entails closed-control-loop implementation collecting, analysing, making decisions, and acting on the network devices. Control-loops will be implemented at various levels, from device to network, which requires the development of a distributed knowledge and decision-making engine that massively relies on the use of monitoring data and on the application of AI/ML and other cyber physical

approaches: (*i*) Address ever-increasing traffic dynamicity, by selecting the appropriate transmission interface (dedicated or dynamic), and by making transmission, routing and repair (self-healing) decisions locally. Similarly, it will deal with the ever-increasing distribution of compute resources in the network by making provisioning, task placement and repair decisions locally; and (*ii*) Reduce operation overheads and minimize overprovisioning, simplify network and service operations, and address users' mobility and inter-layer issues.
KPIs (DoA): KPI 8.1: Speed of decision-making in the sub-second scale by placing the intelligence near the devices, applying advanced AI/ML techniques, accurate model training based on simulation tools, and knowledge sharing among controllers; KPI 8.2: Reduce overheads/overprovisioning by >20%, by proactively adapting the capacity to the demand; KPI 8.3: Reduce OPEX by >20%, by increasing autonomous operations and reducing manual intervention; KPI 8.4: Improve and guarantee service and network availability (> 6x9s availability will be reached by combining MB and PtMP with anticipated degradation detection and proactive decision making).

Obj.8 (O8) Project results

All KPIs of this Objective have been successfully achieved.

KPI 8.1

A comprehensive deep learning (DL)-based optical constellation analysis for in-operation lightpath modelling and power analysis has been proposed. This solution, that enables sub-second scale decision making is based on two main pillars. On the one hand, DL models propagating optical constellation features were trained in a sandbox domain for modelling optical components, such as optical links, nodes, and amplifiers. Then, a target lightpath can be modelled by concatenating specific DL models to reproduce the propagation of optical constellations from transmitter to receiver. On the other hand, two methods for feature extraction were proposed, based on gaussian mixture models and autoencoders (AE). By using those models at the node agent, real-time analysis of the received optical signal can be carried out. In particular, two lightpath analysis use cases has been considered (see figure below).

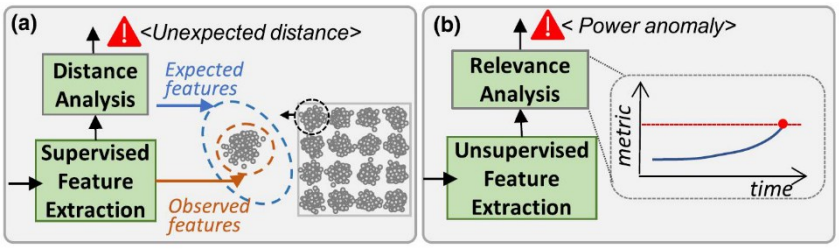

The first use case (labelled as a) is devoted to checking whether the real length of a given lightpath matches with the expected one. This analysis is based on the fact that both LI and NLI noise increase with path length and, additionally, both affect the magnitude and shape of the dispersion of the symbols around the expected constellation points. Therefore, differences can be found by comparing the features of the observed constellation points, extracted with

supervised techniques, and the expected ones. A model is used to detect any significant difference as well as to estimate the real length.

The second use case (labelled as b) explores a different approach to detect anomalies affecting the launch power at the Tx side. Instead of characterizing the gathered constellation through features with the distribution of the constellation points, this use case leverages AEs to compress constellation samples into a reduced set of latent space features in an unsupervised way. The analysis is performed in both forward and backward directions through the AEs to quantify relevance metrics at both the latent feature space and the input. This relevance can be tracked over time to detect any drift or shift directly related to a power anomaly (e.g., power drop) in the Tx.

Details of the comprehensive solution and results supporting the sub-second decision-making statement are provided in [Ru22]. Experimental validation of the distributed platform in support of intelligent decision-making has been assessed in [Go23]. The following capture real-time monitoring data analysis for decision making; in particular, for the use case of supervised analysis of optical constellation features for lightpath distance analysis and misconfiguration detection.

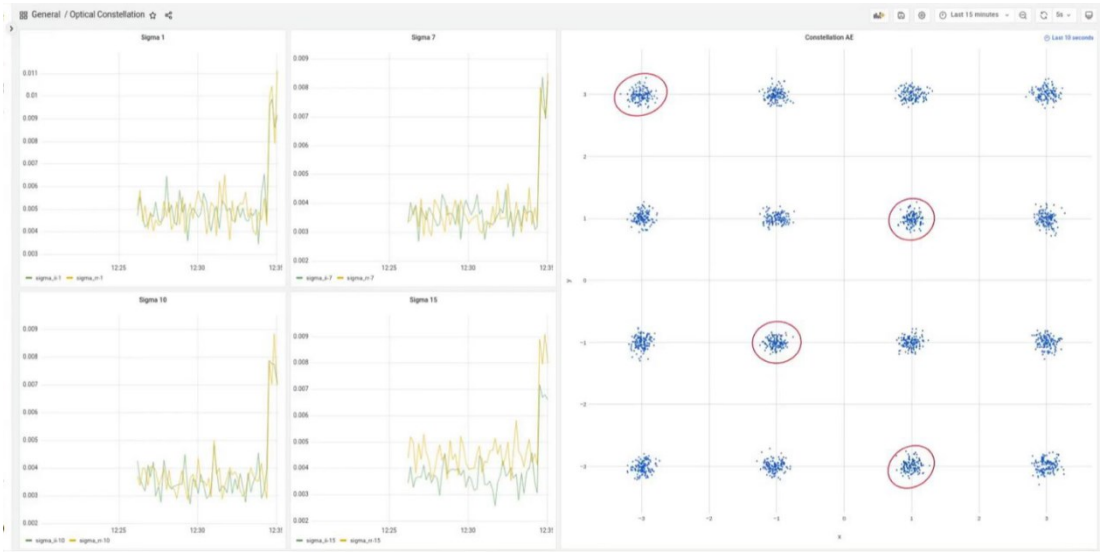

[Ru22] M. Ruiz, D. Sequeira, and L. Velasco, "Deep Learning -based Real-Time Analysis of Lightpath Optical Constellations [Invited]," IEEE/OPTICA Journal of Optical Communications and Networking (JOCN), vol. 14, pp. C70-C81, 2022.

[Go23] P. Gonzalez, R. Casellas, J-J Pedreno-Manresa, A. Autenrieth, F. Boitier, B. Shariati, J. Fischer, M. Ruiz, J. Comellas, and L. Velasco, "Distributed Architecture Supporting Intelligent Optical Measurement Aggregation and Streaming Event Telemetry," in Proc. Optical Fiber Communication Conference (OFC), 2023.

KPI 8.2

Reported in D5.3.

KPI 8.3

Reported in D5.3.

KPI 8.4

Reported in D5.3.

Obj. 9 (O9): Influence major vendors and service providers to adopt B5G-OPEN principles.
Description (DoA): Influence the telecommunications industry on the adoption of B5G OPEN concepts, design methodology, algorithms, and system/node/architectures by means of dissemination, standardization, and exploitation activities. This includes: (*i*) scientific dissemination in peer reviewed international conferences, journals, and magazines; (*ii*) contributions to SDOs and Open-Source Project; and (*iii*) actively contributing to and shaping 5G-PPP white papers, and co-organization of workshops and events within the 5GPPP

Reported in D6.3.

4 AUTONOMOUS SERVICE PROVISIONING AND SELF-HEALING IN MULTI-BAND MULTI-DOMAIN IPOWDM NETWORKS FOR LIVE VIDEO TRAFFIC

This section details the demonstration performed to validate the integration, automation, and real-time management of a multi-band, multi-domain IP over Wavelength Division Multiplexing (IPoWDM) network. The demonstration was aimed at showcasing the network's capability to autonomously provision services, handle live traffic under varying conditions, and implement robust self-healing mechanisms to maintain high performance and reliability.

4.1 DATA PLANE

The data plane architecture is designed to support seamless end-to-end traffic flow, starting from traffic generation at the access network and traversing through the multi-band domain (referred to as Domain 1) and the C-band domain (Domain 2), ultimately reaching the destination nodes. This comprehensive integration enables the network to dynamically manage and route traffic across different optical bands (S, C, and L), adjusting to real-time traffic demands and varying network conditions.

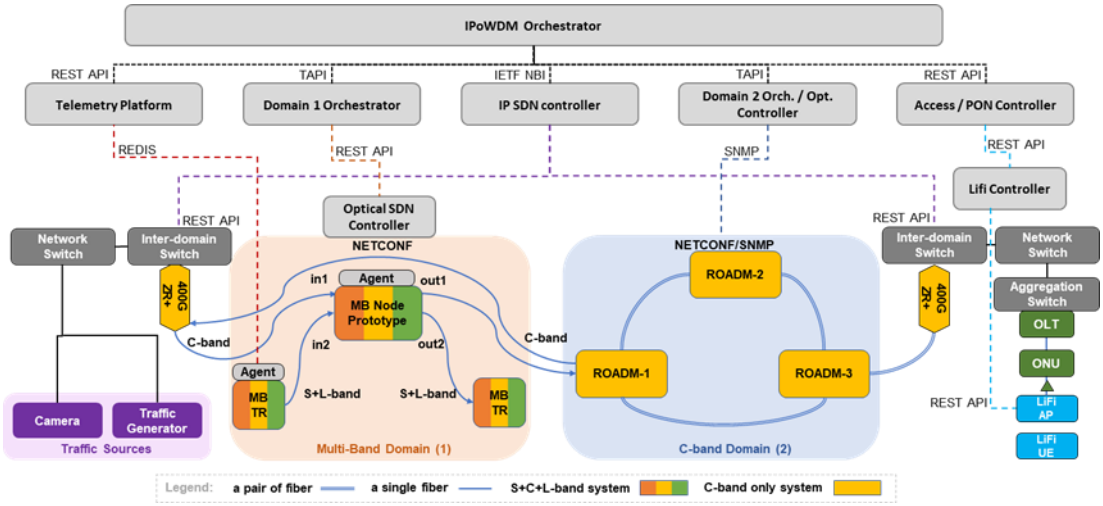

Figure 4-1: Architecture of the demo

A key innovation in this architecture is the SDN-controlled multi-band, semi-filterless add/drop node prototype, which is central to efficient traffic management across the S-, C-, and L-bands. In the C-band domain, a Reconfigurable Optical Add-Drop Multiplexer (ROADM)-based optical network with commercial components was utilized. This segment of the network is responsible for handling high-capacity traffic and is equipped to support dynamic wavelength routing, adapting efficiently to fluctuations in traffic patterns. At the network's edge, the access network handles live traffic, including high-bandwidth video streams sourced from cameras. This IP traffic is converted into optical signals using inter-domain switches, allowing for efficient transmission through the optical network. These devices, integrated with the control plane, facilitate real-time traffic adjustments and resource optimization, ensuring that service quality remains high even under dynamic network conditions.

MB-Node

A key innovation in this architecture is the SDN-controlled multi-band, semi-filterless add/drop node prototype. The MB node prototype enables selected bands bypass and add/drop capabilities for the S-, C- and L-bands. This cost-effective structure is composed of four multiband multiplexers (MB Mux and MB Demux) and an optical matrix switch responsible for routing the bands accordingly. Monitor couplers are also introduced at the input and output for effective monitoring of the ports during validation and operation of the prototype. The switch is fully programmable, allowing for remote operations between the multiple inputs and outputs

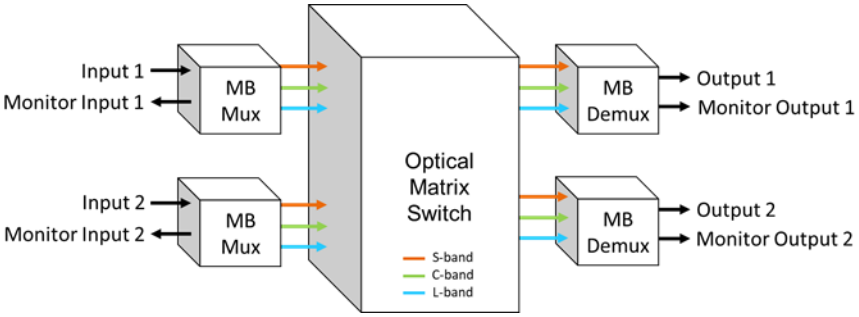

Figure 4-2: Architecture of MB node prototype.

After assembly, the prototype was characterized using a polarization-dependent loss analyzer (PDLA) to verify insertion loss (IL) and PDL of the multiple paths. The values are also presented in Table 3.1. where the specifications of the device are summarized.

Table 0-1: Prototype specifications

Parameter	**Specification**
Operation Bands	S-band: 1460-1522 nm C-band: 1527-1565 nm L-band: 1574-1640 nm
Insertion Loss	< 3.0 dB
PDL	< 0.1 dB

For the use case of this work, the MB node protype was integrated in a multiband (S+C+L) testbed environment, which is shown in Fig. 43. The figure depicts the mentioned setup in detail, the legend section details the diagram and components used as the S+C+L-band ASE source. Other significant components are the S+C+L-band amplifiers that are designed as single-band amplifiers operating in parallel with multiplexing/demultiplexing of the individual bands at the input and output of the block, each block provides a monitor port to allow for monitoring the power spectrum across the testbed. Through the 16x4 optical switch, the optical spectrum analyzer (OSA) can be connected to different monitoring points in order to keep track of what happens through the link. The monitoring points Nx throughout the setup are from each amplifying block, the ASE source, and the input and output ports of the node (except for input 2 monitor port is not used as it is already covered by monitoring point N8), the optical loop in the setup is used only as a through.

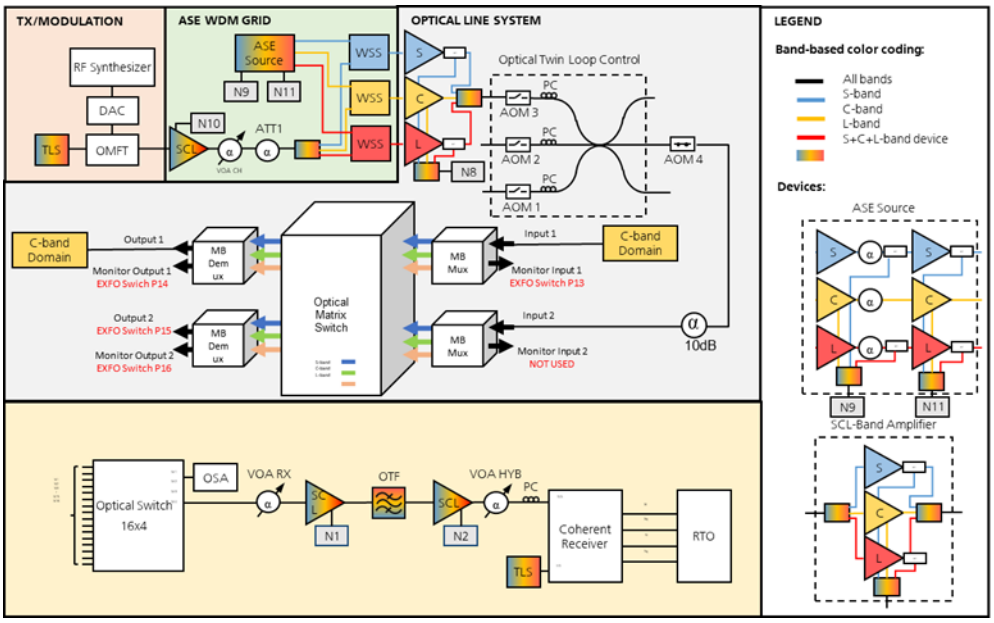

Figure 4-3: Experimental MB (S+C+L) setup integrating the node prototype

LiFi Access

The integration of LiFi technology within the demonstration highlights a key innovation in using light-based communication as a high-performance access technology. LiFi leverages the existing lighting infrastructure to provide reliable, high-speed, and low-latency data transmission, making it an energy-efficient alternative to traditional radio-based wireless access technologies. Its ability to seamlessly coexist with other network technologies, such as 5G and PON, allows for flexible integration in hybrid network environments. The use of LiFi introduces a non-interfering, secure, and high-capacity communication method that is particularly well-suited for environments requiring precise, localized connectivity, such as smart buildings and industrial networks.

In this demonstration, LiFi plays a critical role as part of the overall access network. A LiFi Access Point (AP) is integrated into the network architecture, which is designed to support seamless end-to-end traffic flow across multiple domains. The LiFi AP is the final access point before reaching the end-user device, providing the last-hop communication over light-based wireless technology. The user device in the demonstration is a laptop equipped with a LiFi USB dongle, which is responsible for receiving the LiFi signals from the AP. This setup allows for efficient data transmission between the network and the user device, ensuring low-latency, high-bandwidth communication in the final leg of the traffic flow.

The demo showcases a webcam application (Fig. 44) where LiFi is used as the access technology to establish the connection between the laptop and the network. In the setup (Fig. 45), the LiFi AP connects to the rest of the network, and the user device with the LiFi dongle receives the data, allowing the user to access the webcam feed via a web page on the device. The demo visually illustrates how LiFi can seamlessly integrate into a larger network architecture, supporting real-time, high-quality applications such as a webcam feed. The screenshot taken from a WebCam image demonstrates the low-latency and high-quality transmission made possible by the integration of LiFi into the data plane.

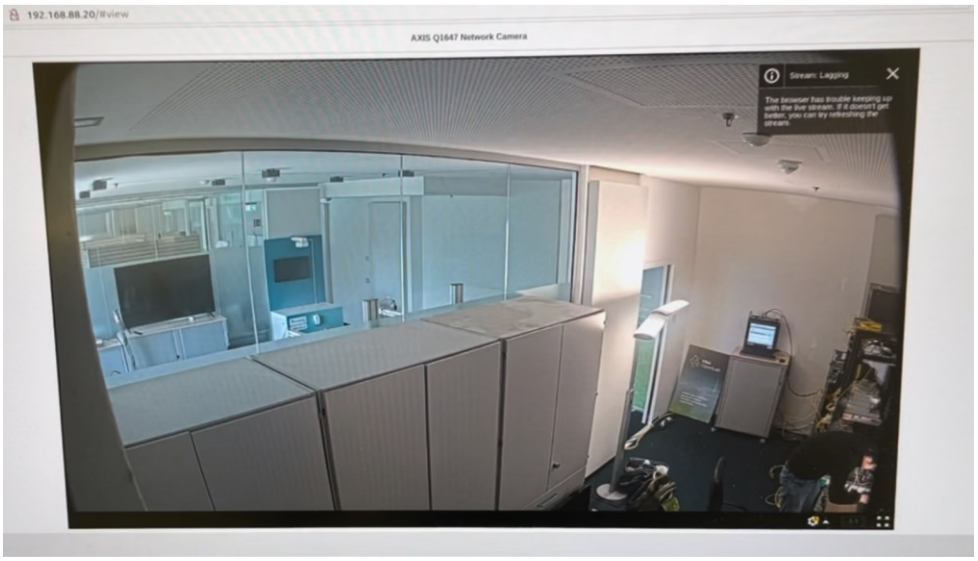

Figure 4-4: Screenshot of the Webcam application on the LiFi enabled user device.

Figure 4-5: the setup of LiFi over PON including (1) the Tibit OLT, (2) the ONU, (3) the LiFi AP, and (4) the LiFi USB dongle.

4.2 CONTROL PLANE

The control plane follows a hierarchical model that enables efficient management of the multi-band, multi-domain IPoWDM network, as depicted in Fig. 41. At the core of this architecture is the IPoWDM Orchestrator, playing the role of the B5G-ONP in this demonstration, which supervises both the IP and optical segments of the network. The orchestrator coordinates with domain-specific controllers using standardized interfaces, ensuring seamless operations across the access, metro, and core network layers. In Domain 1 (the multi-band optical domain), the Domain 1 Orchestrator handles communication with the optical SDN Controller, which is based on the ONOS open-source platform. The SDN Controller manages the SDN-enabled multi-band node prototype and its associated transceivers. It utilizes established protocols and data models, including NETCONF, OpenConfig, and OpenROADM, to execute network configurations. Additionally, custom SDN agents are responsible for key functions such as switching, add/drop operations, and optimizing performance across the optical S-, C-, and L-bands. The Domain 1 Orchestrator gathers topology information from the optical controller and relays it to the

IPoWDM Orchestrator through the Transport API (TAPI). In Domain 2 (the C-band optical domain), the Domain 2 Orchestrator assumes dual roles as both the domain's controller and orchestrator. It manages ROADMs and other optical elements using the Simple Network Management Protocol (SNMP) and YANG models over NETCONF. Communication between the Domain 2 Orchestrator and the IPoWDM Orchestrator is facilitated through an integrated TAPI driver using RESTCONF, providing seamless orchestration across this domain. The IP SDN Controller oversees the inter-domain switches positioned at the origin and destination nodes, ensuring that IP traffic is efficiently integrated with optical domain services for end-to-end traffic flow. By interfacing with the IPoWDM Orchestrator, the IP SDN Controller ensures dynamic traffic routing and optimal resource allocation in response to network conditions. At the network's edge, traffic management is handled by the Access/PON Controller and the LiFi Controller, which dynamically adjust resources to meet real-time demand. This ensures efficient utilization of resources at the edge, particularly for high-bandwidth applications like live video streaming. An integral part of the control plane is the Telemetry Platform, which enables real-time performance monitoring across the network. The telemetry data facilitates proactive network management, allowing the system to detect issues early and initiate self-healing processes. For instance, if traffic quality in the S-band degrades, the system can automatically reconfigure the network to shift traffic to a more stable L-band, maintaining service reliability and performance.

4.3 DEMONSTRATED SCENARIOS

To validate the integration of the control and data planes in the IPoWDM network, various provisioning scenarios were explored. These scenarios demonstrated how the network could autonomously manage connectivity services across different domains. The scenarios involved both parallel and sequential workflows and examined the network's self-healing capabilities in response to degraded performance

Parallel Provisioning

In the parallel provisioning scenario, the network orchestrates service provisioning across the multi-band domain (Domain 1), the C-band domain (Domain 2), and the IP domain simultaneously. This method is designed to significantly reduce setup time.

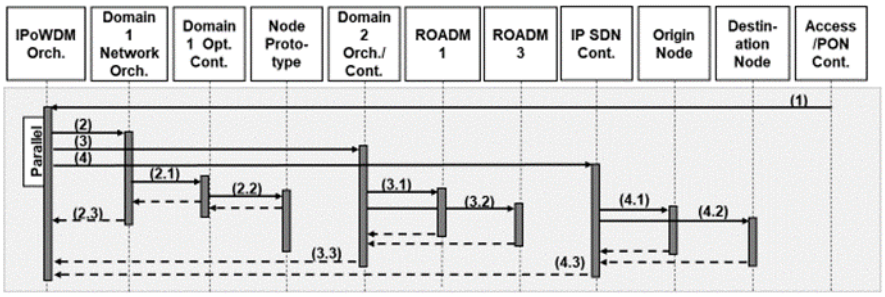

Figure 4-6: Parallel provisioning sequence diagram

As presented in Fig. 4-6, the process begins when the PON Controller detects an increase in traffic demand and notifies the IPoWDM Orchestrator. In response, the orchestrator updates traffic metrics and initiates provisioning across the domains:

- Domain 1 (Multi-band): The IPoWDM Orchestrator sends a request to the Domain 1 Orchestrator, which then communicates with the Optical SDN Controller to configure

the multi-band node prototype. The optical channel is routed through the node, from input port "in1" to output port "out1." This operation is executed through NETCONF commands based on the OpenROADM protocol.

- Domain 2 (C-band): Simultaneously, the IPoWDM Orchestrator directs the Domain 2 Orchestrator to establish an optical path across the ROADMs. This step involves configuring the ROADMs to connect nodes (e.g., ROADM-1 and ROADM-3) for smooth traffic flow.
- IP Domain: In parallel, the IP SDN Controller is instructed to establish IP adjacency between the origin and destination nodes, ensuring that the IP paths are ready to handle the traffic.

Once all these tasks are completed, the orchestrator adjusts traffic parameters to match the increased demand, finalizing the service. The parallel provisioning approach reduces setup time by more than 30% compared to sequential provisioning. However, this method introduces complexity in managing state and error handling due to the simultaneous configuration of multiple domains.

In the Fig. 4-7, we observe how the parallel configuration achieves a significant reduction in processing time, with a decrease from 10,663 ms in sequential mode to 7,099 ms in parallel mode. This represents a major improvement of 34%.

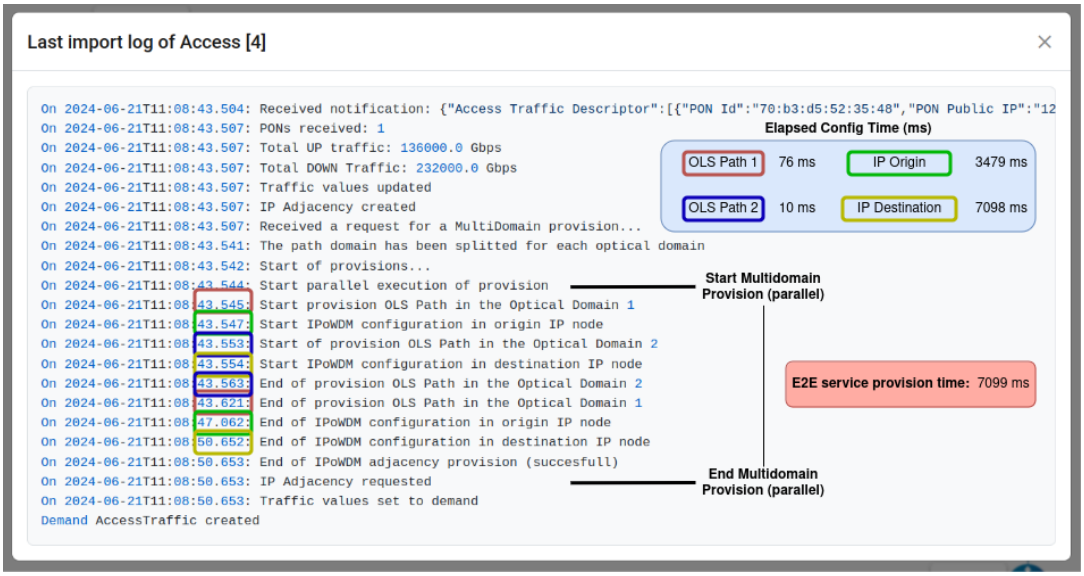

Figure 4-7: Log report of the demo. E2E service provision with parallel mode execution.

Additionally, the following Fig. 4-8 also represent how the IPoWDM represents the succesfully created IPoWDM provision, with the details of how is the optical path that is supporting the newly created IP link. Fig. 4-9 & 4-10 show the views of Domain 1 & 2 Controllers.

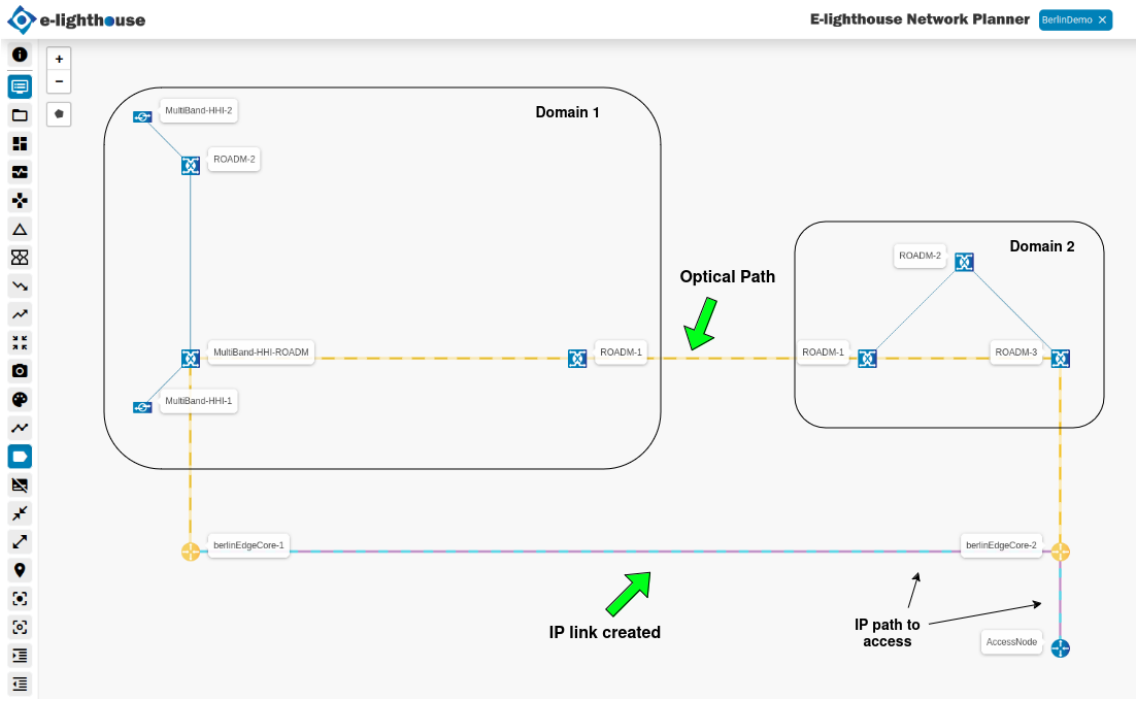

Figure 4-8: Visualization of optical path from the IPoWDM provision visualized by the IPoWDM orchestrator.

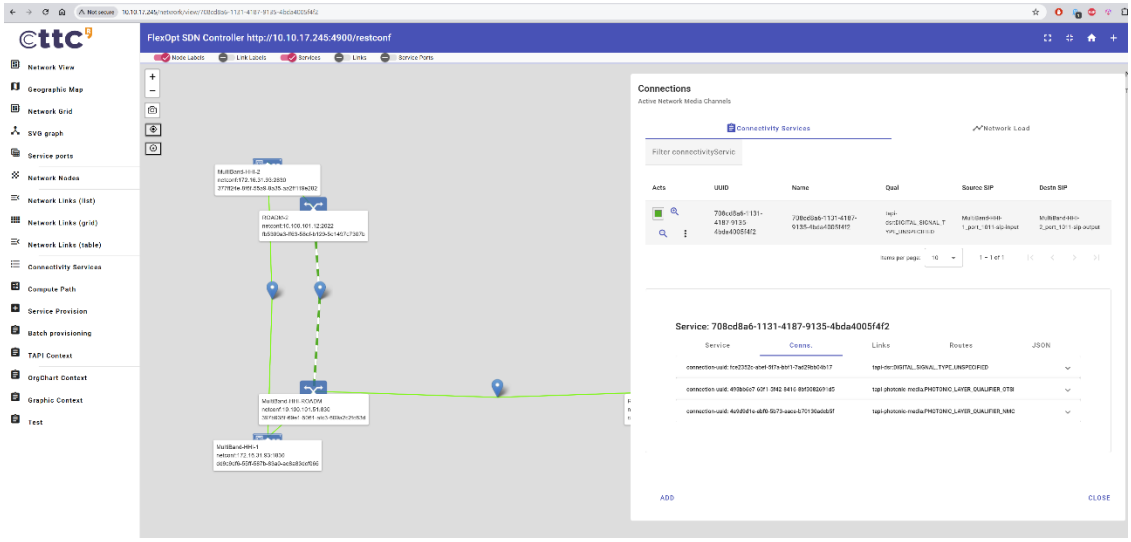

Figure 4-9: Screenshot of the Domain 1 network orchestrator (MB Domain).

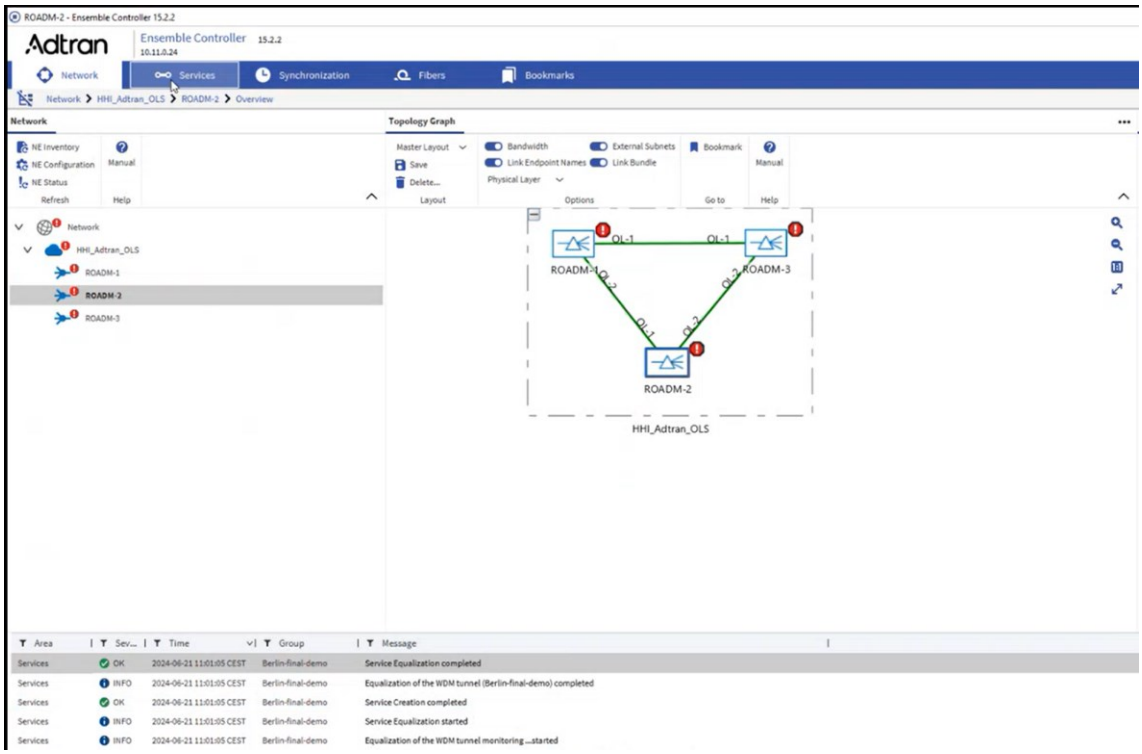

Figure 4-10: Screenshot of the Domain 2 controller (C-band domain optical line system controller).

Sequential Provisioning

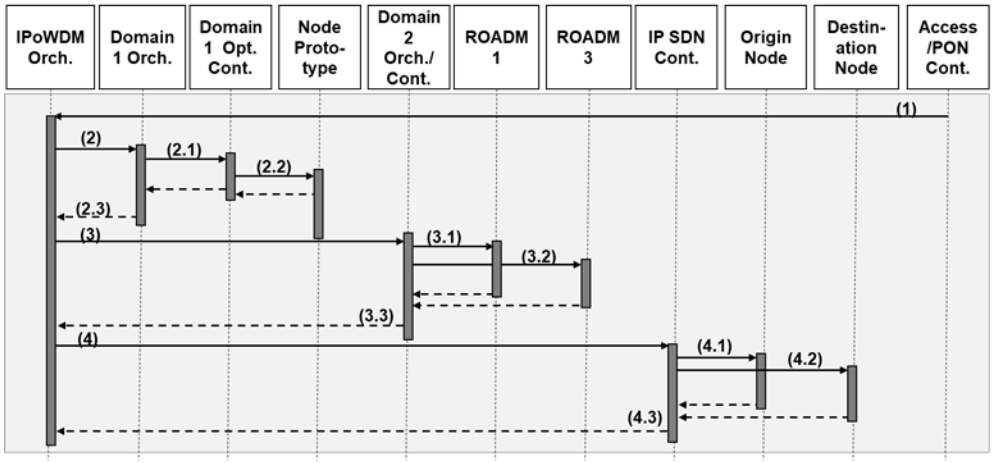

Figure 4-11: Sequential provisioning sequence diagram

In contrast to parallel provisioning, sequential provisioning involves configuring each domain one after the other. Although simpler to implement and manage, this approach takes more time to complete. Each domain — multi-band, C-band, and IP — is set up in sequence, starting from the access network and moving through the metro and core segments. While this method reduces the complexity of managing simultaneous operations, it lacks the efficiency and speed of parallel provisioning, making it less ideal for scenarios with urgent traffic demands or real-time applications.

Self-Healing

The self-healing scenario highlights the network's ability to adapt autonomously to performance degradation by migrating services to a more stable band.

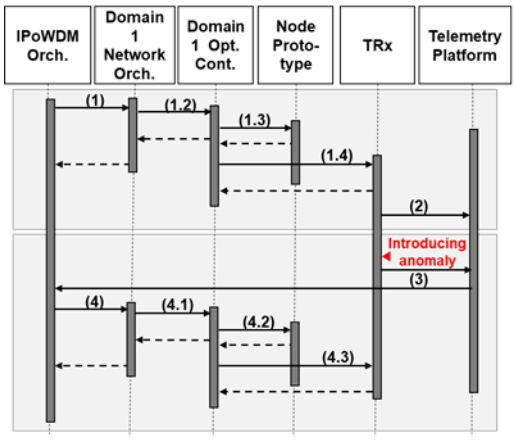

Figure 4-12: Self-Healing sequence diagram

The scenario begins with the IPoWDM Orchestrator provisioning a service over the S-band. The orchestrator configures the multi-band node to route the optical signal from input port "in2" to output port "out2," while the multi-band transceivers are set up with appropriate parameters such as frequency and output power. Throughout the process, the transceivers continuously push performance metrics — such as Bit Error Rate (BER), Signal-to-Noise Ratio (SNR), and Q-factor — to the telemetry platform's data lake for real-time monitoring.

To test the network's adaptive capabilities, an artificial anomaly is introduced using variable optical attenuators (VOAs), significantly degrading the S-band connection's performance. The telemetry platform detects these changes, showing a sharp decline in SNR, a rise in BER, and a drop in Q-factor. Upon recognizing the degradation, the telemetry platform sends an alert to the IPoWDM Orchestrator, recommending a migration to the L-band to restore service quality. In response, the orchestrator initiates a reconfiguration process. The multi-band node is instructed to drop the S-band connection and establish a new L-band connection. A new optical channel in the L-band is provisioned, with the appropriate frequency settings applied to ensure optimal performance. The Optical Spectrum Analyzer (OSA) confirms the successful migration by detecting the presence of the new L-band signal.

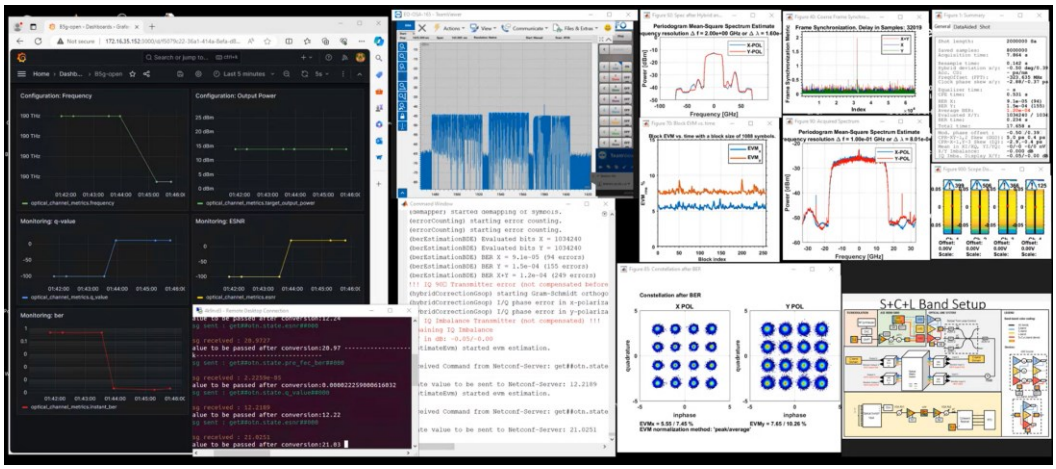

Figure 4-13: Dashboard of the MB domain setup in the lab

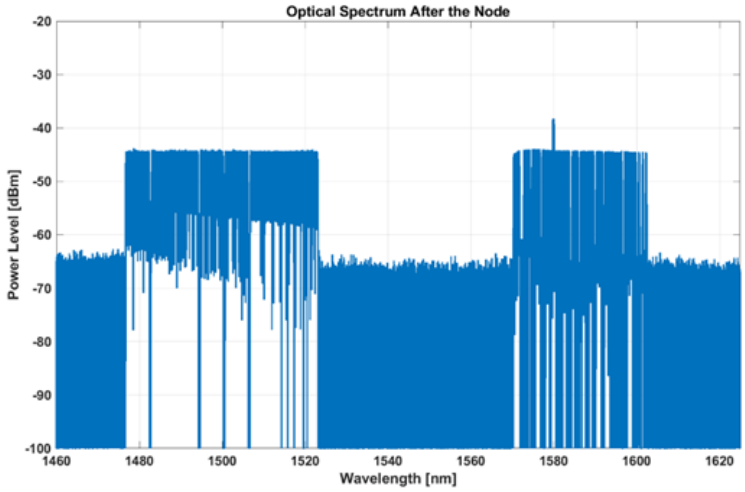

Figure 4-14: Spectrum after reconfiguration

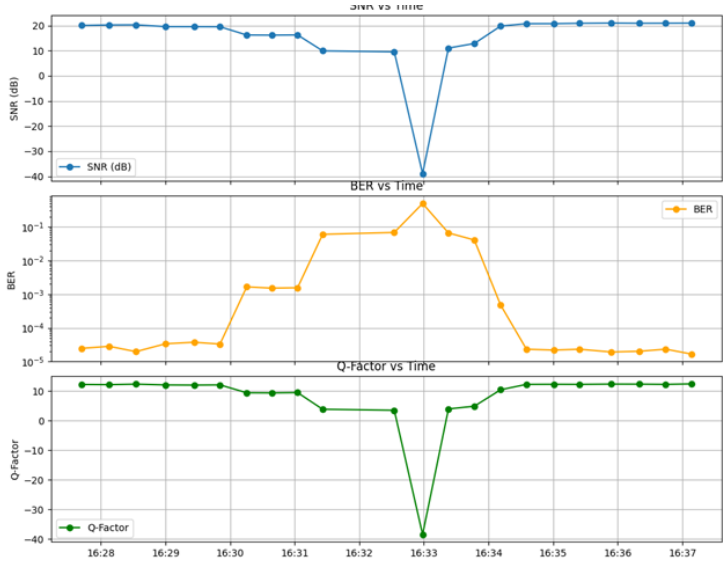

Figure 4-15: QoT Parameter Plots

From the IPoWDM Orchestrator's perspective, we measured an approximate elapsed time of 700 ms for the entire process. This time covers the receipt of the telemetry alert, the detection and processing of the performance degradation, and the handling of the connection migration to the new band or selected path. In Figure 4-16, the logging details from one of the experiment executions illustrate the flow and timing of this reconfiguration.

Figure 4-16: Capture of IPoWDM logs from a successful reconfiguration.

This scenario illustrates the network's autonomous self-healing capability, which allows it to manage Quality of Service (QoS) degradation proactively. By detecting issues and dynamically reconfiguring the optical connection, the network ensures continuous, reliable service even in the face of disruptions.

4.4 CONCLUSION

This project successfully demonstrated a fully integrated multi-band, multi-domain IPoWDM network, utilizing SDN-enabled prototype components and advanced optical pluggable transceivers. The system showcased its ability to autonomously provision services across multiple domains and optical bands, effectively managing dynamic traffic demands, such as live video streams. By employing parallel provisioning, the network significantly reduced setup times, proving its efficiency in high-demand scenarios. Additionally, the system's self-healing capability was highlighted through the automatic migration of services from a degraded S-band to a stable L-band, reinforcing its robustness and reliability. These results underscore the scalability of the IPoWDM architecture, making it a promising solution for high-capacity, low-latency network environments, essential for future network deployments.

5 Disaggregated and Transparent Multi-band Optical Continuum across Access, Horseshoe Aggregation, and Metro IPoWDM Networks

Multi-band optical networks allow to simultaneously attain higher capacity and richer node connectivity [Kra21, Bor21, Kos23, San22, Xin23, Put22]. In parallel, the introduction of IPoWDM technologies exploiting coherent pluggable transceivers is rapidly leading to effective convergence of the IP and photonic layers [Sca23].

Preliminary studies have shown the benefits of transparent traversal across network domains, exploiting dedicated analytical tools for end-to-end estimation of non-linear physical impairments, including multi-band operation [Kos23]. Indeed, the multi-band transparent interconnection between network segments has the potential to reduce the number of expensive and power-hungry opto-electronic conversions [Gio23]. However, no comprehensive validation has been demonstrated yet that integrates multi-band data and control planes. For example, the work in [Bor23] does include control and data plane, but limited to C-band only.

In B5G-OPEN, we propose, implement, and validate an innovative multi-band disaggregated optical network transparently interconnecting cell-site access in the O-band, an aggregation horseshoe operating with both C- and O-bands, and a C-band metro-core network. O-band extends transparently from local exchange in the access domain to include antenna sites to be front-hauled to one of the hub of the horseshoe. The C-band extends transparently from aggregation to metro avoiding electronic regeneration.

5.1 Demonstrated solution for access-metro multi-band optical continuum

Fig. 5.1 shows the traditional network architecture ranging from cell-site access to horseshoe aggregation and metro network. Traditionally, each segment is operated in C-band only and optically terminated at domain borders between access and aggregation and between aggregation and metro.

Fig. 5.2 shows the proposed data plane architecture of next generation Operator's access-metro networks. The cell-site access is operated in O-band, the horseshoe aggregation in both O- and C-bands, while the metro network works in C-band only. Optical bypass in the O-band is performed at Aggregation nodes and in the C-band at Hub nodes. That is, the O-band extends transparently from cell site access to one of the Hub of the horseshoe while the C-band extends transparently from aggregation to metro, avoiding electronic regeneration

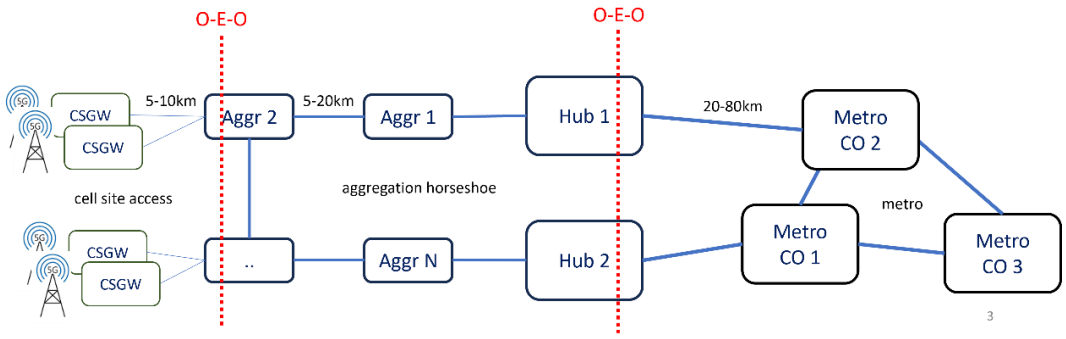

Figure 5.1:- Traditional network architecture ranging from cell-site access to horseshoe aggregation (up to 10 nodes) and metro network. Traditionally, each segment is operated in the C-band only and optically terminated at domain borders.

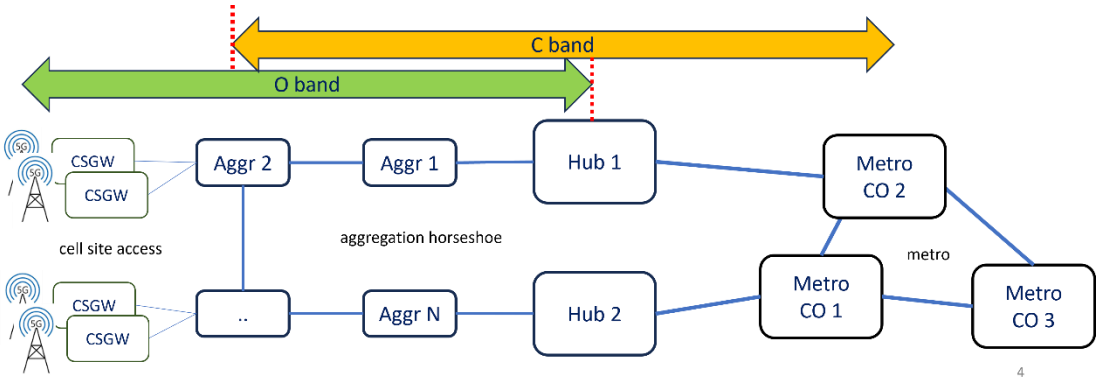

Figure 5.2: -Proposed multi-band network architecture: cell-site access operated in the O-band, horseshoe aggregation in both O- and C-bands, metro network in C-band. Optical bypass in O-band at Aggregation nodes and in C-band at Hub nodes.

The access domain consists of cell-site nodes connected to a horseshoe network including up to ten aggregation nodes (two in the experiment) with one Hub node at each end (*Hub 1* and *Hub 2*). The distance between adjacent aggregation nodes is in the range of 5 to 10 km, each serving an area of few kilometers for both broadband and 5G access. Each node operates in two optical bands, C and O. In each direction, each *Aggr* node includes (i) a pair of passive band splitter/couplers, (ii) a degree-two ROADM with Add/Drop module operating in the C-band and (iii) a prototype of SOA-based ROADM operating in the O-band (Fig. 5.3). The O-band OADM comprises two AWGs with an LWDM grid, two O-band SOAs, two 50:50 splitters for dropping and adding data channels and a microcontroller to control the OADM. The SOAs function as gates and amplifiers for dynamically blocking or passing each channel.

Each Hub node, for what concerns the aggregation segment, includes one band splitter/coupler and a degree-one ROADM in each band. Hub nodes also represent the entry point of the metro network, i.e. they include elements controlled by either the *Aggr* or the Metro SDN Controller (Fig 5.4).

The metro domain (Fig. 5.5) consists of a mesh network, where links are few tens of km long and nodes consist of multi-degree ROADMs in C band only.

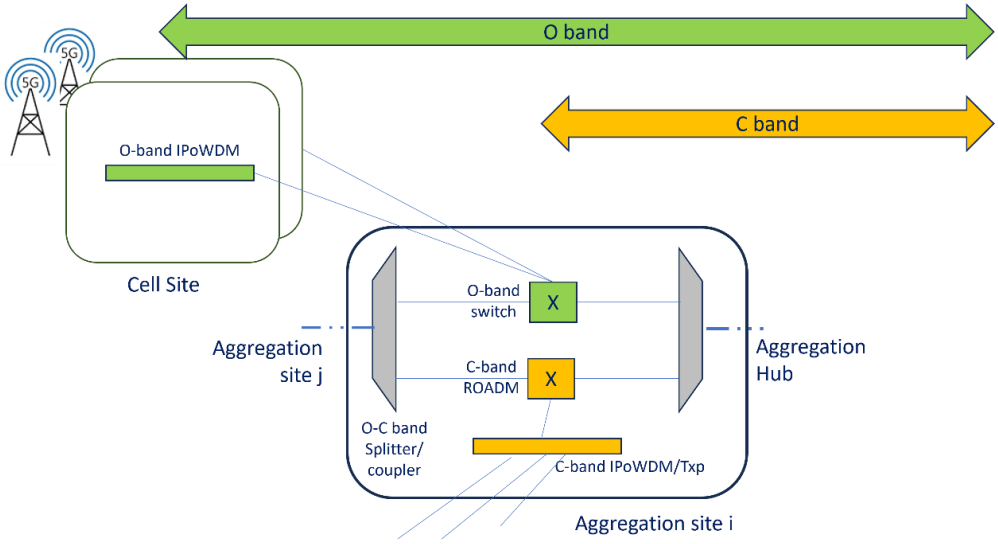

Figure 5.3:- Proposed multi-band network architecture in access and aggregation nodes.

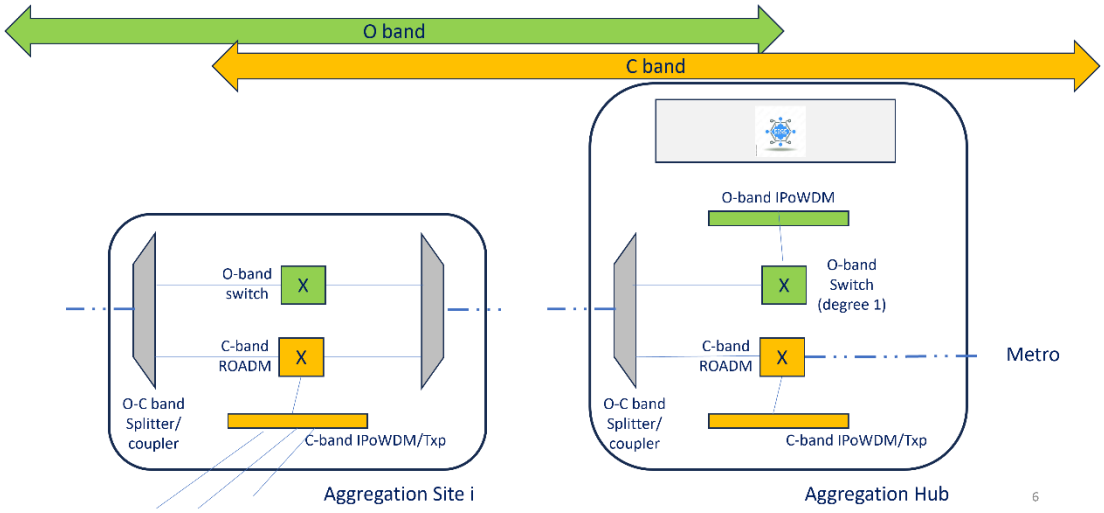

Figure 5.4:- Proposed multi-band network architecture in the aggregation horseshoe

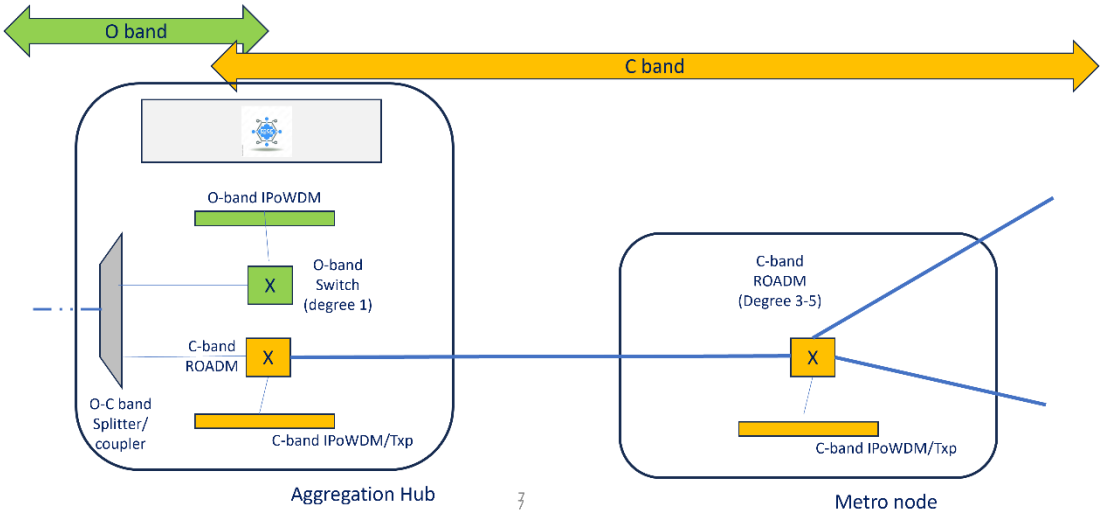

Figure 5.5:- Proposed multi-band network architecture in aggregation and metro nodes.

Fig. 5.6 shows the whole setup implemented in TIM labs in Turin. In this experiment, the aggregation horseshoe includes two hubs and two aggregation nodes while the metro segment encompasses an in-field metro-regional link of 80 km of fiber in the Turin area.

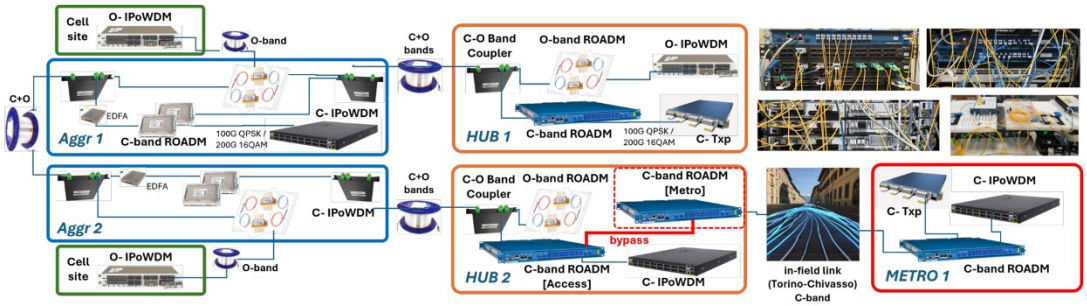

Figure 5.6: -Access-aggregation-metro network implemented at TIM Lab. The metro segment also encompasses a in-field link between the cities of Turin and Chivasso.

Transmission systems in the C-band include 100/200 Gb/s transponders and IPoWDM switches equipped with SONiC operating system and 400ZR(+) transceivers. In the O-band, LWDM 25G transceivers are adopted in Layer3 switches.

Traditionally, access and metro systems are managed as separate domains from both data and control plane perspective, with inefficient electronic termination at Hub central offices. In this work, optical bypass of the IPoWDM box at *Hub2* is implemented for a C-band channel, which transparently reaches remote metro sites. This way, the O-band serves traffic confined within the access and aggregation segments, while the C-band can also be used for high-speed connections transparently crossing the boundary between aggregation and metro.

5.2 DEMONSTRATED CONTROL SOLUTION

To support the proposed optical continuum, several control plane extensions have been designed and implemented.

Fig. 5.7 shows the proposed control plane architecture. In particular, the following control elements, specifically enhanced to manage both intra- and inter-domain IPoWDM connectivity across multiple bands/layers, are included:

A. *Per-domain Optical SDN Controller*.

The optical SDN controllers are based on ONOS, version 3.0.0. One controller is deployed for the aggregation domain and another controller is deployed for the metro segment. The controller has been further extended with respect to the one used in [Gio23]. Current version also supports: (i) devices operating on multiple bands; (ii) establishment of lightpaths using ROADMs ports as endpoints. The latter feature is required to support transparent multi-domain intents.

B. TAPI Network Orchestrator

The TAPI Network Orchestrator is based on CTTC FlexOpt SDN controller and is responsible for inter-working with the per-domain SDN controller. It retrieves topological information from such controller using the controllers' native interface, including devices, ports and per-band spectral information and exports a north bound interface based on standard TAPI data models to the inter-domain, hierarchical controller.

TAPI interfaces have been enhanced to support multi-band networking (multiple media channel pools for a single Optical Multiplex Session, each with its own frequency range) and to include Physical Layer Impairments (PLI).

C. Multi-domain IPoWDM network orchestrator

The Multi-domain IPoWDM network orchestrator is based on the E-lighthouse Network Planner (ENP) software. It interacts with the NBI of a prototype IP SDN controller (based on IETF model RFC 8345), the NBI of the TAPI Network Orchestrators providing access to both optical domains, and an external inventory database with interdomain links and pluggable-to-ROADM connections. It has been enhanced to correlate transparent multi-domain optical and IP layers providing a unified IPoWDM multilayer network view and control.

D. Optical PCE

The optical PCE receives a domainless optical infrastructure view from the IPoWDM orchestrator, and uses a routing engine to derive the optimal operational parameters regarding the intended maximum transparent length per band and the optical transmission technology. In detail, on request for a new connection establishment from IPoWDM orchestrator, it retrieves the optical network topology and configuration from the IPoWDM orchestrator and it executes a PLI-aware RSA computation in order to calculate the path, the selected band and the frequencies assignment. Then, PCE sends a response to IPoWDM orchestrator including the aforementioned information. In this work, simulated annealing is introduced to also estimate the end-to-end optimal launch power per channel/band.

E. Distributed Intelligent Module

Finally, a distributed intelligence module is used to collect and analyze measurements close to the data sources. Measurements are compared to the expected performance obtained using transmission models, so any degradation can be rapidly detected, and its root cause effectively localized [Go23]. In particular, specific transmission models have been developed for the different bands, thus improving the accuracy of the detection and localization.

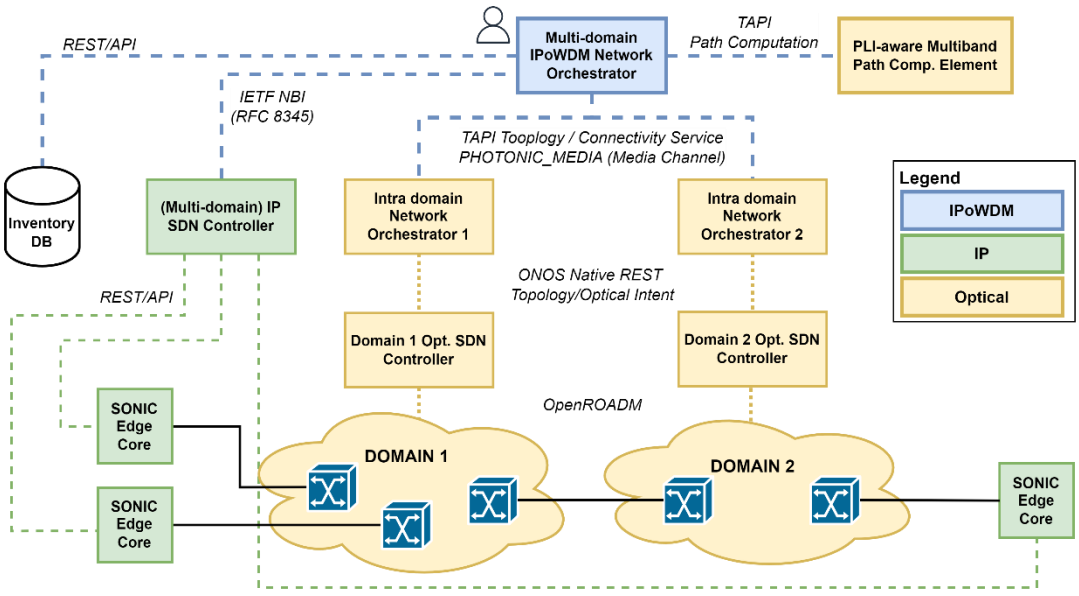

Figure 5.7-: Control plane architecture with B5G-OPEN implemented components

5.3 EXPERIMENTAL RESULTS

The experimental assessment of the multi-band access-metro continuum is validated through the setup of a number of connectivity services.

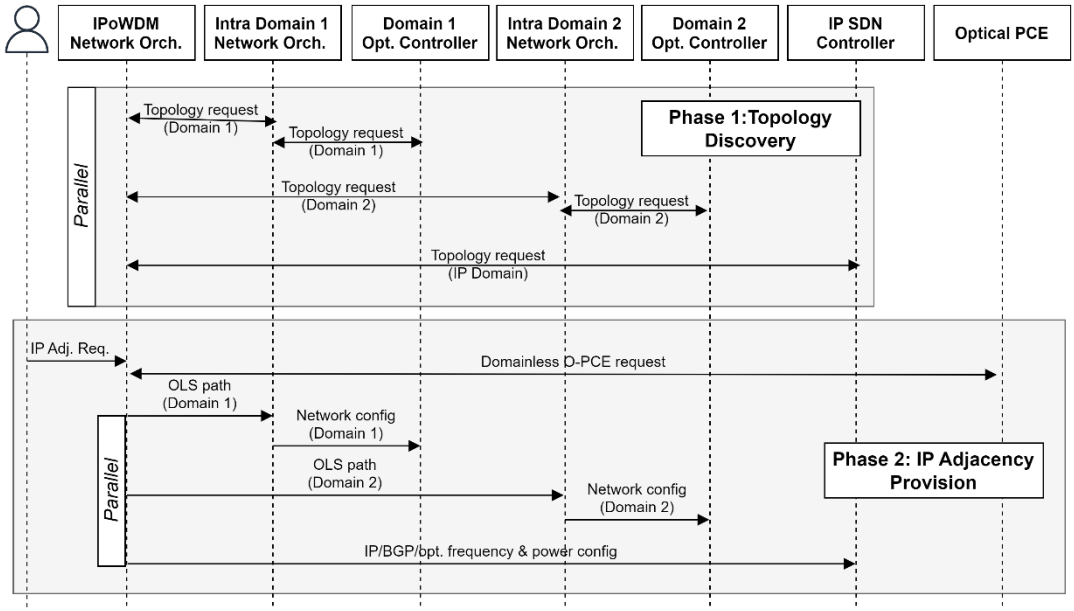

Figure 5.8-: Control plane workflow

Fig. 5.8 illustrates first the IPoWDM topology discovery and then the provision of a cross-domain IP adjacency. In the topology discovery phase, the IPoWDM orchestrator requests in parallel to the TAPI orchestrators and IP SDN controller the topology IP and optical information. The TAPI propagates this request towards the SDN controllers. In the cross-domain IP adjacency provision, (i) the user requests an IP adjacency, (ii) the IPoWDM orchestrator provides the PCE a unified (so-called domainless) optical view of both domains and requests the optical path, spectrum and power computations. For multi-domain optical paths, (iii-a) the IPoWDM provisions in parallel the respective intra-domain OLS paths, that place the intents in the Optical SDN controllers. In parallel, (iii-b) it configures the IP/BGP router aspects, as well as the pluggable frequency and transmission power via the SDN controller. This operation of the IP SDN controller corresponds to the Single SBI management proposal in the TIP MANTRA working group.

The provisioning procedure is successfully applied to six 100G channels among C-Tpx transponders in Aggr and Metro nodes (see OSA view n.1 in Fig. 5.9). Then, the two 400ZR channels among IPoWDM node are successfully established, transparently crossing aggregation-metro boundary (n.2 in Fig. 5.9). Finally, the O-band channels from Access to Hubs are established (n.3 and n.4 in Fig. 5.9).

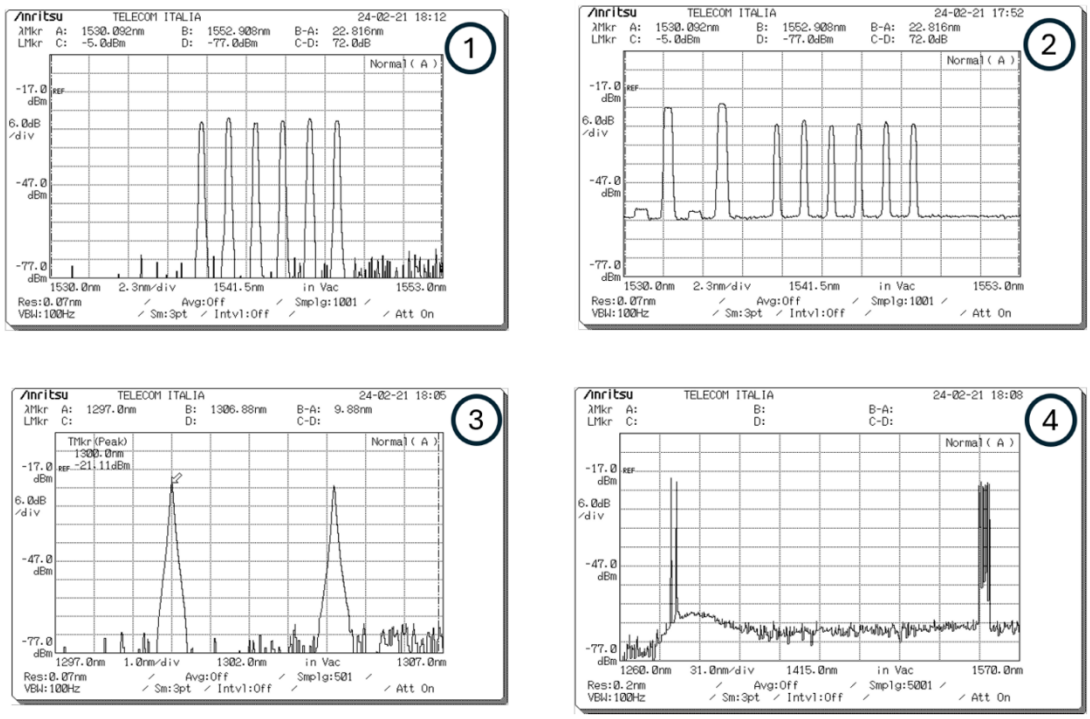

Figure 5.9-: Experimental results: optical spectra (1-4)

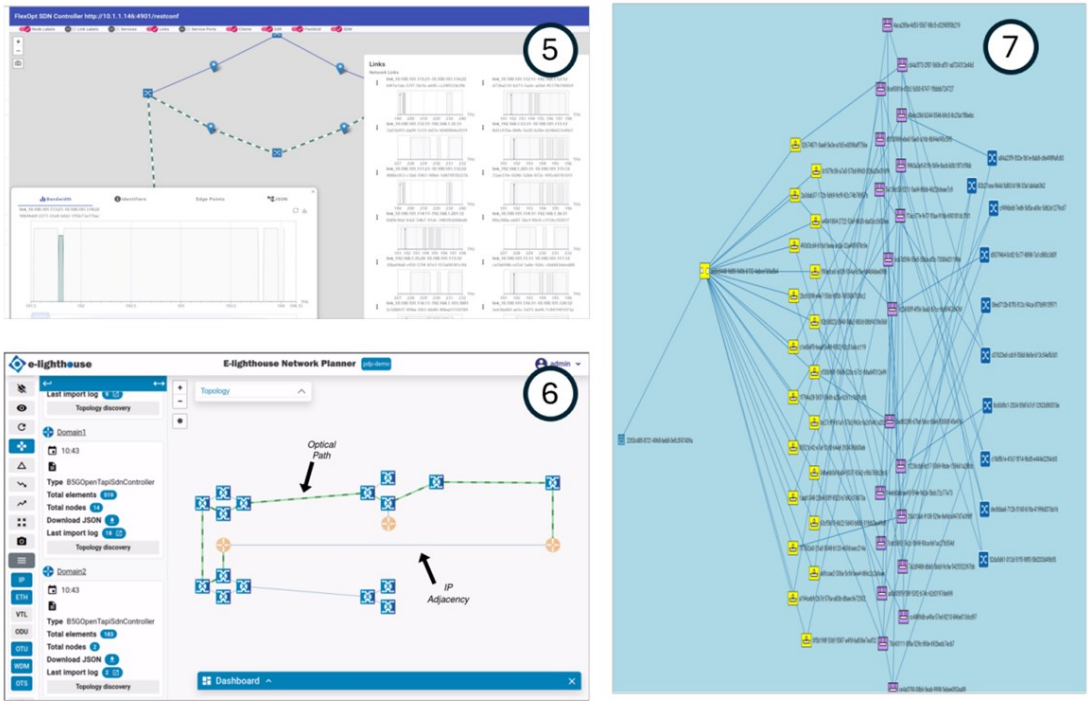

Figure 5:10:- Experimental results: orchestrators' views (5-7)

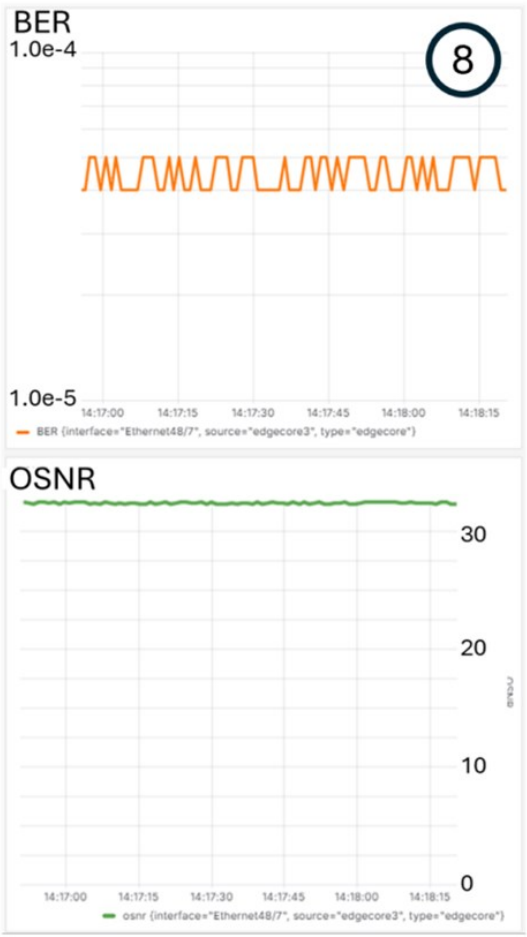

Figure- 5.11: Experimental results: monitoring data on 400ZR

Fig. 5.10 shows the experimental view experienced by the Network Orchestrator. In each domain, the optical path set-up provisioning time is less than 1 second. Moreover, PCE latency is measured to be in the range between 0.5s and 0.6s and it is due to: a) the time needed to retrieve network topology and; b) the time needed for the PLI-aware RSA algorithm to return the selected path, band, channel frequency assignment, and optimal launch powers. The IP/BGP and pluggable configuration requires less than 4 seconds.

From a data plane perspective, the loss of the O-band OADM is 11dB (including the multiband mux/demux). The 10 km fiber loss is 4dB between two Aggr Nodes, and the 5km fiber loss is 2dB from the Access to the Aggr Node. The input power of the data channels at the OADM is 0dBm. During bypass operation, SOA is ON and provides 17dB gain to compensate for the OADM and fiber loss transmission. In the drop operation, the SOA is OFF (no current) and blocks the wavelength. An ON/OFF ratio of 60 dB has been measured which guarantees high isolation and very low cross-talk for wavelength reuse of the added data at the same wavelength. The measured received optical power at the drop port was -15 dBm/ch, which allows error-free of the received Ethernet frames.

The 400ZR C band transceivers operate at around 3.6E-5 pre-FEC BER (Fig. 5.11). Ethernet 25G O-band services at cell sites were error free (overall latency of 60 and 114 us was measured in Aggr1 and Aggr.2 nodes respectively, in compliance with fronthaul requirements).

5.4 KUBERNETES ORCHESTRATION WITH B5G-ONP

In addition to the previous demonstration, within the context of this work we conducted parallel extra experiments focusing on Kubernetes orchestration within the B5G-ONP. These experiments extended beyond the earlier setup by evaluating key performance indicators (KPIs) related to the provisioning of services containing Virtual Network Functions (VNFs) within a Kubernetes environment.

To achieve this, we deployed a Kubernetes cluster to handle VNF instances. The cluster was configured to provision namespaces, services, and deployments under the management of B5G-ONP.

The initial phase of the demonstration begins with the setup of an IP topology, consistent with the configuration from the previous demo. Building upon this base, the experiment advances by integrating B5G-ONP functionalities. The first step introduces a cluster node into the topology, directly connected to edgecore-3. Subsequently, a Kubernetes controller is added to the topology, allowing the orchestration of resources within the cluster. With the controller in place, computational elements inside the Kubernetes cluster are discovered, identifying the available resources for further orchestration (see figure 5.12 below).

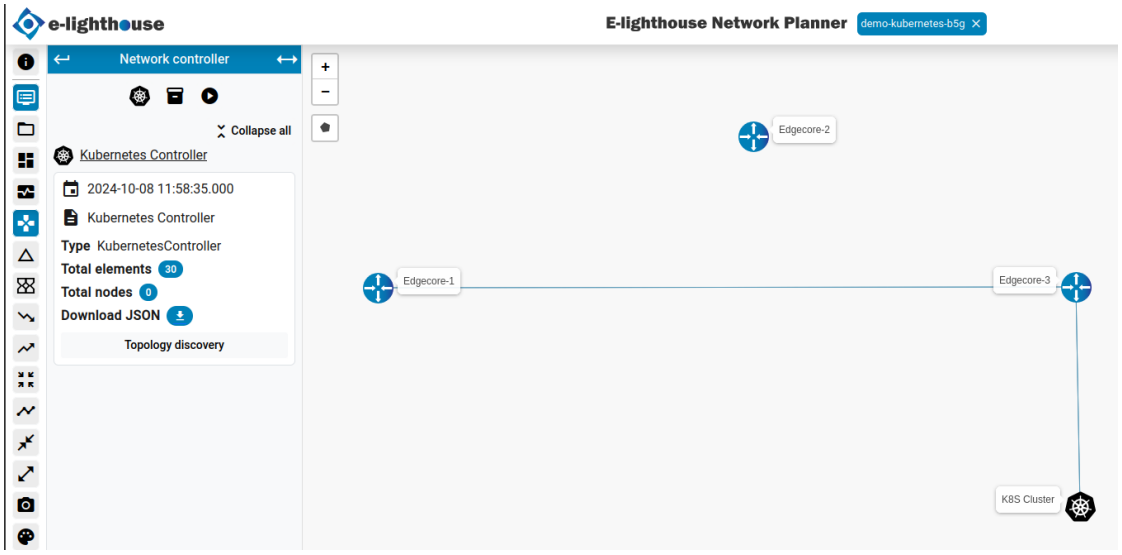

Figure 5.12: -B5G-ONP with Kubernetes Controller and IP topology for VNFs provision.

Once the computational resources are identified, a new namespace is created specifically for the experiment. Within this namespace, a deployment is instantiated to simulate the provisioning of a network service. Additionally, a service is created in the same namespace, associated with the deployment, to ensure the resources within the cluster can be accessed as required.

After setting up the deployment and service, the changes are verified using kubectl commands inside the cluster, confirming the correct functioning of the cluster and its components. Finally, to conclude the experiment, all content created during the process is removed, returning the cluster to its original state (see figures below).

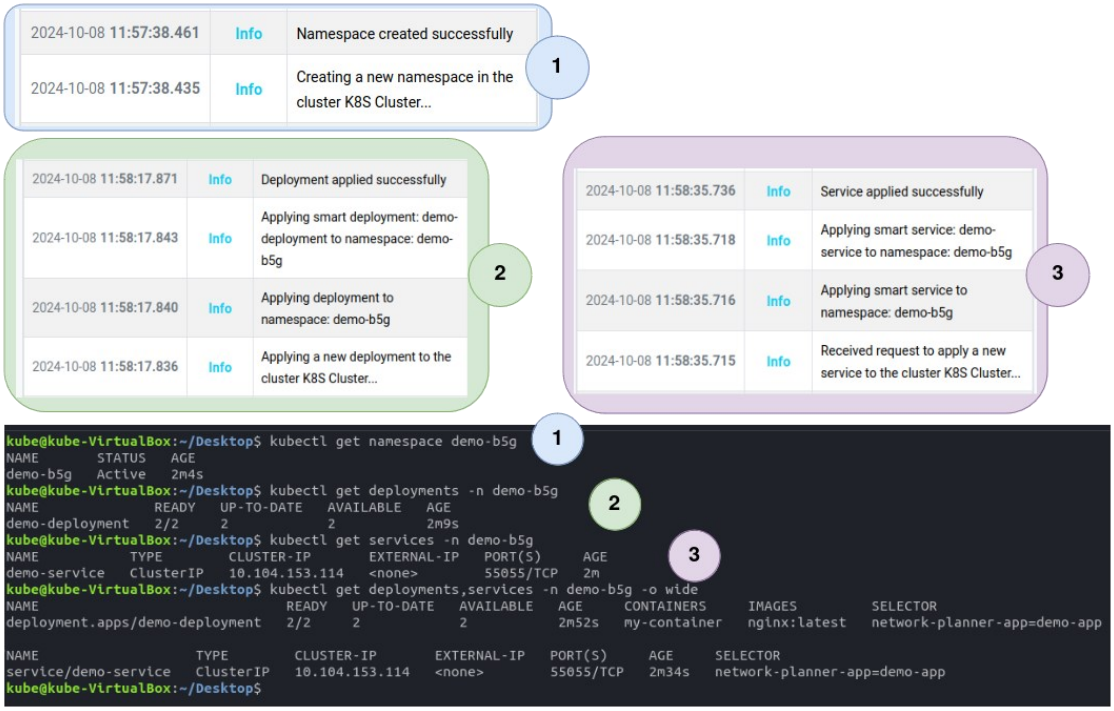

Figure 5.13:-: Capture of logs from B5G-ONP and the state of the cluster with successfully provisioned VNFs.

The KPIs measured during the experiment are as follows:

Action	Namespace (ms)	Deployment (ms)	Service (ms)
Time to create	2.8	379	219
Time to remove	25	353	31

Through this experiment, we successfully validated the integration of Kubernetes-based orchestration with the B5G-ONP architecture, demonstrating seamless interaction between traditional optical network elements and modern cloud-native infrastructure.

5.5 CONCLUSIONS

An innovative disaggregated IPoWDM networks transparently interconnecting access and metro segments and operating over both C- and O-bands is demonstrated. The network is operated through an innovative hierarchical control plane solution extended to compute and enforce transparent end-to-end paths across multiple domains, bands, and layers.

This work involved eight B5G-OPEN Partners. It has been presented at the ECOC 2024 Conf where it was awarded as top scored paper [Mor24]. It also received the invitation for an extended version to appear in the Journal of Optical Communication and Networking (JOCN).

6 FILTER-LESS METRO-ACCESS NETWORK

One of the demonstrations took place at BT labs during the last week of July and first week of September 2024. The demonstration and experiment showed a metro-access network using Infinera's XR Optics connecting a mobile site with a Metro network node through a chain of OADMs that were used to aggregate and drop local traffic. The partners involved included BT, Infinera, OLC-E, CTTC, TuE, and ELIG.

The topology of the metro/aggregation network segments in BT's network is a horseshoe inter-connecting two metro Central Offices (COs) along a chain of access COs as shown in Figure 6.1.

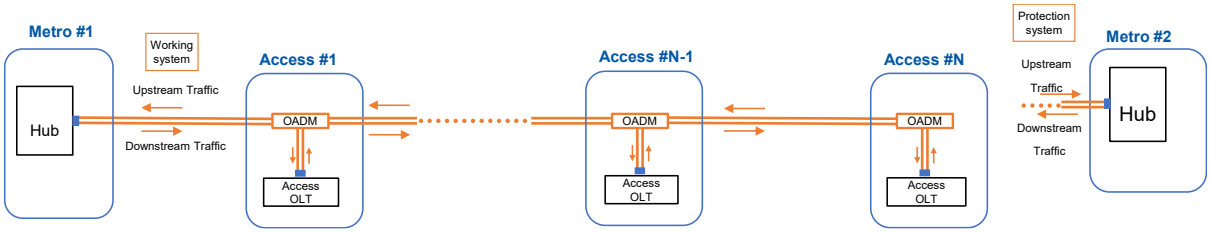

Figure 6-1: Metro-aggregation network in a horseshoe topology

While the main traffic is connected to the Metro CO #1, the connection to the Metro CO #2 is used for resilience.

The initial concept of the demonstration was to simultaneously set up residential connections and mobile traffic using Infinera's XR optics and filter-less OADM that can easily be realised into PICs using SOAs and passive optical splitters. The end-to-end network would be centrally controlled including the PON systems used for residential application. The initial diagram of the demonstration is shown in Figure 6.2.

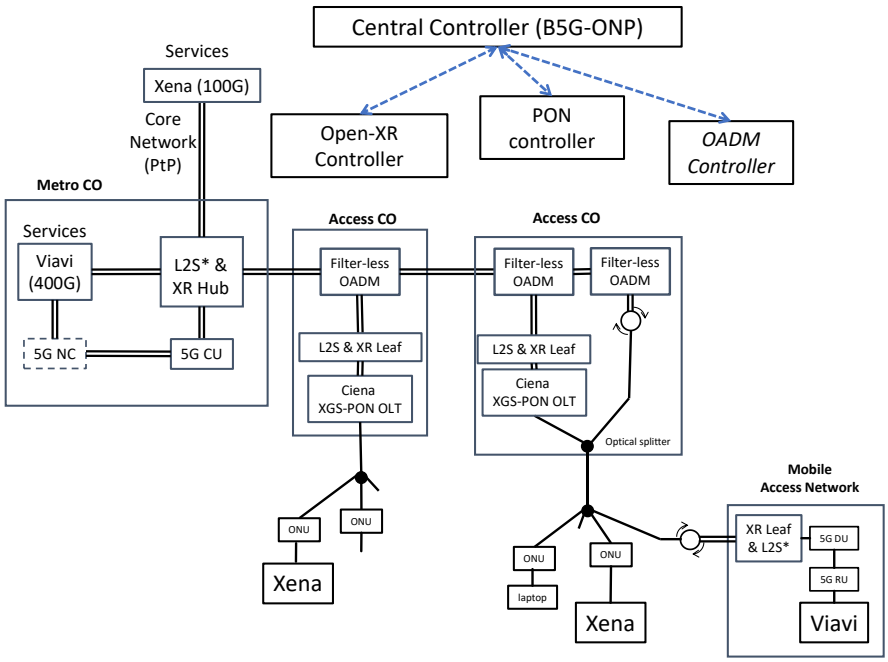

Figure 6-2: Initial diagram of the demonstration setup.

The demonstration concept shows some of the key features addressed during the B5G-OPEN project:

a) Optical continuum: mobile traffic is connected between the cell site and the metro node, optically bypassing the access CO.
b) Multi-Band operation: the mobile traffic uses the fibre C-band to reach a longer distance, while the residential traffic through the PON uses the O-band between customers and access node, and the upper end of the C-band in the downstream towards the customers.
c) Integrated access: both FTTP (residential) and RAN (mobile) use the same fibre infrastructure (single fibre working) in the access network.
d) E2E network orchestration: the central controller (B5G-ONP) manages the service traffic and network configuration for all types of traffic, i.e. both the PON OLT and the XR Optics.

The filter-less OADM, shown in Figure 6.3, uses three or four SOAs (depending on fibre distances) with variable gain, which is controlled by the central controller B5G-ONP, and passive optical splitters.

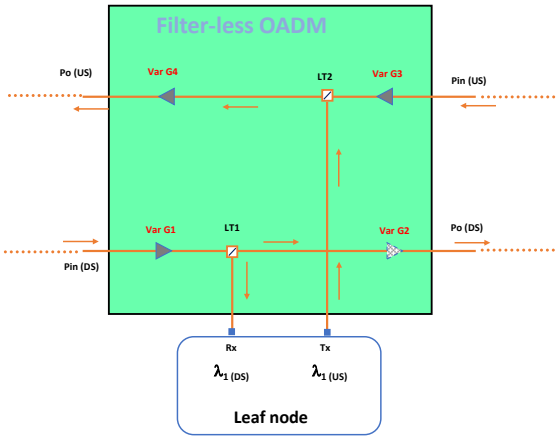

Figure 6-3: Filter-less OADM configuration.

The Filter-less OADM used has three bidirectional ports, West, East, and Local. Figure 6.4 shows the SOA evaluation boards and splitters used in the demonstration.

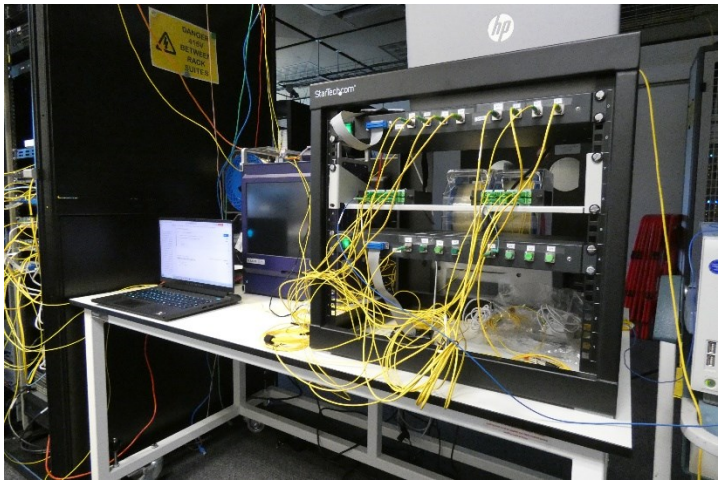

Figure 6-4: Picture showing the SOA evaluation boards and splitters used in the demonstration for the OADMs

We had four XR pluggables available for the demonstration. Due to limitations in the available switches for hosting the pluggables and also of XR configuration, which are still in development, using single fibre working, the final setup of the demonstration used two XR systems at different

wavelengths, one of them configured as a Point-to-Multipoint service for residential traffic, and the other as a Pont-to-Point service for mobile traffic. The final demonstration set-up is shown in Figure 6.5.

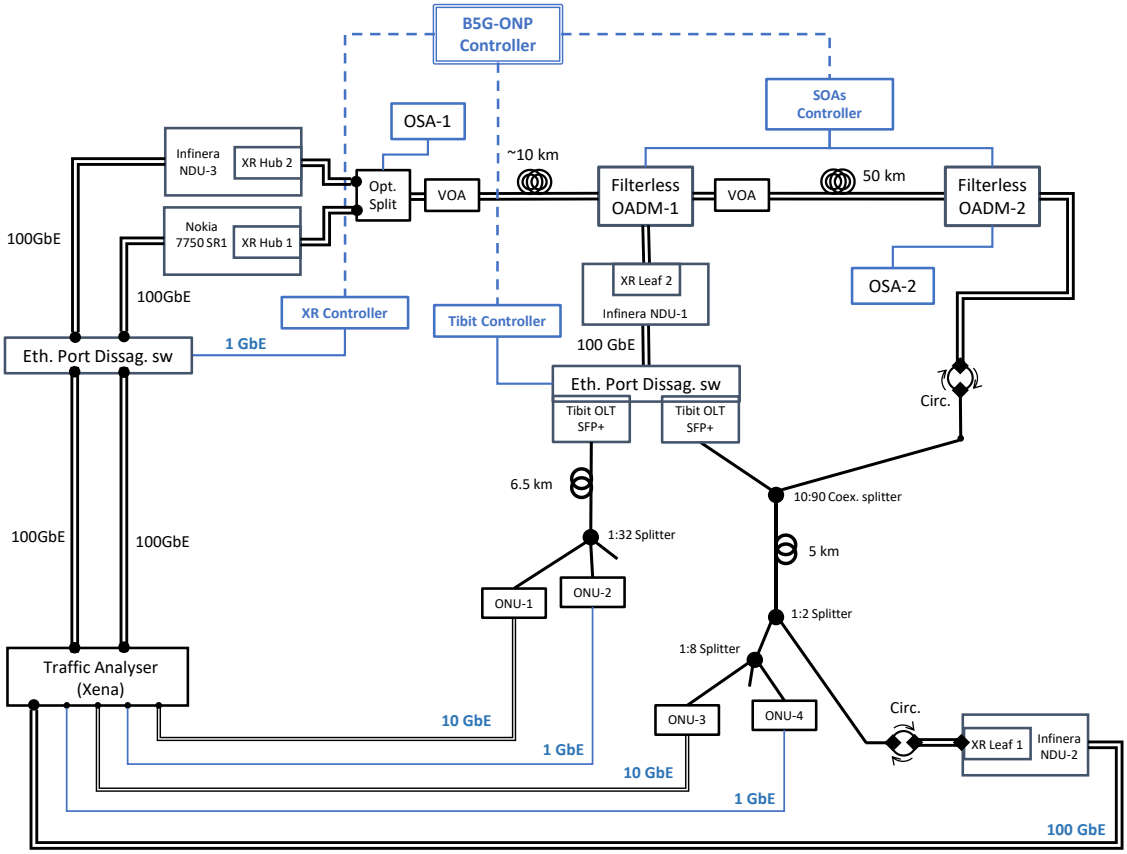

Figure 6-5: Setup of the Filter-less Metro-Access Network Demonstration

The "Filter-less Metro-Access Network" demonstrator used two XR-Systems (each at a different wavelength) and two XGS-PON systems straddling the metro and access network through OADMs. One of the XR systems was configured as a 400G P2MP connection and the second XR as a 100G PtP system that was used to connect to a Mobile network site through both the metro and access network segments. The XR PtP 100G system coexisted in the same access fibre infrastructure as the residential XGS-PON system. As shown in Fig. 6.5.

The XR Hub 1 to XR Leaf 2 connection was established using a Point-to-Multipoint (P2MP) configuration and carried two 5GbE flows and two 1GbE flows over four XR digital subcarriers with a capacity of 100Gb/s, although the XR system had all 16 digital subcarriers active, i.e. 400Gbit/s capacity. The XR Hub 2 to XR Leaf 1 connection was established using a Point-to-Point configuration carrying a single 100GbE flow using four digital subcarriers. In such configuration the XR system has four active subcarriers, i.e. 100Gbit/s capacity.

The fibre distance between the metro node and the first OADM at the first access node was 10 km approximately, and the fibre distance between the first OADM in the first access node and the second OADM in the second access node was 50 km. The local traffic in the first access node was transported over two XGS-PONs. The mobile traffic was connected to the East port of OADM-2. Due to the limitations on the number of XR pluggables we connected the mobile traffic to the fibre infrastructure of the first access node by converting to dingle fibre working.

While the XR pluggables were locally managed, both the PON systems and the SOA gain in the OADMs were remotely controlled depending on optical losses and number of active digital subcarriers.

We inserted Variable Optical Attenuators (VOAs) to run tests in the physical layer and two Optical Spectrum Analysers (OSAs) to show the spectrum content in the metro network. The next few figures show some of the demonstration components and some of the captured spectrum traces.

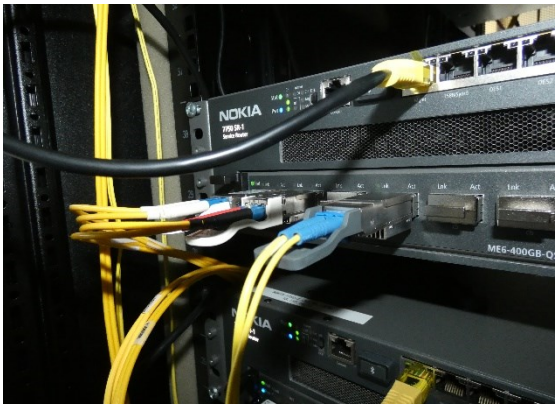

Figure 6-6: XR Hub 1 QSFP-DD connected to a Nokia 7750 SR1

Figure 6-7: Ciena XGS-PON ONUs used in the demonstration

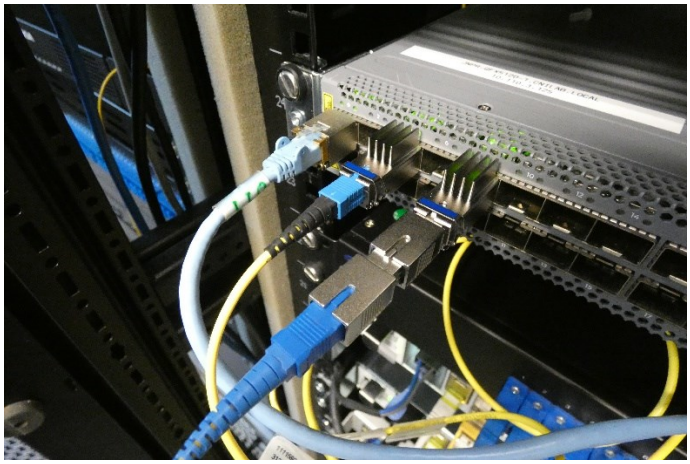

Figure 6-8: Tibit (now Ciena) OLTs connected to a Layer 2 switch

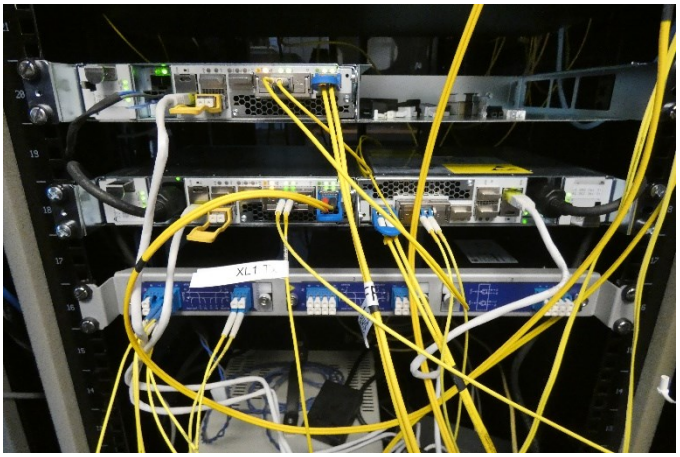

Figure 6-9: Infinera NDUs hosting XR Leaf Nodes and Hub 2

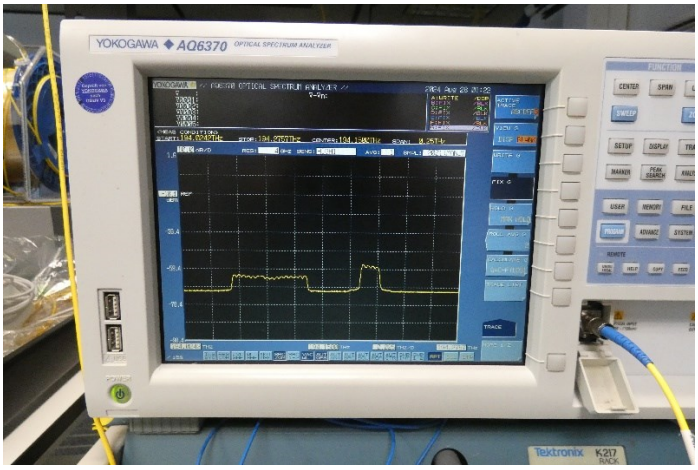

Figure 6-10: Captured spectrum trace showing the two XR systems in the downstream showing the 400G spectrum on the left (P2MP connection) and the 100G on the right (PtP connection).

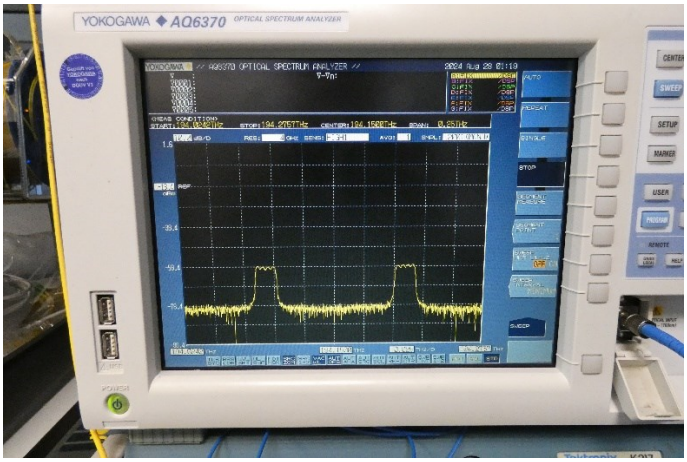

Figure 6-11: Captured spectrum trace showing the two XR systems in the upstream direction.

6.1 PHYSICAL LAYER EXPERIMENTAL RESULTS

Figure 6.12 is a simplification of the setup shown in Figure 6.5 splitting the downstream and upstream connections of the two XR systems. Although the two XGS-PON systems are not shown, they were running throughout the experiments showing no errors in the four different Ethernet flows that they were transporting between the ONUs and the OLTs.

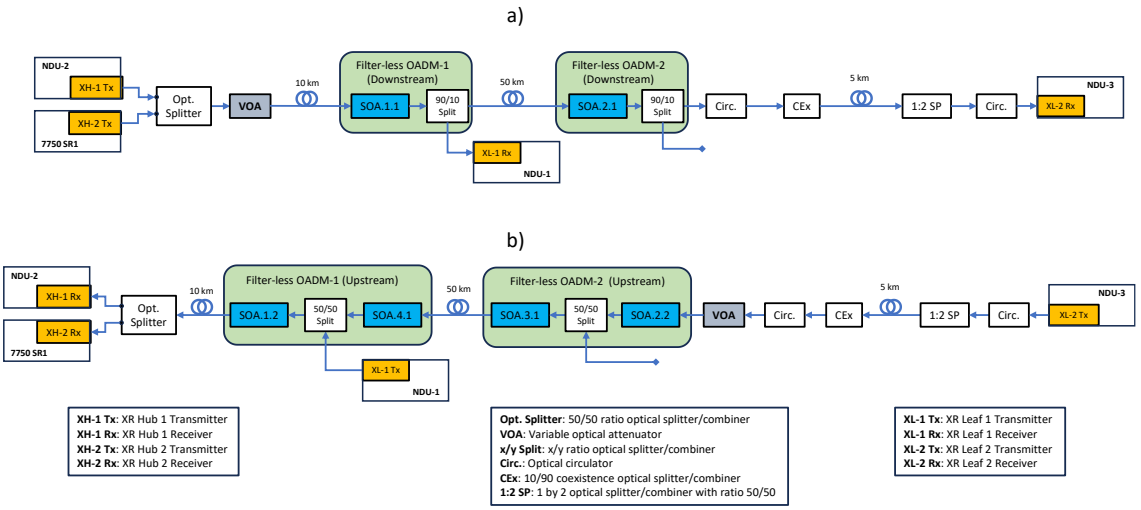

Figure 6-12: Diagrams showing the XR systems connectivity split in a) downstream and b) upstream

The SDN controllers are not shown but they were nonetheless operational. What the demonstration did not include was the algorithm to calculate the configuration of the SOAs gains to establish or re-establish the connections.

The experiments at the physical layer consisted of manually changing the value of the VOA and changing the gain of the SOA if necessary to re-stablish the connection error-free. Although the OADM SDN agent was connected to the central controller B5G-ONP we manually changed the gains though the agent. The starting network configuration was error free.

Figure 6.13 shows the results in the downstream direction for the XR system configured as a P2MP connection between the XR-Hub 1 hosted by a Nokia 7750 SR1 and XR Leaf 1.

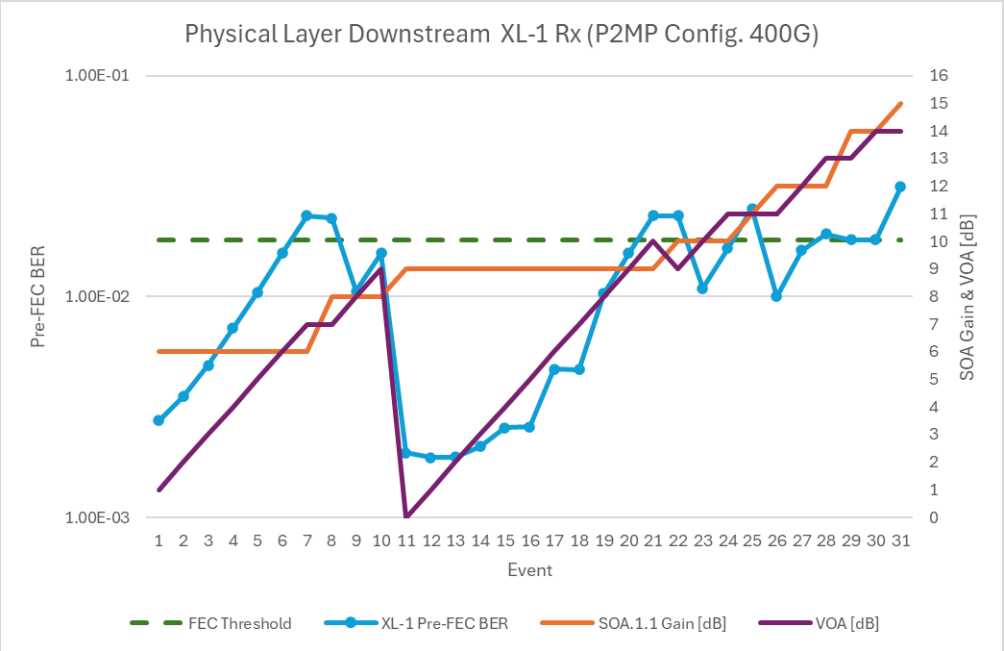

Figure 6-13: Downstream Pre-FEC results as VOA value increased and SOA.1.1 Gain re-configured to re-establish error-free connection at the XR Leaf 1.

Each event represents a change in the value of the VOA, which caused the Pre-FEC to degrade. When Pre-FEC was above the threshold, the connection was starting to show errors at which point the gain of the SOA.1.1 was increased to re-establish an error-free connection. The same method was used in the next three figures. There were some errors in the capture of the values the origin of which we were not able to investigate due to lack of time.

We can see in Figure 6.13 that we were able to increase the VOA to 14dB with an error-free connection, which needed a SOA gain of 14dB.

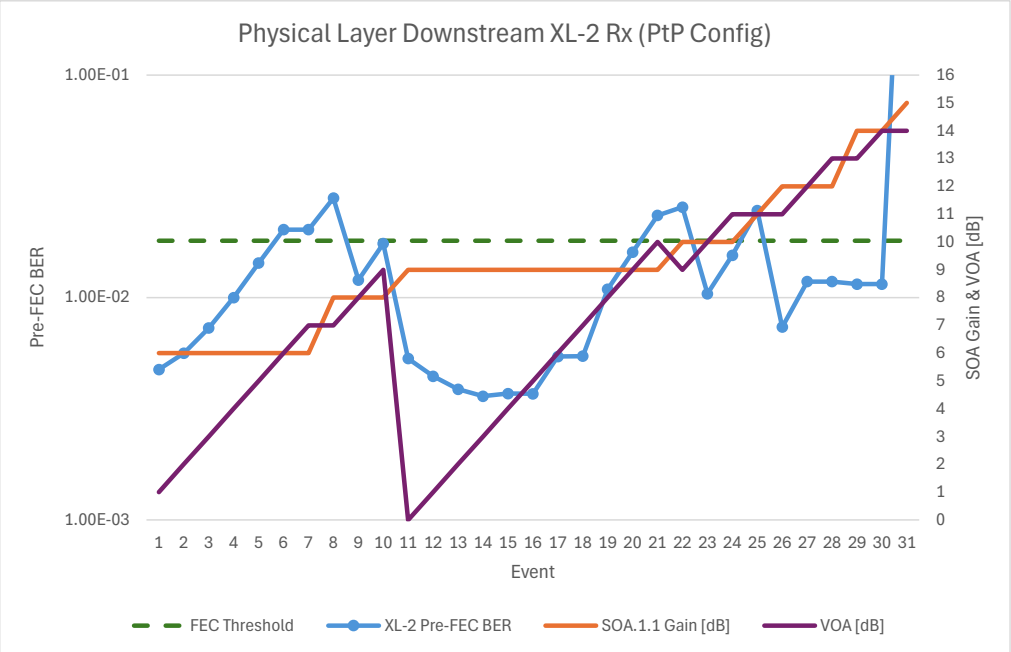

Figure 6-14: Downstream Pre-FEC results as VOA value increased and SOA.1.1 Gain re-configured to re-establish error-free connection at the XR Leaf 2

Figure 6.14 shows the results for the PtP connection where the connection was also error-free for a VOA value of 14dB and a SOA gain of 14dB. It must be noted that both sets of measurements were taken simultaneously. They are shown in two different graphs only for clarity.

The change of VOA value affects both XR systems simultaneously and it is reasonable that being both Leaf nodes configured to receive 100G connections that both can cope with an attenuation up to 14dB. Obviously with this experiment we are only emulating an added insertion loss due to e.g. dirty connector, or a kink in the fibre cable. However, the other main factor of degradation is the OSNR, which is directly linked to the Pre-FEC and only depends on the number of traversed SOAs, being the same in all cases. We have not analysed other potential effects of increasing the transmission distance, although non-linear effects should not degrade the signal since launched optical powers have always been kept around or below 0 dBm.

We have performed the same type of experiments in the upstream direction but inserting the VOA before OADM-2 as shown in Fig. 6.12b).

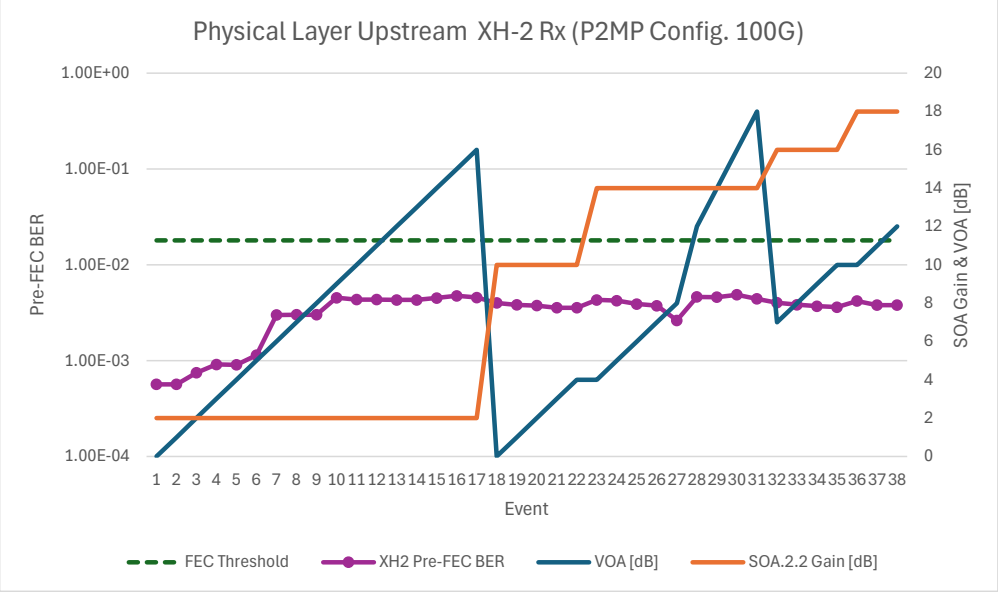

Figure 6-15: Upstream Pre-FEC results as VOA value increased and SOA.2.2 Gain re-configured to re-establish error-free connection at the XR Hub 2

The location of the VOA does not impact the P2MP system and thus we don't expect a big change on its measured BER, which is confirmed by the results shown in Figure 6.15. However, even though the transmission is always error-free, there is a change in the received BER. This is due to two main reasons, the change of the ASE noise generated at the SOA.2.2 when changing its gain, and the change in optical transmitted power at the XR Leaf 1, which automatically changes (in P2MP configuration) to equalise with the in-line transmission at the insertion point in the OADM.

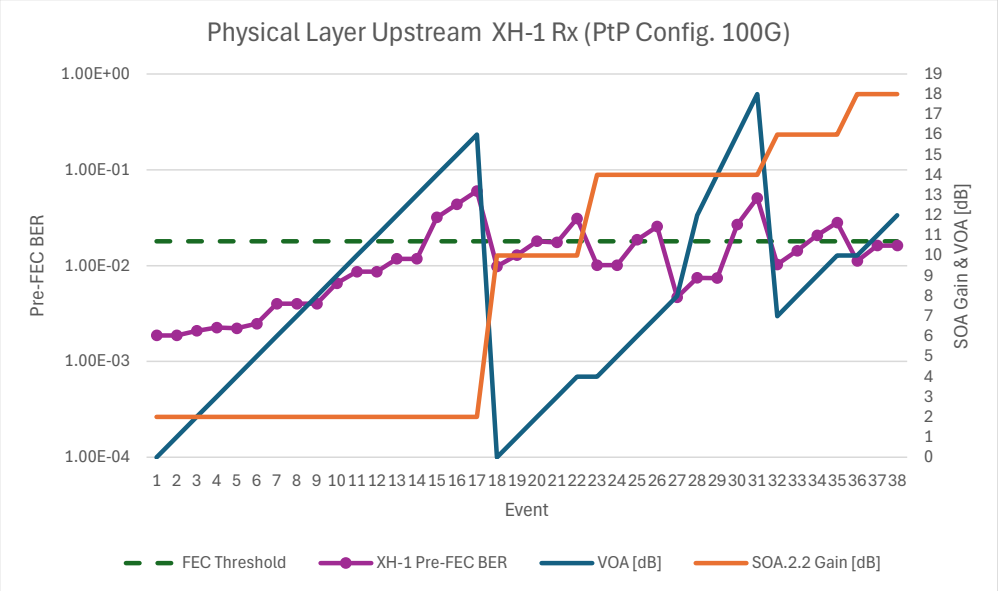

Figure 6-16: Upstream Pre-FEC results as VOA value increased and SOA.2.2 Gain re-configured to re-establish error-free connection at the XR Hub 1

Figure 5.16 shows the impact of changing the VOA value on the PtP XR system between the XR Leaf 2 and XR Hub 1. It shows that increasing the SOA gain up to 18dB (the maximum we were able to configure) the PtP system can cope with a VOA value of 12 dB. However, the maximum value of the VOA the system runs error-free is 14dB, which can be achieved when the SOA gain is configured with a 14 dB gain. Without verification, we can presume this is due to the ASE noise generated by the SOA.

6.2 TIMING EXPERIMENTAL RESULTS

The Filter-less Metro-Access network concept using the XR system is used for mobile applications as described above. In order to share the fibre infrastructure with the residential access network, the dual fibre working system in the metro segment needs to be converted to a single fibre working system in the access segment. This is achieved by using optical circulators as shown in Figure 6.5.

Synchronisation in both frequency and time is crucial for mobile applications, especially on 5G NR using TDD (Time Division Duplex) transmission mode. Therefore, we carried out some experiments on the effect of fibre difference between transmission directions when dual fibre working, and the impact of using introducing single fibre working in the access segment.

The experiment setup was changed to eliminate effects outside of the targeted measurements as shown in Figure 6.17 for the dual fibre working case. Thus, the SOA based OADM were swapped with passive OADMs using passive optical splitters. Only the XR system was used and the PON systems disconnected when necessary. This was due to the lack of enough ports in the NDUs to simultaneously connect the PON OLTs and the Calnex box used in the experiments (Figure 5.18). Also, the SDN network was not used.

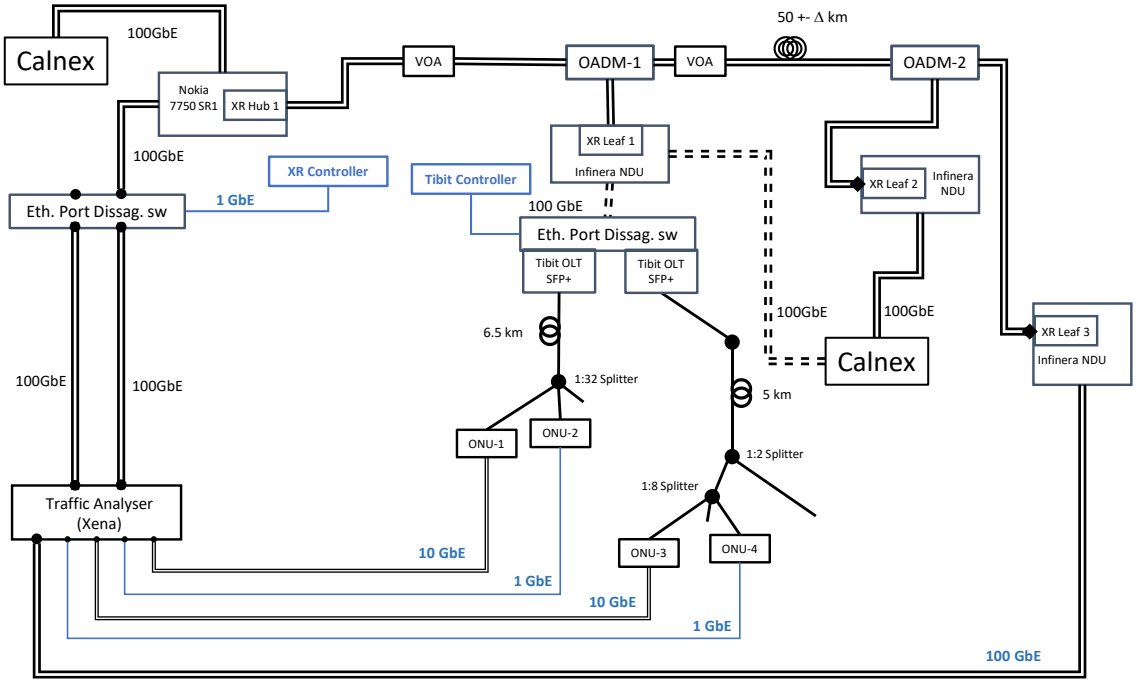

Figure 6-17: Network setup used for the Dual Fibre Working Timing experiments

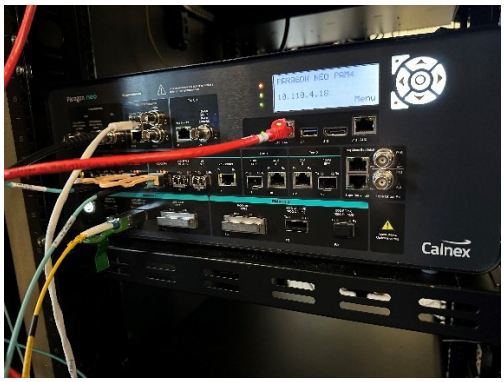

Figure 6-18: Calnex Paragon Neo box used for the Timing experiments

The specific setup diagram was further simplified to carry out the timing measurements. The topology for the dual fibre working tests is shown in Figure 6-19, while Figure 6-20 shows the topology diagram for the single fibre working tests.

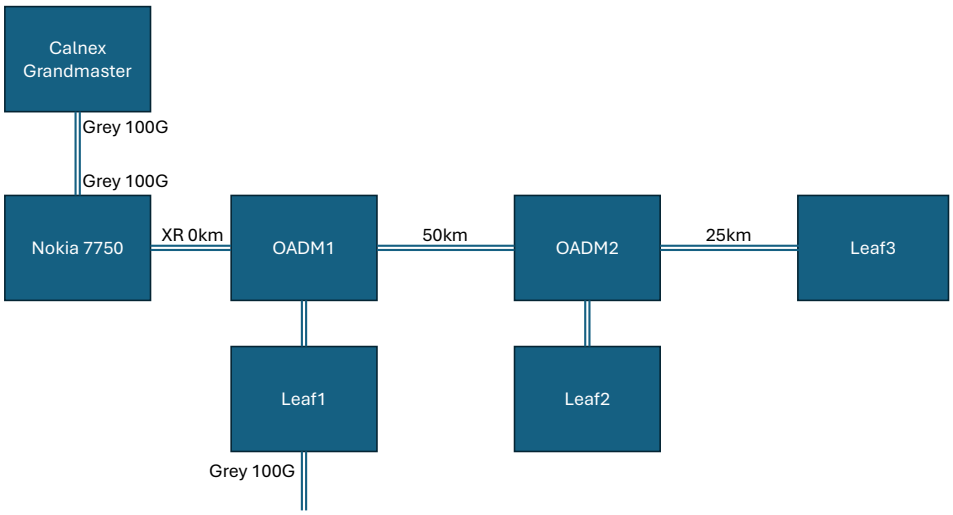

Figure 6-19: Simplified topology diagram for the Dual Fibre Working Timing measurements

The Calnex box was used to introduce distance asymmetries between both directions. First of all, the exact reel fibre lengths were measured, and their difference was compensated. Second, the timing performance of the Nokia 7750 SR1 was also measured and equalised. With this setup a baseline PTP (Precision Time Protocol) performance was measured.

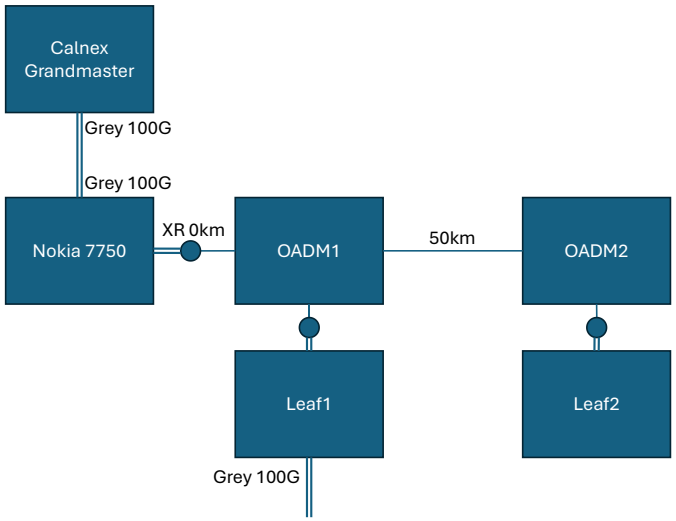

Figure 6-20: Simplified topology diagram for the Single Fibre Working Timing measurements

These experiments took place in September, and at the time of this deliverable report, we are still processing the measurement results.

7 CHROMATIC DISPERSION MONITORING IN MULTI-BAND OPTICAL TRANSMISSION SYSTEMS

One of B5G-OPEN demonstrations took place in CTTC labs in Castelldefels focusing on the monitoring of chromatic dispersion (CD) in multiband (MB) access and metro converged optical networks [Boi24]. The partners involved in the demo were NOKIA and CTTC. In particular, the research specifically targets CD monitoring across multiple bands including S-, C-, and L-bands using a multiband bandwidth/bitrate variable transceiver (MB BVT). Two slices of the MB sliceable BVT (S-BVT) prototype, developed in B5G-OPEN, were used in the demo. An additional slice operating in the L-band, developed as part of the SEASON project (G.A. No. 101096120), was also incorporated to extend the monitoring study and capabilities towards evaluating additional wavelengths within the L-band.

In traditional networks, the C-band has been widely used for optical communication, but MB technology arises as a suitable solution to further increase network capacity. Therefore, exploring the use of additional optical bands such as S- and L- bands is crucial for the future development of high-capacity optical networks. These additional bands offer more bandwidth, thus enabling flexible and higher-capacity transmission for both access and metro network segments. CD arises as a critical parameter for predicting non-linear impairment in long-distance and high-speed optical transmission, so it needs to be accurately monitored across all these bands to ensure optimal network performance. This work addresses this challenge by proposing a method that utilizes orthogonal frequency division multiplexing (OFDM)-based transceivers to monitor CD properties in a heterogeneous fiber network.

The main research objectives of the demo are here summarized:

1. Investigate the performance of CD monitoring over the S-, C-, and L-bands using MB BVTs.
2. Integrate the monitoring solution in an experimental optical networking testbed to demonstrate its accuracy and applicability in heterogeneous fiber topology scenarios.
3. Validate the proposed solution using different fiber types, such as standard single mode fiber (SSMF) and Teralight (TL) fiber, at varying lengths and channels/wavelengths across the optical bands.

7.1 METHODOLOGY

The proposed monitoring method employs OFDM-based MB BVTs to monitor CD properties over the C+L+S bands. This is achieved by capturing and analyzing the power spectrum density (PSD) of the received OFDM signals using an advanced digital signal processing (DSP) block. The steps involved in the methodology include:

1. **Analytical Model**: The linear OFDM channel is modeled using a transfer function equation that correlates the frequency and wavelength of the signal with the accumulated CD. This model is used to estimate CD by identifying notches (zero points) in the PSD.

$$PSD(f) = P_0 \left|\cos\left((f\lambda)^2 \frac{D_\lambda * L}{c}\right)\right|^2 10^{\alpha * f} + N_0 \text{ , (6.1)}$$

where α is an attenuation coefficient related to the scope bandwidth, N_0 is accounting for multiple electrical and optical noise and is a background level, D_λ is the dispersion coefficient at the wavelength λ, L the fiber length. α is fixed for all the experiment 0.2 dB.GHz^{-1}. Figure 7-1 shows a typical PSD (cross markers) with fitted curve from Eq. (6.1) in dashed line.

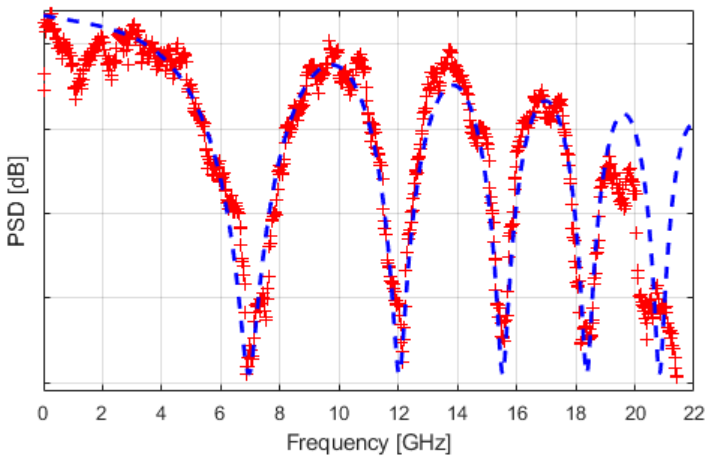

Figure 7-1 Power spectral density of detected signal after 75 km of propagation in SSMF. Crosses are experimental points; dashed line is the fit based on Eq. 6.1.

2. **Measurement Process**:
    - Record a 2048-point PSD vs. frequency for each lightpath with central wavelength λ_j.
    - Use a moving average filter to smooth the monitored PSD.
    - Calculate the notches in the PSD by estimating the accumulated CD based on known fiber parameters.
    - Determine the dispersion parameter D(λ) using a three-term Sellmeier formula.

$$D(\lambda) = \frac{S_0}{4}\left(\lambda - \frac{{\lambda_0}^4}{\lambda^3}\right) \qquad (6.2)$$

    where λ_0 is the zero-dispersion wavelength and S_0 is the dispersion slope at λ_0.

3. **Accuracy Evaluation**: Different fiber types (SSMF and TL) are tested with varying lengths (50 km and 75 km) to evaluate the accuracy of the method. Results are compared with expected values from theoretical models to validate the measurement accuracy.

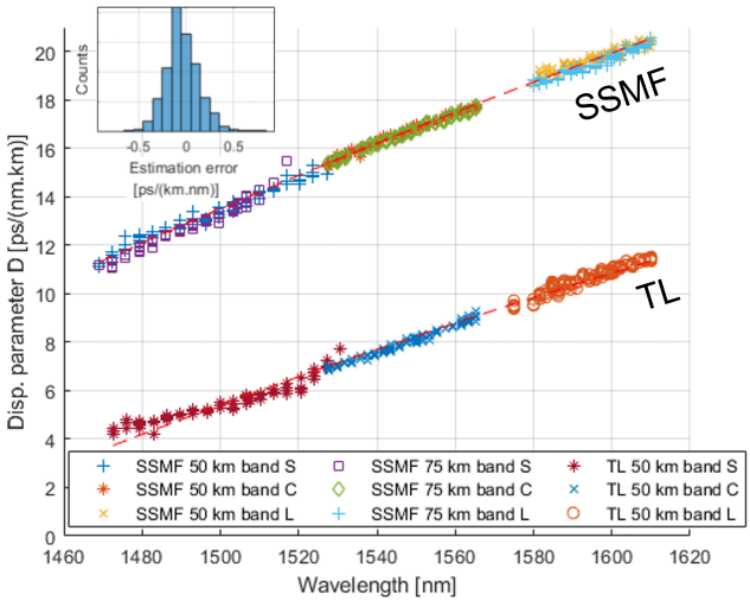

Figure 7-2 Dispersion parameter D as a function of the wavelength obtained from the fitting with Eq. (6.1) for different fiber types and fiber lengths. Red dashed lines are the results of the fit with Eq. (6.2) for each fiber type. Inset: histogram of the estimation error.

The results of the fit for all fiber types, lengths, and channel wavelengths are shown in Figure 7-2. For each fiber type, the fitting was performed using Eq. (6.2) by minimizing the root mean square error to obtain the fiber parameters λ_0 and S_0. The resulting fit, depicted as a dashed red line in Figure 7-2, matches well for SSMF but shows deviations at low wavelengths for TL, likely due to reduced accuracy in areas with low accumulated dispersion. The obtained parameters for each fiber type and length are displayed in Table 6.1. The inset histogram in Figure 7-2 illustrates good overall performance, with a standard deviation of 0.19 ps/(km.nm) and a mean error of -0.03 ps/(km.nm).

Table 6.1 Tested fiber type, length and fitted parameters

Fiber	Length [km]	λ_0 [nm]	S_0 [ps/(km.nm^2)]
SSMF	50	1335	0.0968
	75	1337	0.0966
TL	50	1416	0.0703

7.2 EXPERIMENTAL TESTBED INTEGRATION

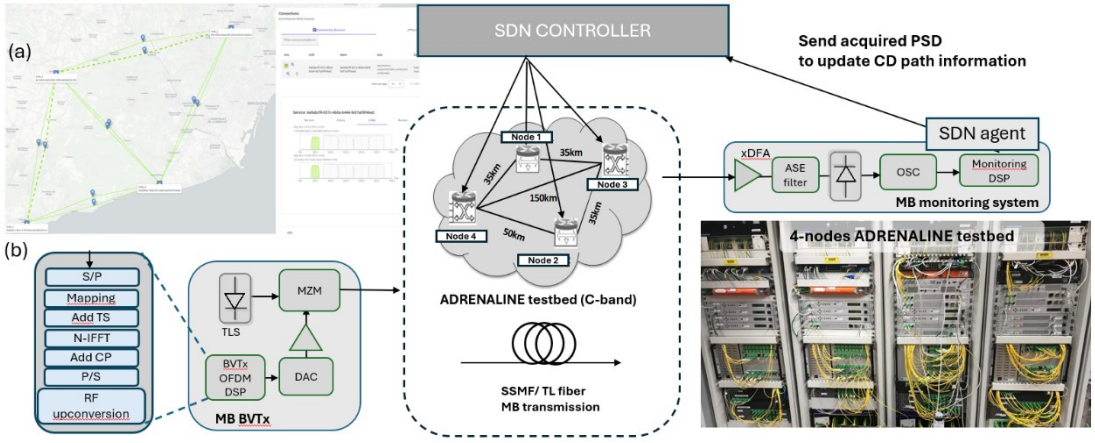

Figure 7-3 Experimental setup for CD monitoring. (a) GUI of the SDN controller to stablish the optical path. (b) Setup used to perform the experiment with the MB BVT: The OFDM data are generated, sent through the optical testbed or Fiber spool, amplified, filtered, and then sampled by an oscilloscope. The monitored data are sent to the controller via the SDN agent.

The proposed monitoring method has been integrated and validated within the ADRENALINE testbed, available at CTTC lab [Mun17]. Specifically, the ADRENALINE testbed is an open, disaggregated software defined networking (SDN)/Network Functions Virtualization (NFV)-enabled infrastructure that integrates packet/optical transport networks with edge/cloud computing. It is designed to support beyond 5G, 6G, and IoT/V2X services. The ADRENALINE photonic mesh network consists of four nodes (N1-N4, as shown in Figure 7-4), including two reconfigurable optical add-drop multiplexers (ROADMs) and two optical cross-connects (OXCs). The network features five bidirectional flexi-/fixed-grid dense wavelength-division multiplexed (DWDM) amplified optical links covering up to 150 km each, totaling 600 km of optical fiber. The 35 km links are SMF, the 50 km link is TL and 150 km is LEAF (see Figure 7-4).

Figure 7-4 ADRENALINE fiber spools with SSMF and TL paths.

The integration process involves configuring the SDN controller to establish new services between different nodes, where the MB BVT transceiver measures and reports the PSD of detected signals for each optical path. The controller then fits the PSD data using a predefined function to calculate the accumulated dispersion of each link.

The study demonstrates 29 services starting from Node 3 and connecting to other nodes (Node 1, Node 2, Node 4). For single-link routes (e.g., N3-N1 and N3-N2), CD properties can be directly measured and determined without additional processing. However, for multi-link routes (e.g., N1-N4 and N2-N4) the dispersion estimation becomes more complex due to the combined effects of multiple fiber segments with varying CD characteristics. In these cases, a correlation algorithm is applied to accurately determine link-specific properties based on the cumulative dispersion data. The experimental results validate the accuracy of the CD measurements and show how the SDN controller can leverage this information to optimize path computation based on CD, ensuring improved network performance and flexibility.

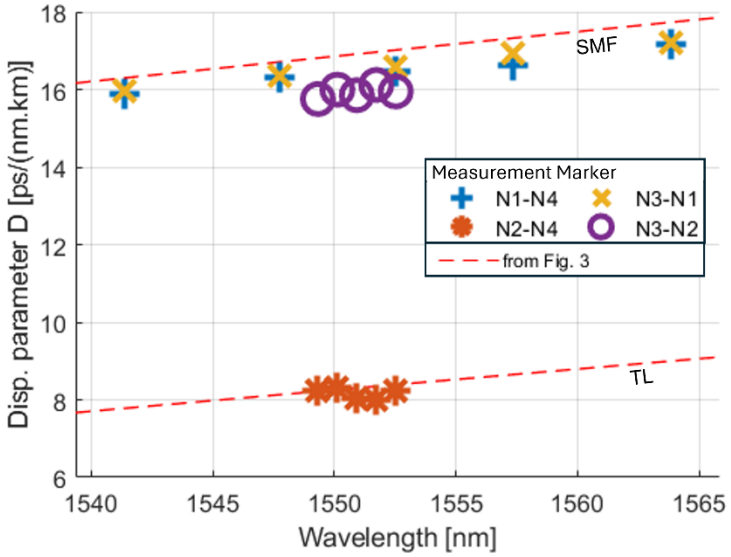

Figure 7-5 Dispersion parameter D as a function of the wavelength obtained from the fitting with Eq. (6.1) for different fiber types and fiber lengths. Red dashed line is the results of Figure 7-2.

In particular, Figure 7-5 shows the dispersion parameter obtained for each link (represented by the measurement markers). The red dashed lines correspond to the fitted results from Figure 7-2. It should be noted that the link N2-N4 represents the TL fiber spool characterized earlier. For the TL fiber (indicated by red stars), the properties were estimated using the correlation algorithm, and the results show excellent agreement with the previous characterization, with a standard deviation of 0.18 ps/(nm·km). Additionally, this monitoring approach revealed a deviation from the average fiber parameters for the N3-N2 link.

The final step involves incorporating the updated and accurate CD values into the SDN controller's path computation function (see Figure 7-6). This allows the SDN controller to use CD as a traffic engineering metric, enabling it to prioritize paths with lower accumulated dispersion, which is particularly beneficial for double sideband (DSB) transmitters that are more sensitive to dispersion effects. The updated link properties can be shown in the controller graphical interface depicted in Figure 7-7.

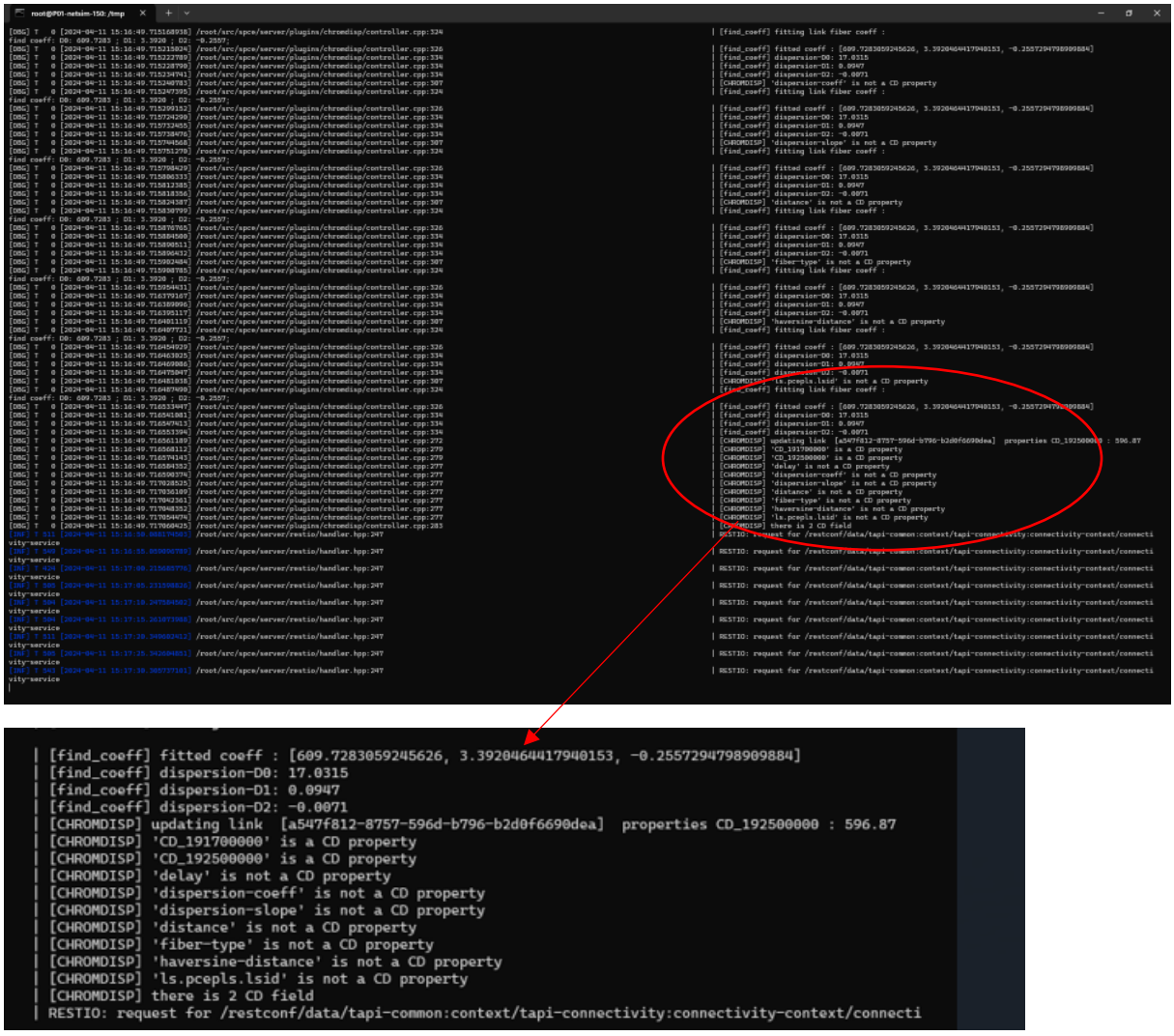

Figure 7-6 Example of logs for path N3-N1-N4 of the ADRENALINE testbed at 1557.36 nm where the calculated accumulated dispersion is depicted.

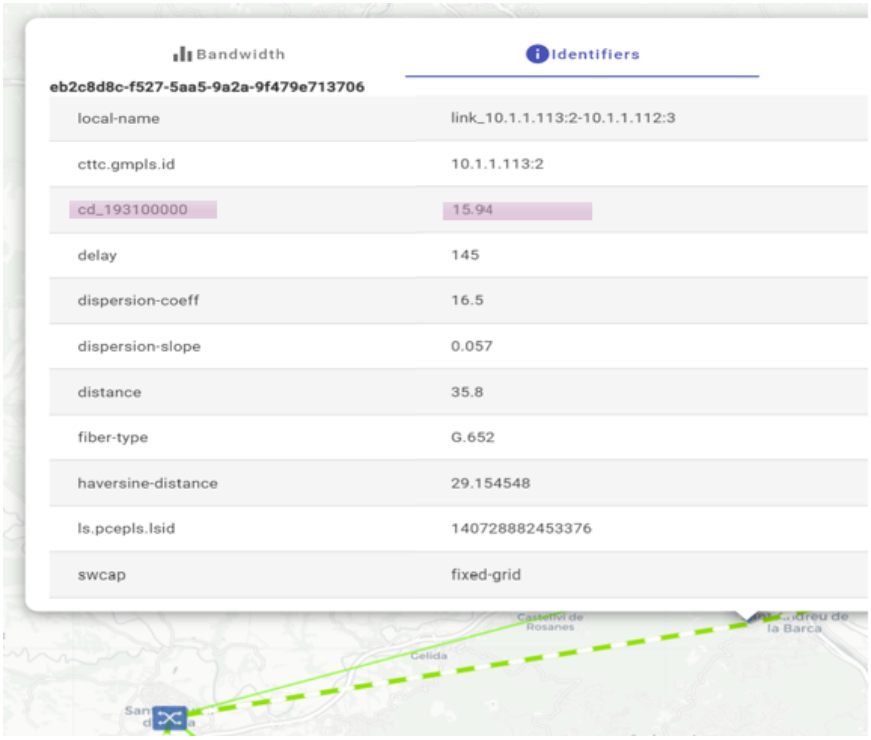

Figure 7-7 Example of updated link properties in the controller graphical interface.

This demo demonstrates a technique for monitoring the CD characteristics of optical fibers using an OFDM-based MB BVT. The results demonstrate high accuracy, with a small standard deviation of 0.19 ps/(km·nm). The proposed monitoring solution is integrated into an optical networking testbed, providing a complete end-to-end workflow for evaluation and validation.

8 PACKET-OPTICAL NETWORK USING COHERENT PLUGGABLE TRANSCEIVERS

The experimental setup of TID in the Madrid laboratory is aimed at evaluating the performance of the proposed B5G-OPEN architecture in which coherent pluggable are hosted in packet optical routers. The aim is to verify experimentally that the distances that can be bridged are aligned with the target network defined in B5G-OPEN.

8.1 METHODOLOGY

It is important to emphasize that the testing is conducted in a controlled environment with standardized test procedures to guarantee accurate and reliable results. The TID IPoWDM benchmark test comprises up to four activities as follows:

- **TX Performance:** The pluggable module transmitter will be tuned and set to maximum power. At this stage, the TX output of the pluggable module will be connected directly to an Optical Spectrum Analyzer (OSA). The activity will assess the minimum and maximum configurable frequency and the adjustment granularity for both transmitted optical power and frequency.

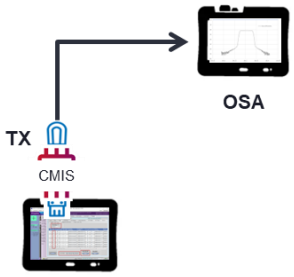

Figure 7-1- TX Optical Power Testing

- **RX Optical Power Sensitivity:** A Programmable Variable Optical Attenuator (PVOA) will be used to establish a loopback between the pluggable module's transmitter and receiver. The process can be considered complete once the PVOA loss has been increased until errors are observed.

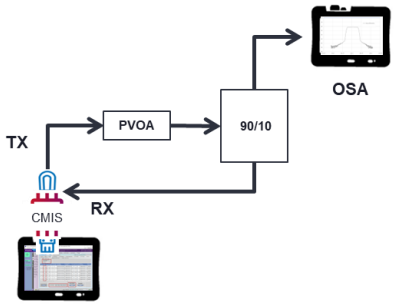

Figure 7-2 -RX Optical Power Sensitivity Testing

- **RX B2B OSNR Sensitivity:** A back-to-back (B2B) noise loading setup was implemented (for details, refer to **Figure 7-3, RX B2B OSNR Sensitivity Testing**). A PVOA will be used to control the noise injection; the PVOA loss will be reduced until errors are observed.

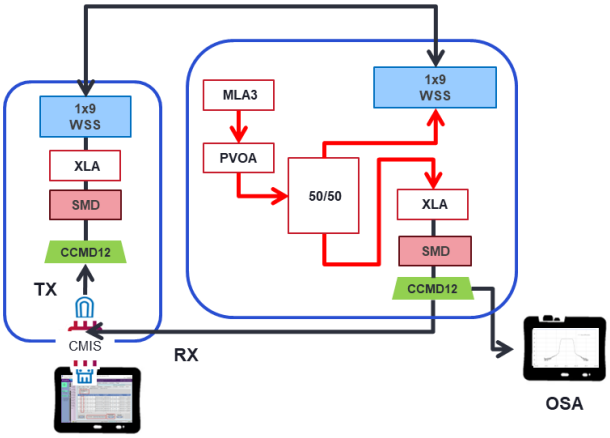

Figure 7-3 -RX B2B OSNR Sensitivity Testing

The test setup must be configured to ensure that both the total optical spectrum (CHC, Channel Control) in the OLS and the optical spectrum intended to be used by the optical carrier (NMCC, Noise Measurement Channel Control) allow noise floor visibility both left and right of the optical carrier. **See Figure 7-4 System Noise (ASE) floor,** to have details for the Total ASE comprising all noise sources.

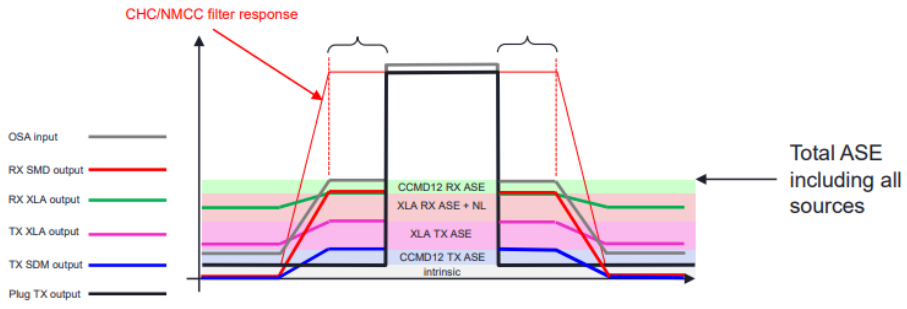

Figure 7-4- System Noise (ASE) floor

- **OSNR Performance vs Span:** The initial three test packages are designed to assess the fundamental functionalities (set TX optical, power, set frequency, frequency offset, transmission mode (AppSel), etc.) and capabilities (receiver sensitivity to optical power and tolerance to noise) of the system. The fourth testing package, OSNR Performance vs Span, will use the data gathered in the first three testing packages as baseline parameters. Those baselines will be used to evaluate OpenZR+ pluggable modules installed in the Telefonica Test Bed, with the aim of measuring performance over multiple spans and ROADM nodes. This testing package will enable Telefonica to assess the effect of incremental transmission penalties due to fibre impairments, the incremental penalties due to WSS modules present, and the ZR+ pluggable module performance when exposed to OSNR degradation due to going through up to six ROADM nodes. The Telefonica Test Bed (**See Figure 7-5 Telefonica Testbed**) has been equipped

with noise generators (MLA3 ASE) at the Tapia and Paloma nodes. The Tapia noise generator will be used to feed the ASE holders in both directions of the system.

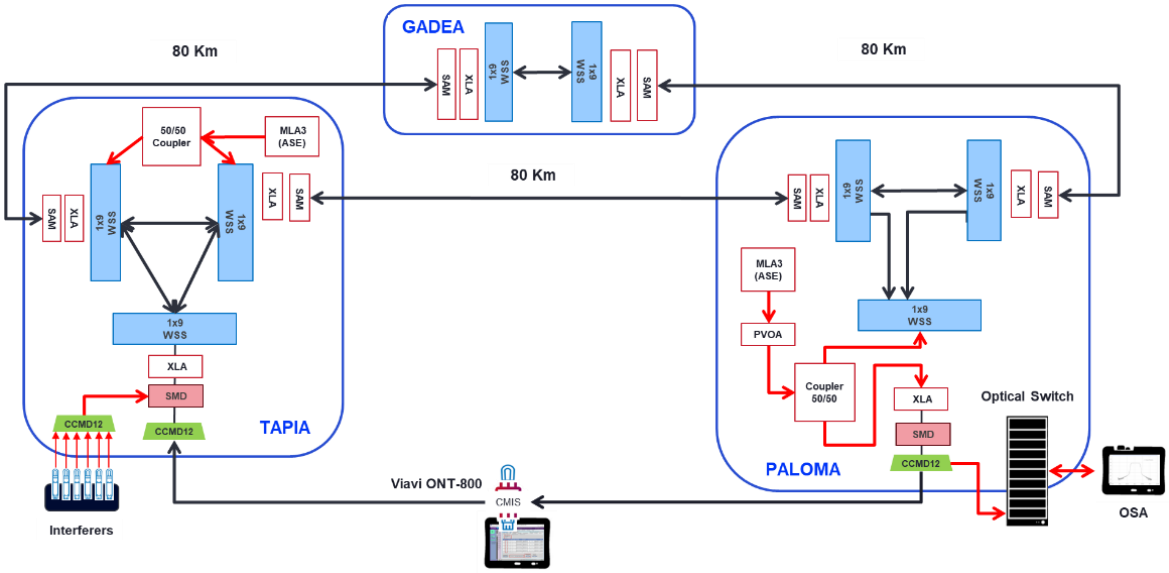

Figure 7-5 Telefonica Testbed

8.2 TEST ENVIRONMENT – GENERAL SETUP

To emulate a "brown-field" scenario, the optical spectrum (C-band) was filled with an ASE channel and interferers flanking the Signal Under Test (test probe). **See Figure 7-6 Optical Spectrum as configured in the Test Bed**-. To have details about the disposition of the ASE holders, the "Interferers", and the Signal Under Test at the center of the usable Optical Spectrum.

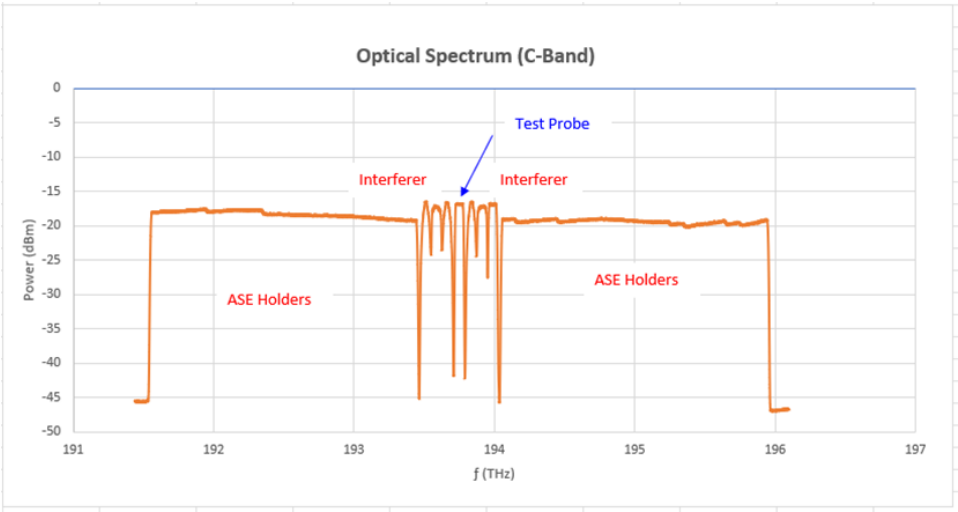

Figure 7-6 -Optical Spectrum as configured in the Test Bed

The “Interferers” were generated using optical signals from another ZR+ pluggable module. The decision was made to proceed with further testing after the initial package was completed. This revealed differences in the transmission profile of the tested pluggable modules. The differences were particularly noticeable about the pulse shaping, with both the pulse width and pulse flatness differing significantly. **See Figure 7-7 TX Optical**

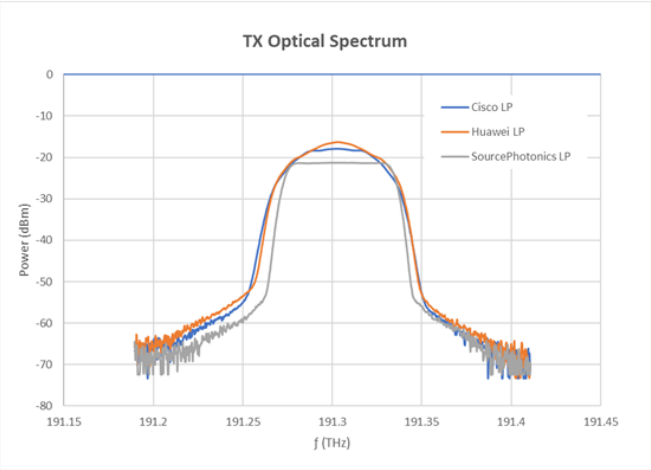

Figure 7--7 TX Optical Spectrum Differences

To accommodate both the ASE Holders and the Interferer, it was necessary to prepare and follow an Optical Channel plan where all ASE Holders and Interferers were configured for a 100 GHz and 75 GHz width, respectively. The width differences were due to the need to cover the non-used optical spectrum using ASE Holders while at the same time ensuring that the appropriate width was provided for a 60 GBaud, 16-QAM, oFEC (Open Forward Error Correction) ZR+ optical signal. The figure below presents the Channel Plan as configured in the Test Bed.

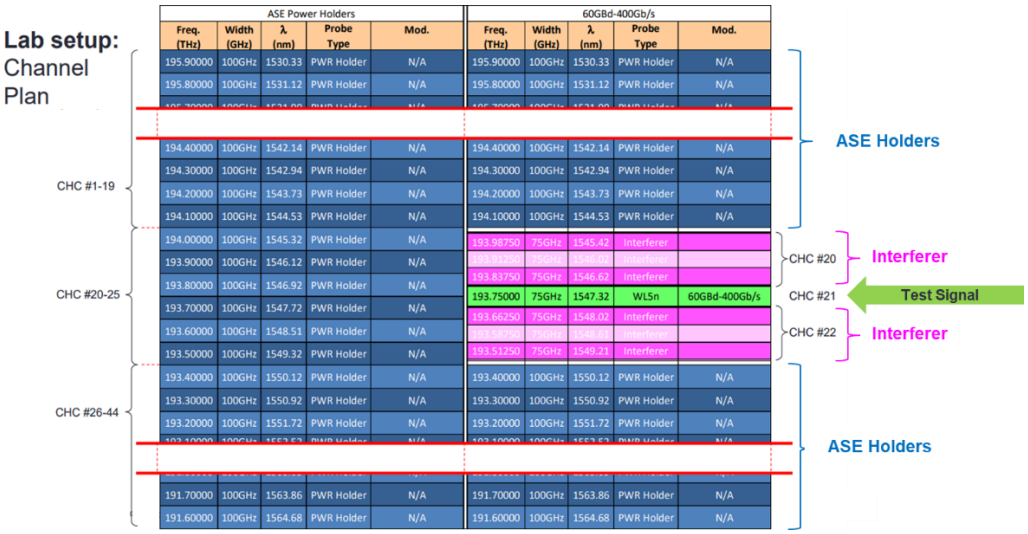

Figure 7-8 -Channel Plan

8.3 TEST ENVIRONMENT – REFERENCE MEASUREMENTS

After the propagation of the Signal Under Test across the system, there were two reference measurements taken:

a. A Power Hunt experiment was completed to evaluate the variations in performance (BER) of the pluggable module in relation to the optical power transmitted into the media (optical fibre). **See Figure 7-9 Power Hunt.**

b. The Back-to-Back (B2B) noise loading was performed to measure the BER versus the RX OSNR. This measurement was described in Figure 7-2 Optical Power Sensitivity Testing / RX OSNR Sensitivity (B2B) provided a baseline for the effective available OSNR margin. The comparison with the B2B NL curve will give an indication of the transmission penalties. **See Figure 7-10 Back-to-back Noise Loading.**

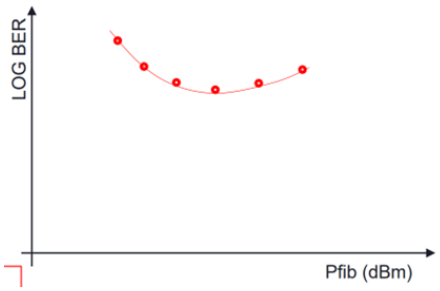

Figure 7-1 Power Hunt

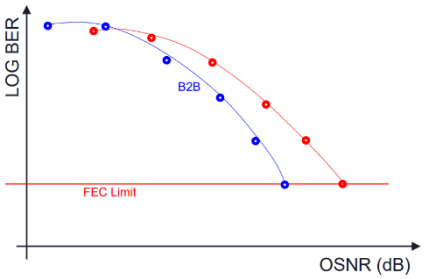

Figure 7-2 Back-to-Back Noise Loading

8.4 TEST ENVIRONMENT – TRANSMISSION TESTING

Once the Test Bed has been configured and reference measurements are taken, the ZR+ pluggable module (Device Under Test - DUT) will be inserted into the Viavi ONT-800 (host device). The ONT-800 CMIS Graphical User Interface will be used to read the AppSel Codes advertised by the DUT and then select the AppSel Code to enable the transmission of a 60 GBaud, 16-QAM, oFEC optical signal.

The propagation of the optical signal will be unidirectional, and it can be compared to a loopback that starts in the DUT transmitter. It goes across the Test Bed comprised of six (6) ROADM Nodes with an 80 km span in between and finally arrives at the DUT receiver.

The Test Bed was equipped with an optical switch to facilitate the measurement of optical spectra along the propagation path. The Optical Switch Monitor Port was connected to the OSA. The optical spectrum measurement points were connected to the Optical Switch Input Ports as described **in Figure 7-11 Span Test Sequence**

The Span Test Sequence starts with the manual propagation of the Optical Signal transmitted by the ZR+ pluggable module (The Device Under Test – DUT). Because of the unidirectional

propagation, it will be possible to emulate the corresponding transmission conditions for the optical signal going across the spans and WSS modules. The **Figure 7-11 Span Test Sequence** show the numbered markers for each defined optical spectrum measurement point. The list below presents the summary for the total reach and the quantity of WSS after traversing the spans.

- Marker-8: Back-to-Back, 0x span (0 km and 2 WSS-Local). NOTE. The Optical Signal will always go through the Back-To-Back structure. The Optical Signal will ingress via WSS Local at Tapia Mux-Structure and egress via WSS Local at Paloma Demux-Structure.
- Marker-9: Back-To-Back + 1x span (80 km and 2x WSS Degree)
- Paloma WSS Degree facing Gadea: Back-To-Back + 2x spans (160 km and 3x WSS Degree)
- Marker-10: Back-To-Back + 3x spans (240 km and 4 WSS Degree)
- Paloma WSS Degree facing Tapia: Back-To-Back + 4x spans (320 km and 5 WSS Degree)
- Marker-11: Back-To-Back + 5x spans (400 km and 6 WSS Degree)
- Marker-12: Back-To-Back + 6x spans (480 km and 7 WSS Degree)

Once the first three spans have been traversed, the Optical Signal will be sent back (loopback at Tapia WSS Degree facing Paloma) for it to be propagated in reverse across span-4, span-5, and span-6.

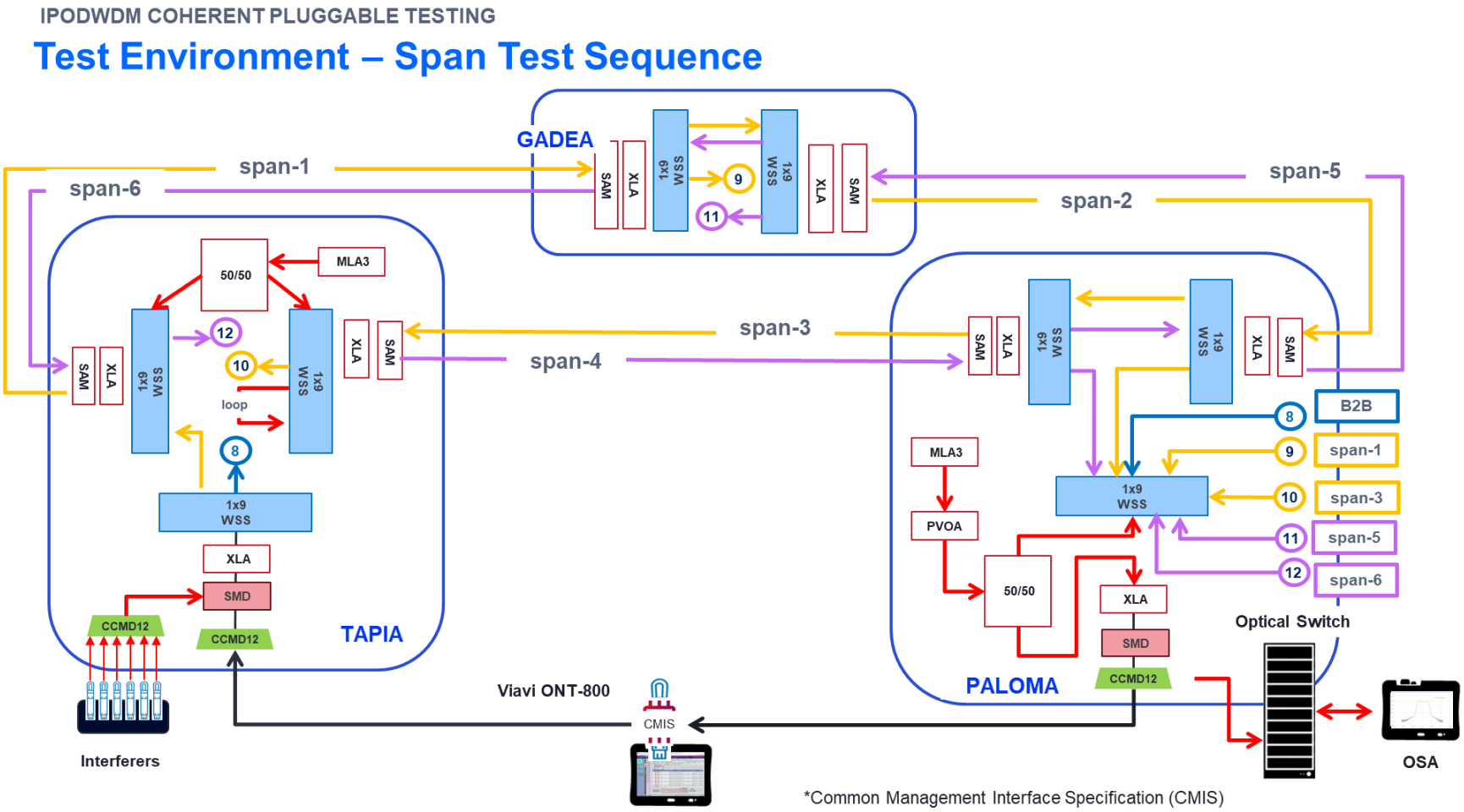

Figure 7-11 Span Test Sequence

8.5 TESTING RESULTS – TRANSMITTER TESTS

The testing for the Transmitted Optical Power of all available coherent pluggable modules was completed, and modules performed within their own specification as stated in the datasheet. The procedure involved connecting the TX output to a calibrated Optical Spectrum Analyzer (OSA), tuning the transmitter to 193.75 THz, and setting the power to maximum. Then, the maximum output power was verified, and the adjustment precision was tested by decreasing the power in 0.1 dB increments. Furthermore, the spectral width was verified at 3dB, 10dB, and 20dB down points, as well as the overall TX Optical Signal-to-Noise Ratio (OSNR). The tuning step size was tested by adjusting the TX frequency by 0.1 GHz. Additionally, TX spectrum OSA traces were captured at the minimum frequency of 191.250 THz and the maximum frequency of 196.125 THz. These tests ensure a thorough evaluation of the module's performance across its operational range.

The testing activities revealed noticeable differences in pulse shaping and pulse flatness among the tested modules. See **Figure 7-7 Optical Spectrum Differences,** that presents the TX profile of three pluggable modules.

When the pluggable transmission profile was evaluated in relation to TX masks as defined in OpenZR+ MSA Section 11.4.10 Tx spectral masks (for 60Gbaud signalling it became evident that there were significant differences in terms of pulse flatness. See the images below, which correspond to three of the tested pluggable modules.

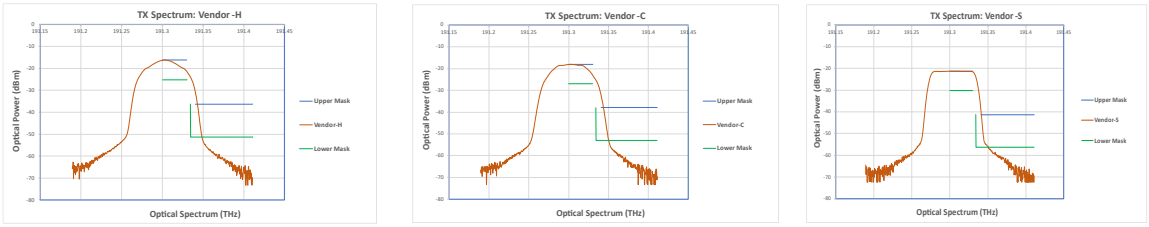

Figure 7-12- Module TX Profile vs OpenZR+ TX Mask

The OSA traces also revealed differences in both pulse width and pulse flatness. For further information, see images below. The figure to the left shows a wider pulse that also has 47.8 GHz of its provisioned spectrum, allocated within the bandwidth corresponding to a 3dB down marker. The figure on the left shows a narrow pulse that also exhibits better Pulse Flatness, allowing for the allocation of 58.8 GHz of its provisioned spectrum within the bandwidth corresponding to the 3dB down marker.

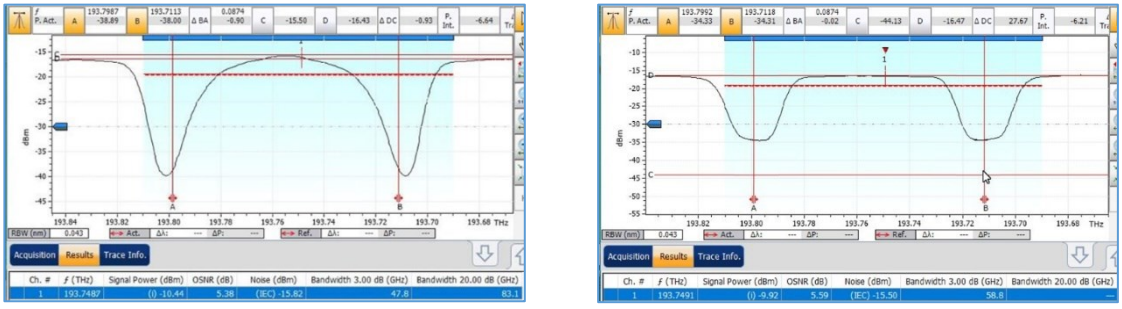

Figure 7-13 -OSA Pulse Width Comparison

Based on empirical observations, it can be concluded that flat and narrow pulses perform well in terms of reach and OSNR. It was not within the scope of the testing to determine the exact reason for this behaviour.

8.6 TESTING RESULTS – RX POWER SENSITIVITY TESTS

The testing for the Received Optical Power of all available coherent pluggable modules was completed, and all modules performed within their own specification, as detailed in the datasheet. The testing procedure began by connecting the probe TX and RX to a Programmable Variable Optical Attenuator (PVOA), a 90/10 coupler, and an Optical Spectrum Analyzer (OSA) as illustrated in **Figure 7-2 RX Optical Power Sensitivity Testing.** The transmitter was tuned to 193.75 THz, and its power was set to maximum. The PVOA loss was gradually increased until Pre-Forward Error Correction (FEC) errors were recorded, after which the received optical power threshold for error occurrence was recorded. Subsequently, the PVOA loss was reduced to facilitate recovery. After that, the PVOA loss was increased in 0.1 dB increments to identify the precise point at which Pre FEC errors reappeared. Finally, the PVOA loss was reverted to the last value where the traffic was error-free, and the RX Optical Power Sensitivity was measured.

The testing activities revealed that all pluggable module receptors performed better than their data sheet specifications. Furthermore, the plot of RX Power (dBm) versus Q-Factor (dBQ) exhibits similar behaviour. See which illustrates the relationship between RX optical power and Q-factor. The figure below shows the optical receiver “plateau” for optical power values below its receiver overload point. As the optical power decreases and goes out of the plateau, the Q-Factor decreases rapidly until it reaches the optical receiver breaking point.

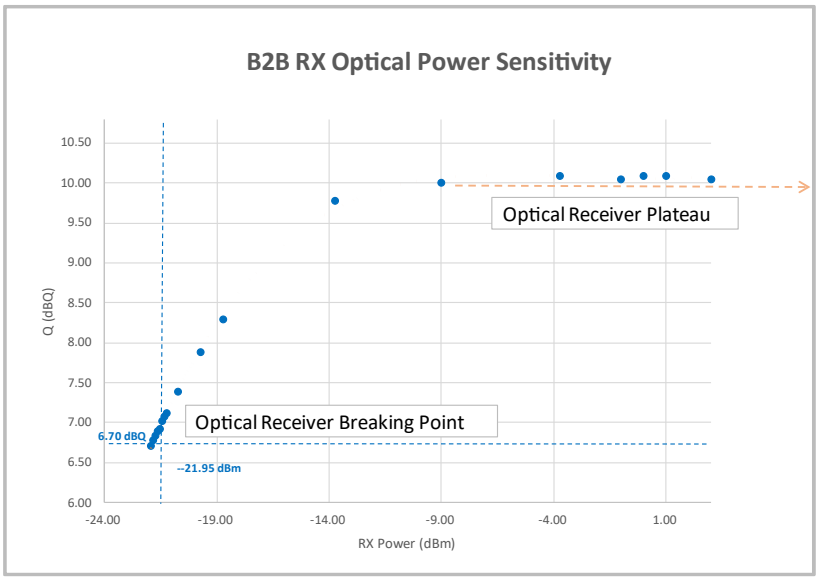

Figure 7--14 RX Optical Power vs Q-Factor

8.7 TESTING RESULTS – TRANSMISSION PERFORMANCE TESTS

A transmission performance test was conducted in two distinct environments, one for High Power (HP) and the second for Low Power (LP) pluggable modules. For each environment, both interferers and the Signal Under Test were equipped with the same type (HP/LP) of pluggable module. The Transmission Performance Testing was executed as an extension of the RX B2B OSNR sensitivity test, whereby the signal under test was propagated across ROADM nodes of the OLS by the procedures outlined in section 7.4 of the test environment – transmission testing. The procedure for this test is analogous to that of the RX B2B OSNR Sensitivity Test. Once the Signal was successfully propagated across a given Span and had a Pre-FEC (Q-Factor) margin to spare, the noise loading procedure was executed until the breaking point value for OSNR Sensitivity of the pluggable module receptor was reached.

8.7.1 Transmission performance – RX OSNR Measurements

RX OSNR testing utilises the TX OSNR (Head-End OSNR) right at the output of the Tapia Mux structure. See SW-1 marker in Fig**ure 7-15 Tapia ROADM Node.** The TX OSNR will not be the same for each DUT due to DUT's specific characteristics (pulse width, pulse flatness) and the characteristics of the Mux structure (Optical Amplifiers, Filter Response). The Mux structure at Tapia was configured for a channel width (CHC = 575 GHz) to accommodate both interferers and the signal under test. However, interferers will not be enabled during the TX OSNR measurement, as the focus is on capturing the noise floor, which only affects the signal under test. Once all the necessary configurations and conditions were met, we proceeded to measure the actual TX OSNR of the Signal Under Test (before it entered the first WSS-Degree facing Gadea). This measurement will be recorded as OSNR1.

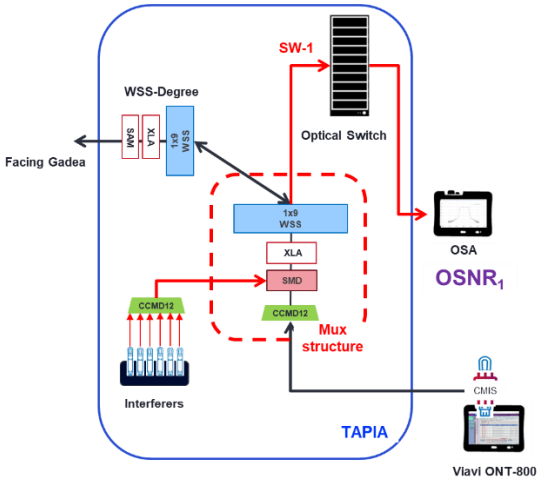

Figure 7--15 Tapia ROADM Node

The Signal Under Test is exposed to other noise sources (at each ROADM node) and impairments (related to the transmission media) from the moment it enters the OLS (@Tapia WSS-Degree facing Gadea) until it exists the OLS (@Paloma CCMD12). The previously described conditions, when combined with the signal under test, result in a second OSNR measurement. This measurement will be recorded as OSNR2. See Figure 7-16 RX OSNR Measurements To have measurement points references in the Test Bed.

The final RX OSNR value will be obtained by compounding OSNR1 and OSNR2 according to the equation below.

$$\frac{\mathbf{1}}{(\boldsymbol{RX\ OSNR})} = \frac{\mathbf{1}}{\boldsymbol{OSNR_1}} + \frac{\mathbf{1}}{\boldsymbol{OSNR_2}}$$

Equation 1 OSNR Compound

Transmission Testing: RX OSNR Measurements

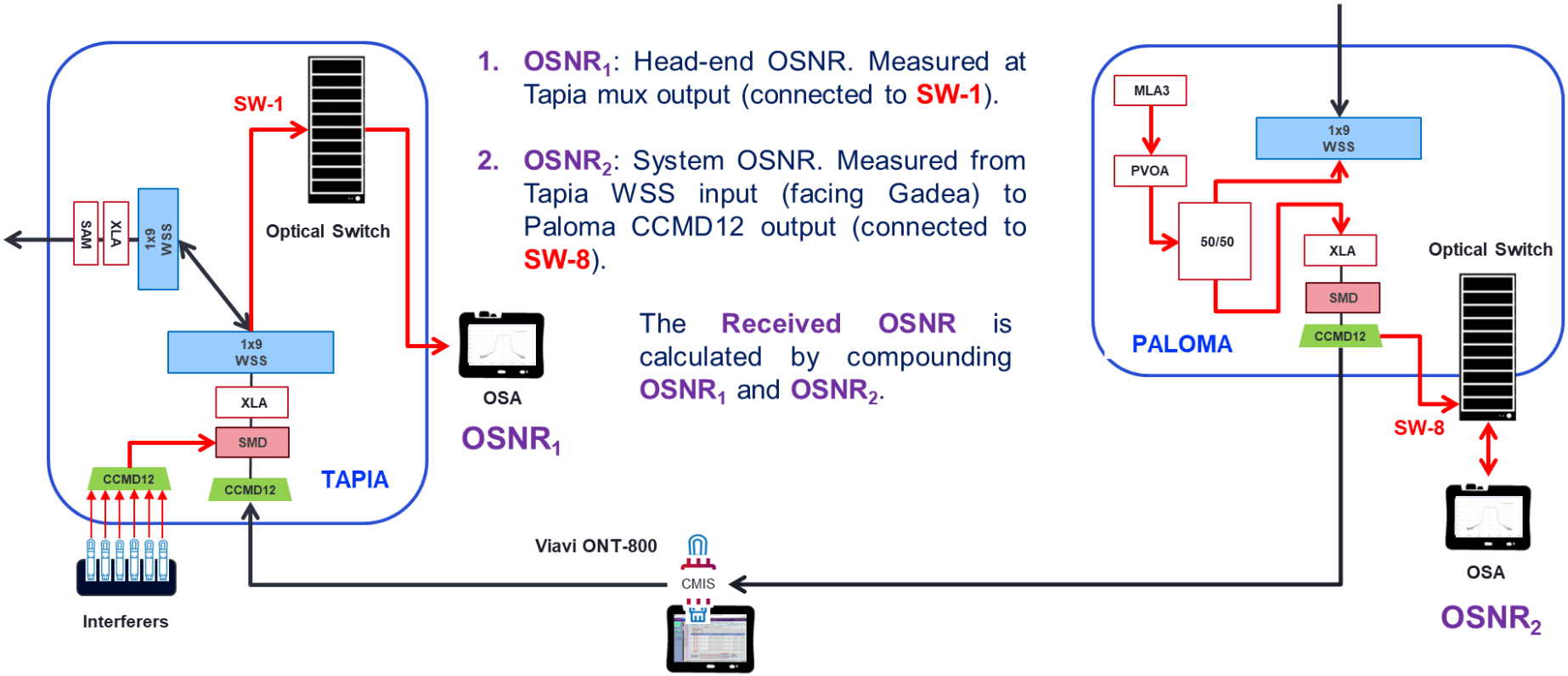

Figure 7-16 RX OSNR Measurements

8.7.2 Transmission Testing – Findings High Power vs Low Power

The empirical evidence indicates that there is no significant difference between Low-Power (LP) and High-Power (HP) pluggable modules in terms of OSNR Sensitivity Limit (Required OSNR). This verifies that the transmitted optical power alone affects signals exhibiting the same TX profile (pulse shaping, pulse flatness, 3dB bandwidth). **Figure 7-17 RX OSNR vs Q-Factor for Lower Power Modules and Figure 7-18 RX OSNR vs Q-factor** I present the plots of HP and LP modules, respectively. Both plots show a small horizontal shift between successive curves corresponding to the incremental transmission penalties.

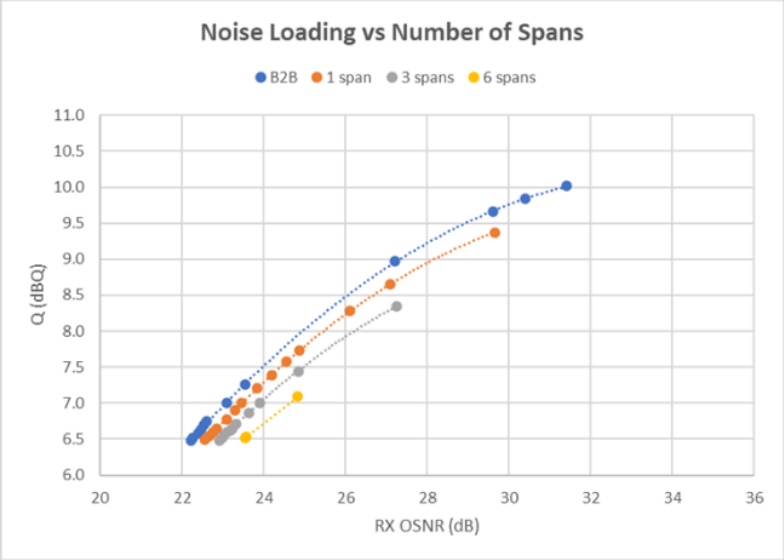

Figure -7-17 RX OSNR vs Q-Factor for Low-Power Modules

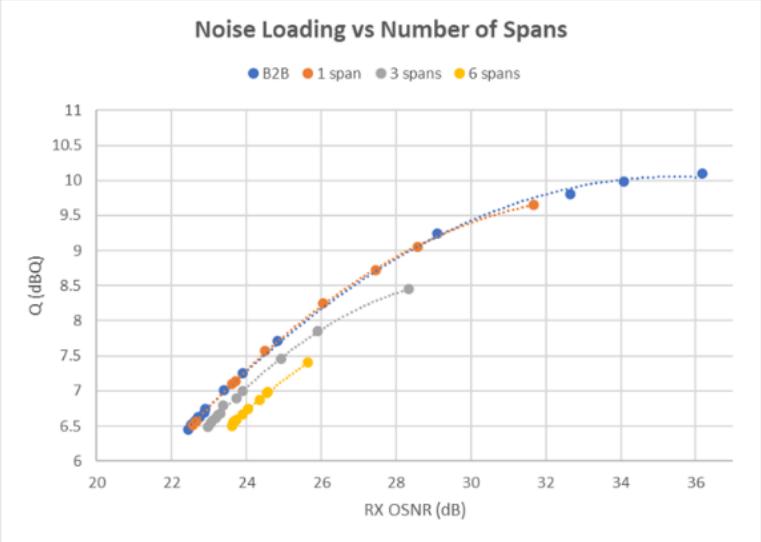

Figure -7-18 RX OSNR vs Q-Factor for High-Power Modules

The main difference shows up in relation to the higher Transmitted Optical Power (Launch Power) that translates into a higher TX OSNR (Delivered OSNR). See **Figure 7-19 Noise Loading vs Number of Span: HP/LP.** The plots below refer to the Noise Loading versus Number of Span testing for HP versus LP pluggable modules. The limit of the OSNR RX (which

is associated with the FEC failure point) is (approximately) the same for the two evaluation scenarios. It is notable that high-power pluggable modules permit an initial higher delivered OSNR (due to their higher transmit optical power) in comparison to low-power pluggable modules.

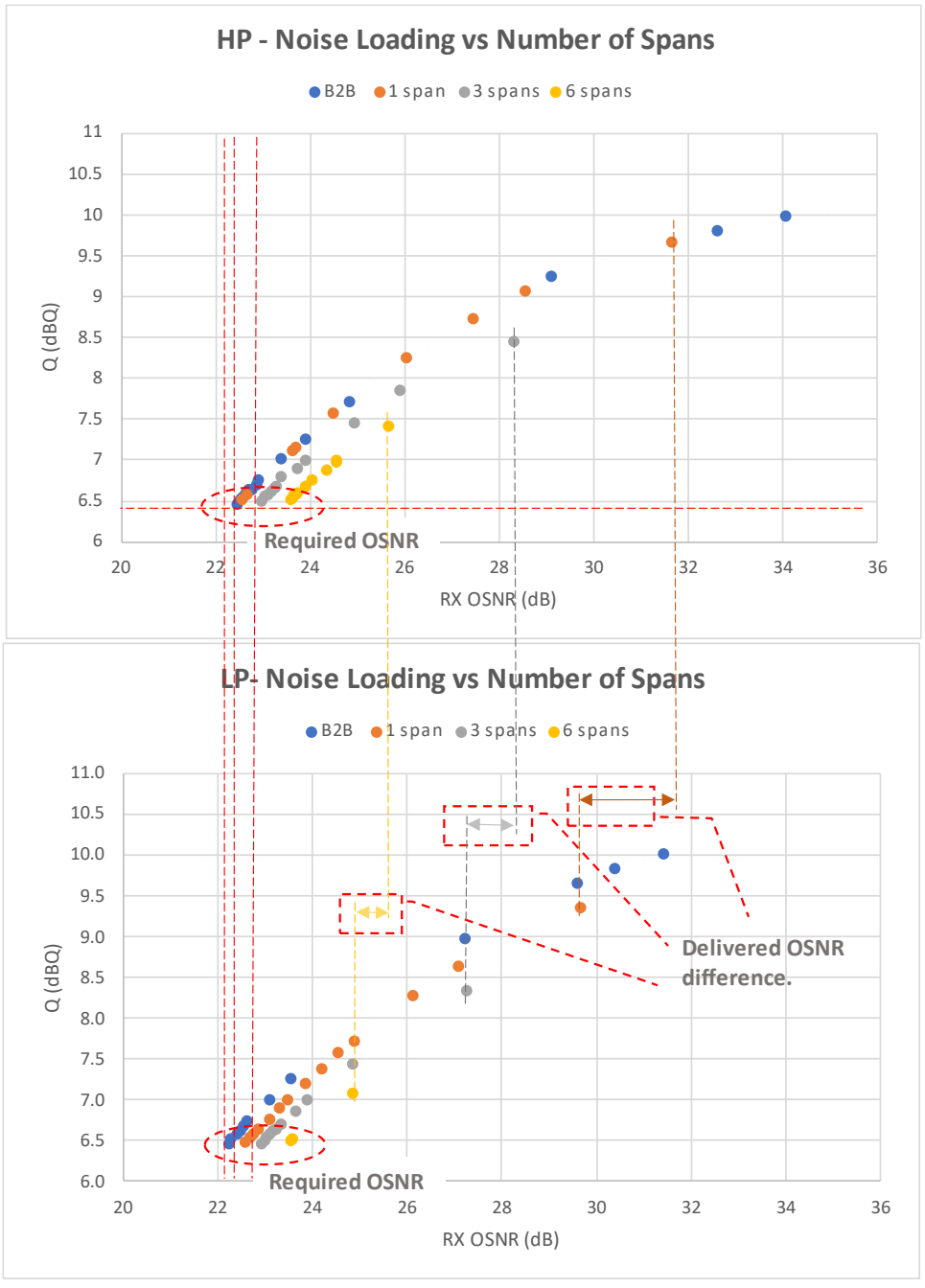

Figure -7-19 Noise Loading vs Number of Span: HP/LP

8.7.3 Transmission Testing – Delivered and Requirement OSNR

The delivered OSNR at the RX input may be adversely affected by the number of spans. This is due to an increase in overall system noise, resulting from the insertion of noise by each optical amplifier and ROADMs as the signal passes through the system. See **Figure 7-20 Delivered OSNR at Rx input**. The High-Power (blue) and the Low-Power (pink) curves demonstrate a difference in performance due to variations in both the OSNR1 and the TX power profile. It is important to note that each span the signal under test passes through adds a ROADM node to the path. If we assume that the loss introduced by two B2B WSS modules is equivalent to 19 dB and that this loss will be compensated by introducing an optical amplifier, then from an OSNR perspective, each additional span is equivalent (approximately) to having two fibre spans instead.

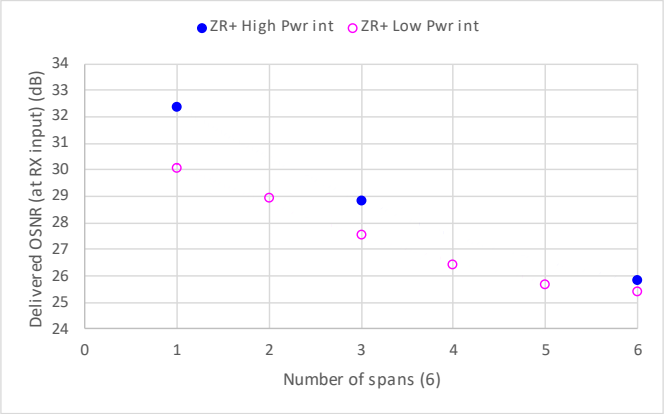

Figure 7-20 Delivered OSNR at RX input

The Required OSNR increases with the number of spans due to increasing transmission penalties. This is a result of incremental filtering and PDL/PMD penalties, which are incurred as a result of WSS, adding to fibre penalties. See **Figure 7-21 Required OSNR at FEC limit**. The high-power (blue) and low-power (pink) curves show minimal difference, as the OSNR sensitivity remains consistent despite the higher OSNR1 values for the high-power pluggable modules.

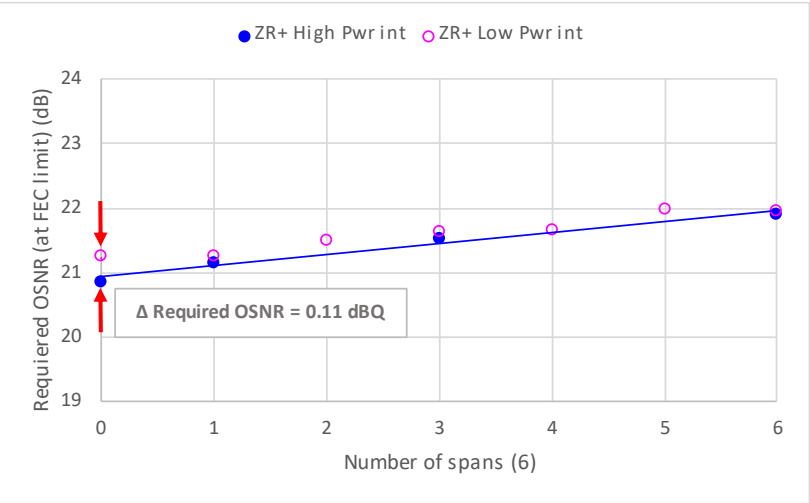

Figure 7-21 Required OSNR at FEC Limit

8.8 CONCLUSIONS

The Test Bed was configured to emulate a “brown field” optical network comprising three ROADM nodes with an 80 km fibre span between them. The optical spectrum was assumed as fully occupied. Due to the unidirectional signal propagation across the OLS, the maximum reach of the Signal Under Test was 480 km across six fibre spans.

Testing results indicate that Low-Power OpenZR+ MSA-compliant pluggable modules can reach 480 km through six ROADM nodes, provided that the module in question has an appropriate TX profile. The same principle applies to high-power pluggable modules. Having more "launch" (TX) optical power does not guarantee the maximum reach for current testing conditions.

Based on the Test Bed described above, it can be reasonably assumed that both Low-Power and High-Power OpenZR+ MSA compliant pluggable modules will successfully reach 480 Km across 6x ROADM nodes, provided that the modules have the appropriate TX profile. However, low-power modules may not always be the optimal choice due to their limited TX optical power budget, which makes them suitable for use in optical networks with a highly populated optical spectrum or data centre interconnection (DCI) applications only. Highly populated optical links represent an opportunity for low-power modules usage because the TX optical power demanded of a new optical signal will not be high because the required optical power input (OPIN) for the link optical amplifier has already been met.

When it comes to high-power pluggable modules, its usage is not restricted due to available TX optical power budget. High-Power pluggable modules have sufficient TX Optical Power within the 0 dBm to +1 dBm range for spectrum equalisation purposes, allowing them to coexist with standard (non ZR+) coherent transponders.

NOTE: In general, highly populated optical links are those optical links whose spectrum already supports optical signals to such an extent that each optical signal does not use all its TX Optical Power for TX Optical Power equalization purposes because of this, we confirm that LOW power plugs may coexist with HIGH power plugs. On the other hand, to create the “Composite” TX Optical Power that will be fed into an optical amplifier, thus ensuring that the optical amplifier will operate without falling into “noisy” working conditions.

9 SUMMARY

This deliverable concludes the B5G-OPEN technical developments by reporting on several experimental demonstrations that brought together the different components developed in the project. We provide a short conclusion of each individual demo below to summarize the deliverable.

The demonstration reported in chapter 4 showcased a fully integrated multi-band, multi-domain IPoWDM network using SDN-enabled prototype components and advanced optical transceivers. We demonstrated autonomous services provisioning across various domains and optical bands, effectively managing dynamic traffic like live video streams. We showed that parallel provisioning significantly reduces service setup times, showcasing its efficiency in high-demand scenarios. Moreover, we presented the system's self-healing capability through automatic service migration from a degraded S-band to a stable L-band, upon detected anomalies, highlighting its robustness to failures.

The demonstration presented in chapter 5 showed an innovative disaggregated IPoWDM networks transparently interconnecting access and metro segments and operating over both C- and O-bands. The network is operated through an innovative hierarchical control plane solution extended to compute and enforce transparent end-to-end paths across multiple domains, bands, and layers.

The demonstration presented in chapter 6 showed a metro-access network using XR Optics connecting a mobile site with a metro network node through a chain of OADMs that were used to aggregate and drop local traffic. The demo showcases an optical continuum where mobile traffic connects between the cell site and metro node, bypassing the access CO. In terms of multi-band operation, mobile traffic utilizes the C-Band for longer distances, while residential traffic employs the O-Band and the upper C-Band. Additionally, both FTTP (residential) and RAN (mobile) share the same fibre infrastructure. The central controller (B5G-ONP) manages service traffic and network configuration for all traffic types, ensuring end-to-end network orchestration.

The demonstration reported in chapter 7 focused on monitoring chromatic dispersion (CD) in multiband (MB) converged optical networks. This demo showcases a technique for monitoring the CD characteristics of optical fibers using an OFDM-based MB BVT. The results demonstrate high accuracy, with a small standard deviation of 0.19 ps/(km·nm). The proposed monitoring solution is integrated into an optical networking testbed, providing a complete end-to-end workflow for evaluation and validation.

The demonstration presented in chapter 8 focused on investigating the pluggable transceivers for B5G-OPEN related networking scenarios, in particular B5G-OPEN architecture in which coherent pluggable are hosted in packet optical routers. The aim is to verify experimentally that the distances that can be achieved are aligned with the target network defined in B5G-OPEN. We concluded that both Low-Power and High-Power OpenZR+ MSA compliant pluggable modules will successfully reach 480 Km across 6x ROADM nodes, provided that the modules have the appropriate TX profile.

10 REFERENCES

[And24.1] I. Andrenacci, M. Lonardi, P. Ramantanis, S. Almonacil, et al. "Machine-learning-based technique to establish ASE or Kerr impairment dominance in optical transmission," in JOCN, vol. 16, no. 4, pp. 481-492, 2024

[And24.2] I. Andrenacci, et al. "Machine Learning-Driven Low-Complexity Optical Power Optimization for Point-to-Point Links Impaired by PDL," OFC 2024

[Boi24] F. Boitier, L. Nadal, F.J. Vílchez, P. Ramantanis, J. M. Fàbrega, A. May, M. Svaluto Moreolo, R. Casellas and P. Layec, “Monitoring of Chromatic Dispersion in Multiband Access and Metro Converged Optical Network”, ECOC, Frankfurt, 2024.

[Bor21] G. Borraccini et al., “Cognitive and autonomous qot-driven optical line controller,” J. Opt. Commun. Netw. 13, E23–E31 (2021).

[Bor23] G. Borraccini et al., “Experimental demonstration of partially disaggregated optical network control using the physical layer digital twin”, IEEE Transactions on Network and Service Management, 2023.

[Gio23] A. Giorgetti et al., “Modular control plane implementation for disaggregated optical transport networks with multiband support”, in ECOC, 2023.

[Kos23] E. Kosmatos et al., “SDN-enabled path computation element for autonomous multi-band optical transport networks,” J. Opt. Commun. Netw. 15, F48–F62 (2023).

[Kra21] R. Kraemer et al., “Multi-band photonic integrated wavelength selective switch” J. Light. Technol. 39 (2021).

[Mor24] Roberto Morro, Emilio Riccardi, Anna Chiado’ Piat, Annachiara Pagano, Alessio Giorgetti, Evangelos Kosmatos, Shiyi Xia, Henrique Freire Santana, Nicola Calabretta, Pol Gonzalez, Luis Velasco, Andrea Sgambelluri, Pablo Pavon-Marino, Enrique Fernandez, Jordi Ortiz, Alexandros Stavdas, Chris Matrakidis, Filippo Cugini, Laia Nadal, Ramon Casellas, Oscar Gonzales De Dios, “Field Trial of Transparent Multi-band Multi-domain Disaggregated IPoWDM Networks”, ECOC 2024, *top scored*

[Mun17] R. Muñoz et al., "The ADRENALINE testbed: An SDN/NFV packet/optical transport network and edge/core cloud platform for end-to-end 5G and IoT services," 2017 European Conference on Networks and Communications (EuCNC), Oulu, Finland, 2017, pp. 1-5, doi: 10.1109/EuCNC.2017.7980775.

[Put22] B. Puttnam, R. Luis, G. Rademacher, Y. Awaji, and H. Furukawa, “Wideband transmission in single and multi-core fibers”, in 2022 Conference on Lasers and Electro-Optics (CLEO), 2022.

[San22] C. Santos, B. Shariati, R. Emmerich, C. Schmidt Langhorst, C. Schubert, and J. K. Fischer, “Automated dataset generation for qot estimation in coherent optical communication systems”, in European Conference on Optical Communication (ECOC) 2022, Optica Publishing Group, 2022, Tu2.4.

[Sca23] D. Scano et al., “Hybrid sdn orchestration in multi-layer network with sonic packet-optical nodes and coherent pluggables”, in OFC, 2023, M3Z.13.

[Xin23] X. Yang et al., “Qot estimation improvement with inputs refinement tool for c+l networks”, in 2023 Optical Fiber Communications Conference and Exhibition (OFC), 2023.

[Ve23.1] L. Velasco, P. González, and M. Ruiz, “An Intelligent Optical Telemetry Architecture,” in Proc. OFC, 2023.

[Ve23.2] L. Velasco, S. Barzegar, and M. Ruiz, “Using a SNR Digital Twin for Failure Management,” in Proc. IEEE International Conference on Transparent Optical Networks (ICTON), 2023.

[Ru22] M. Ruiz, D. Sequeira, and L. Velasco, "Deep Learning -based Real-Time Analysis of Lightpath Optical Constellations [Invited]," IEEE/OPTICA Journal of Optical Communications and Networking (JOCN), vol. 14, pp. C70-C81, 2022.

[Go23] P. Gonzalez, R. Casellas, J-J Pedreno-Manresa, A. Autenrieth, F. Boitier, B. Shariati, J. Fischer, M. Ruiz, J. Comellas, and L. Velasco, "Distributed Architecture Supporting Intelligent Optical Measurement Aggregation and Streaming Event Telemetry," in Proc. Optical Fiber Communication Conference (OFC), 2023.